EUROPEAN COMMISSION
5th EURATOM FRAMEWORK PROGRAMME 1998-2002
KEY ACTION : NUCLEAR FISSION

HTR-E

High-Temperature Reactor Components and Systems

CONTRACT N°
FIKI-CT-2001-00177

Work Package 1 – deliverable 7b
Design studies of horizontal hot gas duct with its thermal insulation

D. Vanvor

Framatome ANP GmbH

Germany

Contributors :
L. Briottet (CEA)
A. Buenaventura (Empresarios Agrupados)

Dissemination level : RE
Document N° : HTR-E-02/08D-1-1-5-1-B
Status : Final
Framatome ANP GmbH identification N° : NGPS3/2002/en/0054 rev. A-01

FRAMATOME ANP

Final-Report	Ref. (Department/Year/Language/Serial No.) **NGPS3/2003/en/0054**	Rev. **A-01**

Subject/Title
Final Report Deliverable 7b of HTR-E: Continuous Hot Gas Duct for GTMHR Reactor Design

Place	Date
Erlangen	30.01.2004

Prepared by	Department	Tel.	Signature
D. Vanvor	NGPS4	94380	Sign. Vanvor
Reviewed by Dr. Brinkmann	NGPS4	96630	Sign. Brinkmann

Project
HTR

Handling Instructions
restrictive

Export Classification (Reports with techn. content)
AL: ECCN:

Released by concerned department (content, handling, distribution)

released for external distribution

Proj.-Code	UA	DCC	Contents Code	Doc. Ident. No.
ZFY116	BE	M -BB		0600258153

Goods labeled with "AL not equal to N" are subject to European or German export authorization when being exported out of the EU. Goods labeled with "ECCN not equal to N" are subject to US reexport authorization. Even without a label, or with label "AL:N" or "ECCN:N", authorization may be required due to the final whereabouts and purpose for which the goods are to be used.

Summary

Pages of Text: 12 Appendices 89 p Pages total: 101

This report serves as information for the members of WP1 of the HTR-E (EC Project: FIKI-CT-2002-00177) and is intended as an input for the SINTER network. It is the contribution of Framatome ANP GmbH to Deliverable 7b of WP1 of the HTR-E.

In this final report the results of the following individual reports are summarized and evaluated.

- Final Report NGPS3/2002/0032 from 08/02/2002; FANP GmbH (Reference 1)
- Intermediate Report NGPS3/2003/en/0005 from 25.02.2003, FANP GmbH (Attachment 1)
- HTR Hot Gas Duct Configuration Trade-off Doc.N0 092-110-E-00002, EA (Attachment 2)
- Work-Report NGPM5/2003/en/0285 from 30.12.2003, FANP GmbH (Attachment 3)

Distribution

Dr. Brinkmann NGPS4	BALLOT NZ
Mr. Ebert NGPS4	GAUTHIER NZ
Briottet CEA (Members of WP1)	HITTNER NZ
	LECOMTE NZ
	BESSON NFPVEI

List of revisions

Rev.	Date	Scope of revision	Section/Page
A	30.01.2004	First edition	All
A-01	05.04.2004	Review by intervention of WP-Leader	Page 4, 8 and 9

Table of Contents

1 Introduction

This report specified in detail the design and design criteria for a continuous horizontal hot gas duct (based on report [1]). The design is based on the GTMHR reactor design (helium turbine as heat sink in a one loop plant.) Special data come from Mr. Alan Gerber, FANP SAS (Attachment 1).

The review of the preliminary design for the mechanical design was carried out by EA (Attachment 2). In addition further Finite Element-analyses were carried out by FANP GmbH (Attachment 3)

2 Design Conditions

2.1 Normal Working Conditions

Normal working conditions are fixed by FANP SAS (see attachment 1). Therefore we have the following data:

<u>Hot gas side:</u>

Helium inlet temperature:	850 °C
Helium outlet temperature:	848.4 °C
Helium pressure:	70.8 bar
Helium mass flow:	316.19 kg/s

<u>Cold gas side:</u>

Helium inlet temperature:	487.9 °C
Helium outlet temperature:	487.8 °C
Helium pressure:	71.6 bar
Helium mass flow:	318.2 kg/s

2.2 Transient Working Conditions

Starting with the normal operating conditions, the following transient conditions are defined: [1)]

<u>Hot gas side:</u>

Helium inlet temperature:	starting at 850 °C → ending at 850 °C in 8.83 s
Helium outlet temperature:	starting at 848,4 °C → ending at 848,4 °C in 8.83 s
Helium pressure:	starting at 70.8 bar → ending at 1.6 bar in 7 s
Helium mass flow:	starting at 316.19 kg/s → ending at 0 kg/s in 7 s

<u>Cold gas side:</u>

Helium inlet temperature:	starting at 487.9 °C → ending at 284.81 °C in 8.83 s
Helium outlet temperature:	starting at 487.8 °C → ending at 284.71 °C in 8.83 s
Helium pressure:	starting at 71.6 bar → ending at 1.6 bar in 7 s
Helium mass flow:	starting at 318.2 kg/s → ending at 0 kg/s in 7 s

[1)] FANP GmbH has interpreted the transient conditions from attachment 2, chapter 3.3.2, as a turbine rupture and a depressurization of the primary loop. The Ref. 3 from attachment 2 is not available to FANP GmbH.

2.3 Geometric Data

Geometric data are set by FANP SAS (see attachment 1). Therefore the following data are used:

Cold gas duct inner diameter:	2,300 mm
Hot gas duct outer diameter:	1,700 mm
Hot gas duct inner diameter:	1,450 mm
Hot gas duct wall thickness:	25 mm (support wall thickness)

2.4 Material data

Material data are set by FANP SAS (see attachment 1). Therefore the following data are used:

Metal alloy 1.4876 (X10NiCrAlTi32-21 or X10NiCrAlTi32-20)

This material is used for all metal structure inside the hot gas duct except the support tube.

Metal alloy 1.4571 (X6CrNiMoTi17-12-2)

This material was chosen primarily for the support tube of the hot gas duct.

Insulation material

All insulation areas are filled with fibre mats, containing min. 95% Al_2O_3 and approx. 5% SiO_2 ceramic materials. This fibre material is manufactured in mat form and is delivered in pad form.

3 Design of the continuous hot gas duct

FANP GmbH produced a draft for a hot gas duct module using the geometric data given above and the mechanical design module common in the nuclear industry.

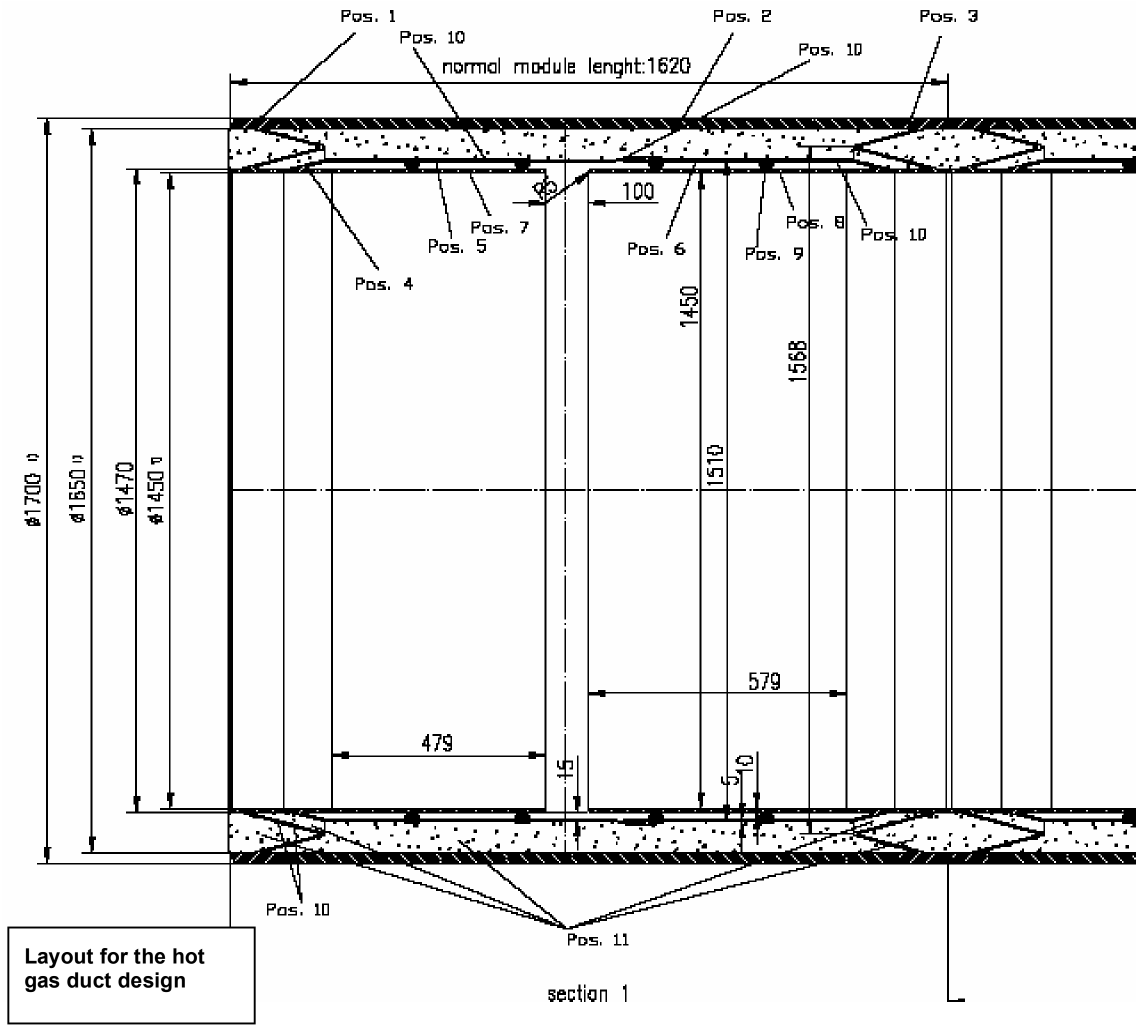

Layout for the hot gas duct design

This design was developed based on the experience FANP GmbH had gained from previous HTR-projects and was characterized by the following points:

- Shop fabrication from assembly modules
- All welds within the module were already tested by X ray or Ultra Sonic method in the factory.
- Only two site welds required between the modules on site.
- Site welds can be tested by Ultra Sound.
- All components are optimized for stress-loading.
- All welds are outside of the high-load areas and can be fully tested.

Further details can be found in attachment 1.

3.1 Structural analysis by EA

The report (attachment 2) was checked regarding content on the following points:

a) Input data used (Geometry, loading, materials)
b) Methods and verification procedures
c) Results and conclusions
d) Variants A, B and C

3.1.1 Input data used (Geometry, loading, materials)

With regards to geometry, the essential main dimensions, named in 2.3 were given in the text. On the basis of the reference of the FANP report ZFY116-0600191597 it is assumed that the Finite Element-Model was taken from the structure of the engineering drawing.

The following corrections – basis for a more detailed investigation - are necessary regarding the technological properties used on page 3-1:

- The data on specific heat, Cp, is given in KJ/kgK not in J/kgK.
- The data for E-Module E are given in Pa not in MPa.

On the basis of this necessary information about consistency of units in the FEM calculations, these corrections can matter whereby the specific material heat is not relevant for the static calculations. But these variables definitely matter for the transient analysis on heat transfer.

On the basis of the high stresses included (see page 4-3) it is assumed that the non-linearity in the behavior of the material remains unconsidered. It is therefore also assumed that an elastic behavior was used, since there was no indication that a plastic deformation (strain) was undertaken.

3.1.2 Methods and verification procedures

As a reference to the applied standard, only the ASME II Dev. 1-NH is on page 4-3. There are no references to be found on the generally accepted approach of primary and secondary diaphragm and bending stresses. There is a reference to an acceptable secondary stress of $2Rp_{0,2}$ on page 4-3. This stress limit has to be investigated in further work. It is also valuable to confirm in the report to what extent time-dependant temperature methods are considered. For the component being tested it is necessary to conduct a verification analysis for expansion with time and temperature dependant limits in accordance with KTA 3221. This means limits of stress and expansion with time and temperature dependant limits under detailed examination of fatigue levels and classification of stress and binding as well as a relax action and creep.

3.1.3 Results and conclusions

The conclusions on pages 4-3 to 4-5 (4-7) have need further work, so that the chosen construction for the design input satisfies the requirements of a preliminary optimized design. FANP GmbH has therefore decided to confirm the design using the data available at the present time with its own FEM analysis.

3.1.4 Variants A, B and C

In the report attachment 2, the reference solution A is considered according to ZFY116-0600191597 of the FANP GmbH with FEM-Analysis and also thermosleeves created by EA in an S-curve-form (type B) or a stair-form (type C) and additional variations.

These EA designs were not included by FANP GmbH in its own considerations for the following reasons:

- Both the type B and the type C include welds which are not acceptable as primary system components in the German nuclear industry.
- None of the chosen welds can be tested for accuracy by an X-ray or an Ultra Sonic-test.
- The installation of individual hot gas duct components as shown in the FANP GmbH drawings is not possible for the selected thermosleeve-forms without a gap in the insulated area.

3.1.5 Filter type A and B

In chapter 5.2.1 of appendix 2, it is assumed that ceramic rings are placed between the perforated piping and the flow duct. This assumption leads to unavoidable consequences during depressurization events.

In the design FANP GmbH used round spacers between both metal sheets. A larger flow cross section ensures the outflow of the helium gas that penetrated the insulation from the insulation space in the drainage column and from the draining column in the free flow cross section.

The filter for the pressure relief of the isolated area which is shown in FIGURE E of appendix 2 does not fulfill the following tasks, which are believed to be mandatory:

- Minimization of the pressure difference between the drainage gap and the free flow cross section
- Stress-strain compensation of different stresses between the liner tube and the support pipe due to the tendency for helium friction welding when movement occurs.
- Low flow velocity within the isolated area through pressure relief.
- The design does not comply with German nuclear regulations.

The installation of this device as well as the installation of the hot gas duct component between the L-Shape is not believed to be carried out (see positioning of the welds, support pipe and liner).

4 FEM analyses concerning continuous, horizontal hot gas duct

The present design for the hot gas duct, especially the spacres between the inner liner and the support tube, is evaluated for the operational conditions and on Accident Load Case. For the incident and accident conditions conclusions are made.

The evaluation is based on the preliminary KTA 3221.1 and KTA 3221.2. The hot gas duct with operating conditions of 488°C at the support tube und 850°C at the inner liner is classified for Temperature category III. With respect to the classification the structural analyses include evaluation of primary and secondary strains and stresses and the consideration of elastic-plastic material behaviour together with the assessment of creep behaviour. The threshold values are time-temperature depending values.

The evaluation is done by the FE-Method with the computer code ANSYS 7.1.

Details see Work-Report NGPM5/2003/en/0285 from 30.12.2003 (attachment 3).

With respect to the available information and made estimations it can concluded that the design resist the load for the normal operation (usage factor 0,11). Critical items are stress concentration with respect to material and geometrical discontinuities. Welds has to be minimized in principle and not considered here

The investigated design for the hot gas duct seems to resist the defined loadings, but not all load cases were considered and material discontinuities were neglected. Furthermore it should be considered that welds have to be minimized and the geometrical design should preclude any stress concentration. A final statement and design optimization should include further load cases and the check if any further loads from boundary conditions has to be considered (e.g. seismic loads).

5 Conclusions

Based on the continuous hot gas duct reference design (attachment 1), thermo mechanical calculations have been carried out for both the normal operating conditions and transients. In particular, the design of the continuous horizontal hot gas duct and the behavior of the thermal insulation were analyzed.

This review took place with the current available data and took into account a normal operation as well as a general plant transient. At a later date additional analyses for loop calculations will have to be carried out.

Taking into account the comments regarding EA as well as the additional analyses performed by FANP, the design is acceptable. The selected design can be retained for further development.

However, FANP GmbH recommends the production of the support pipe out of the 1.4876 material because of planned high cold gas temperatures. As a result unacceptably high temperatures at the support pipe under accident conditions can be avoided and a structural integrity can be assured.

In conclusion the following must be pointed out:

The analyses carried out by FANP GmbH used estimates from earlier HTR-projects. The material data were taken from the KTA-regulations “draft” in Germany.

Up to now no standards (HTR-L) or material data (HTR-M) concerning the functional design for components for a HTR has been specified. Therefore it cannot be ruled out that an upgrading of the chosen design will be necessary due to the application of a binding standard at a later date.

6 References

1. Final Report NGPS3/2002/0032 from 08/02/2002; FANP GmbH

7 Attachments

1. Intermediate Report NGPS3/2003/en/0005 from 25.02.2003, FANP GmbH
2. 092-110-E-M-00002, HTR Hot Gas Duct Configuration Trade-off, EMPRESARIOS AGRUPADOS
3. Work-Report NGPM5/2003/en/0285 from 30.12.2003, FEM Analysis on continuous hot gas duct Framatome ANP GmbH

Attachment 1

Intermediate Report NGPS3/2003/en/0005 from 25.02.2003, FANP GmbH

FRAMATOME ANP

Intermediate Report	Ref. (Department/Year/Language/Serial No.) NGPS3/2003/en/0005	Rev.

Subject/Title
Continuous horizontal hot gas duct
Detailed design for GM-HTR reactor design

Place	Date
Erlangen	2003-02-25

Prepared by	Department	Tel.	Signature
D. Vanvor	NGPS3	94380	gez. Vanvor

Reviewed by

Project
HTR-E

Handling Instructions
restricted

Export Classification (Reports with techn. content)
AL: ECCN:

Dr. Brinkmann	Dr. Brinkmann
gez. Brinkmann	gez. Brinkmann
Released by concerned department (content, handling, distribution)	released for external distribution

Proj.-Code	UA	DCC	Contents Code	Doc. Ident. No.
ZFY116	BE		1123, 1435, 1436	06001 91 597

Summary

Pages of Text: 5 Appendices 6 Pages total: 11

This report serves as information for the members of WP1 of the HTR-E (EC Project: FIKI-CT-2001-00177) and is intended as an input for the SINTER network. It is the contribution of Framatom ANP GmbH to Deliverable 7b of the HTR-E.

The information is especially needed for the FEM-analysis for the hot gas duct to be prfotmed by EMPRESARIOS AGRUPADOS (EA), Mr. Arturo Buenaventura Pouyfaucon.

Distribution

Dr. Brinkmann, NGPS3	Mr. Ballot, TH, f.i.o.
Mr. Ebert, NGPS3	Mr. Bogusch, RGR, f.i.o.
Members of WP1 of HTR-E	Mr. Friebe, NGPS3, f.i.o.

Framatome ANP GmbH

List of revisions

Rev.	Date	Scope of revision	Section/Page
0	2003-02-25	First issue	All

Table of Contents

1 Introduction

This report describes the design for a continuous horizontal hot gas duct in detail. The design is based on the data from Mr. Alain Gerber from NFEVES (see attachment 1) for the hot gas duct for the GT-MHR reactor design.

The continuous horizontal hot gas duct is split in several sections. Each normal section is 1620 mm long. For connecting to the upper core structure or the helium turbine inlet we need shorter sections, but for the FEM-analyses made by EA the longest section should by calculate.

In the attachments 3 to 5 the detailed construction for the continuous hot gas duct is shown.

2 Normal working conditions

Normal working conditions are fixed by NFEVES (see attachment 1). Therefore we have the following data:

<u>Hot gas side:</u>

Helium inlet temperature:	850 °C
Helium outlet temperature:	848,4 °C
Helium pressure:	70,8 bar
Helium mass flow:	316,19 kg/s

<u>Cold gas side:</u>

Helium inlet temperature:	487,9 °C
Helium outlet temperature:	487,8 °C
Helium pressure:	71,6 bar
Helium mass flow:	318,2 kg/s

3 Materials

The materials chosen are specified in our e-mail dated 13. January 2003 (see attachment 2).

For the fibre insulation you must calculate with a thermal conductivity of 0.55 W/mK at the temperature of 850 °C.

4 Special data

In completion we specified following data:

- Each insulation fibre area is filled with 90 Vol% helium.
- The shown depressurisation gaps in the positions 1, 5 and 6 are only pre designed. This design must be confirmed by the FEM-calculations.
- The shown depressurisation gap between position 5 / 6 and 7 (15 mm) and the ring outlet inside the liner (100 mm) are only pre designed. This design must be confirmed by the FEM-calculations.

VANVOR Dieter NGES3

Von: GERBER Alain NFEVES
Gesendet: Montag, 10. Februar 2003 17:23
An: Arturo Buenaventura Pouyfaucon (E-mail)
Cc: VANVOR Dieter NGES3; Laurent BRIOTTET (E-mail); BREUIL Eric NFEVEI; HAMY Jean Marie NFEVEK
Betreff: GT-MHR : nominal working conditions

Dear Arturo,
In your E-mail to M. Vanvor dated January the 9th about "HTR-E, WP1, Task D7b, Hot gas duct", you ask nominal working conditions data. These are the following (GT-MHR data) :

1 - NOMINAL OPERATING CONDITIONS

Hot gas size :

Helium inlet temperature : 850°C (= core outlet)
Helium outlet temperature : 848,4°C (=turbine inlet)
Helium pressure : 7,08 MPa
Helium mass flow : 316,19 kg/s

Cold gas side :

Helium inlet temperature : 487,9°C (=recuperator outlet)
Helium outlet temperature : 487,8°C (=core inlet)
Helium pressure : 7,16 MPa
Helium mass flow : 318,2 kg/s

2 - NORMAL OPERATION, LOAD CYCLING

The reactor load can be decreased from 100% to 30% (and inversely) at two load changes levels :
- low load change : 0,6% per minute
- rapid load change : within the range of 6% to 10% per minute.

- At 0,6% per minute, on both hot and cold gas sides :
  * Transient induced temperatures variations are not significant.
  * Transient induced pressure variations is about 0.042MPa per minute
  * Transient induced flowrate variations is 1,9 kg/s per minute

- We have performed some calculations in the past concerning load change from 100% to 30% at 10% load change level. It can be retained in a conservative approach :
  * Outlet core temperature is regulated, so there is no variation of hot gas side temperatures
  * Cold gas side temperature variation is -9K per minute at transient beginning, +1,14 K per minute at end.
  * For both hot and cold gas sides, transient induced flowrate variation is -12,23 kg/s per minute in transient beginning, then -1,74 kg/s per minute at the end.

- No data available for 30% to 100% transient, our fisrt calculations are not correct (code problems). Moreover it depends of Helium Service System capacity to fill the helium inventory. In a first approach, inverse data of transient from 100% to 30% should be retained.

3 - GEOMETRICAL DATA
- Cold gas duct inner diameter : 2300 mm
- Hot gas duct outer diameter : 1700 mm
- Hot gas duct inner diameter : 1450 mm
- Hot gas duct wall thickness : 25 mm

4 - NEXT DATA
As promised in the november meeting in Juelich, we will produce envelope operation data for transient conditions in March 2003.

****
FRAMATOME-ANP PVES
Tél. : (33)4 72 74 71 96
Fax : (33)4 72 74 73 30
E-mail : alain.gerber@framatome-anp.com
****

Attachment 2-1

VANVOR Dieter NGES3

Von: VANVOR Dieter NGES3
Gesendet: Montag, 13. Januar 2003 14:44
An: 'abp@empre.es'
Cc: BREUIL Eric NFEVEI; 'laurent.briottet@cea.fr'; BRINKMANN Gerd NGES3
Betreff: AW: HTR-E, WP1, Task D7b, Hot Gas Duct

Dear Arturo Buenaventura,

To your E-Mail we take position as follows:

Objective and scope of the analysis
We need a FEM analysis of all construction units of the hot gas duct. This meens for detail:

- for the liner and the perforated pipe with a boil pressure of about 10 bars at 900 °C
- for the Vee-shaped spacers for a temperature differenz of about 600 K
- for the support pipe for a boil pressure af about 10 bars at 540 °C

But this data must be spezifide by NFEVEI!

Detailed geometry of the Hot Gas Duct:
This data and design specifications have to be fixed bei NFEVEI !

Materials:
Metal alloy 1.4876 for the liner, perforated pipe and the hot side of the vee-shaped sacer
Basis for the material parameters are the standards indicated according to German "Stahlschlüssel, 2001). In this steel key as basis standard the EN 1009-1 indicates. In Germany also the material sheet SEW 470 is permissible.

The material is classified as follows:
1.4876 X10NiCrAlTi32-21 / X10NiCrAlTi32-20
in USA: Type B 163, UNS No. N 08800 or N 08810 (AISI/SAE)
France: AFNOR Z 10 NC 32-21
Spain: UNE F.3314 - X 10 NiCrAlTi 32-20
GB: B.S. NA 15 (XH)
Japan: JIS NCF 800 (TP)

Metal alloy 1.4571 for the cold side of the vee-shaped spacer an the support pipe
Basis for the material parameters are the standards indicated according to German "Stahlschlüssel, 2001). In this steel key as basis standard the EN 10028-7 and EN 10088-1 one indicates.

The material is classified as follows:
1.4471 X6CrNiMoTi17-12-2
in USA: Type 316TI, UNS No. S 31635 (AISI/SAE)
France: AFNOR Z 6 CNDT 17-12
Spain: UNE F.3535 - X 6 CrNiMoTi 17 12 2
GB: B.S. 320 S 31
Japan: JIS SUS 316 Ti

The boundary conditions and Nominal working conditions:
This data and design specifications have to be fixed bei NFEVEI !

Best regards

===

-----Ursprüngliche Nachricht-----
Von: Arturo Buenaventura Pouyfaucon [mailto:abp@empre.es]
Gesendet am: Donnerstag, 9. Januar 2003 18:08

Attachment 2-2

An: VANVOR Dieter NGES3; BREUIL Eric NFEVEI
Cc: 'Briottet Laurent (E-mail)'; Alfredo Orden (E-mail); Maite Dominguez (E-mail)
Betreff: HTR-E, WP1, Task D7b, Hot Gas Duct

Ref: 092-110-CE-EA-SV-03/0001

Dear Mr Vanvor,

As discussed during last HTR-E Meeting held in FZJ (Nov. 2002), we will carry out the themo-mechanical analysis of the horizontal Hot Gas Duct between the reactor and the PCU.

We are willing to start working as soon as possible, so we request from you the required input data for the analysis:

Objective and scope of the analysis (different types of analysis you require us to perform, results you need, etc..)
Detailed geometry of the Hot Gas Duct (Diameter, etc..)
Materials (if German reference, the equivalence or directly the list of characteristics)
The boundary conditions (fixing of reactor side and PCU side Hot Gas Duct extremities)
Nominal working conditions

We are aiming to have the FE Model and calculations for nominal working conditions by March 2003.

Best regards,

Arturo Buenaventura
Empresarios Agrupados
Mechanical Department
Tf: +34 91 309 80 00
Fax: +34 91 591 26 55

Continuous horizontal hot gas duct
vertical cross section, scale 1:5

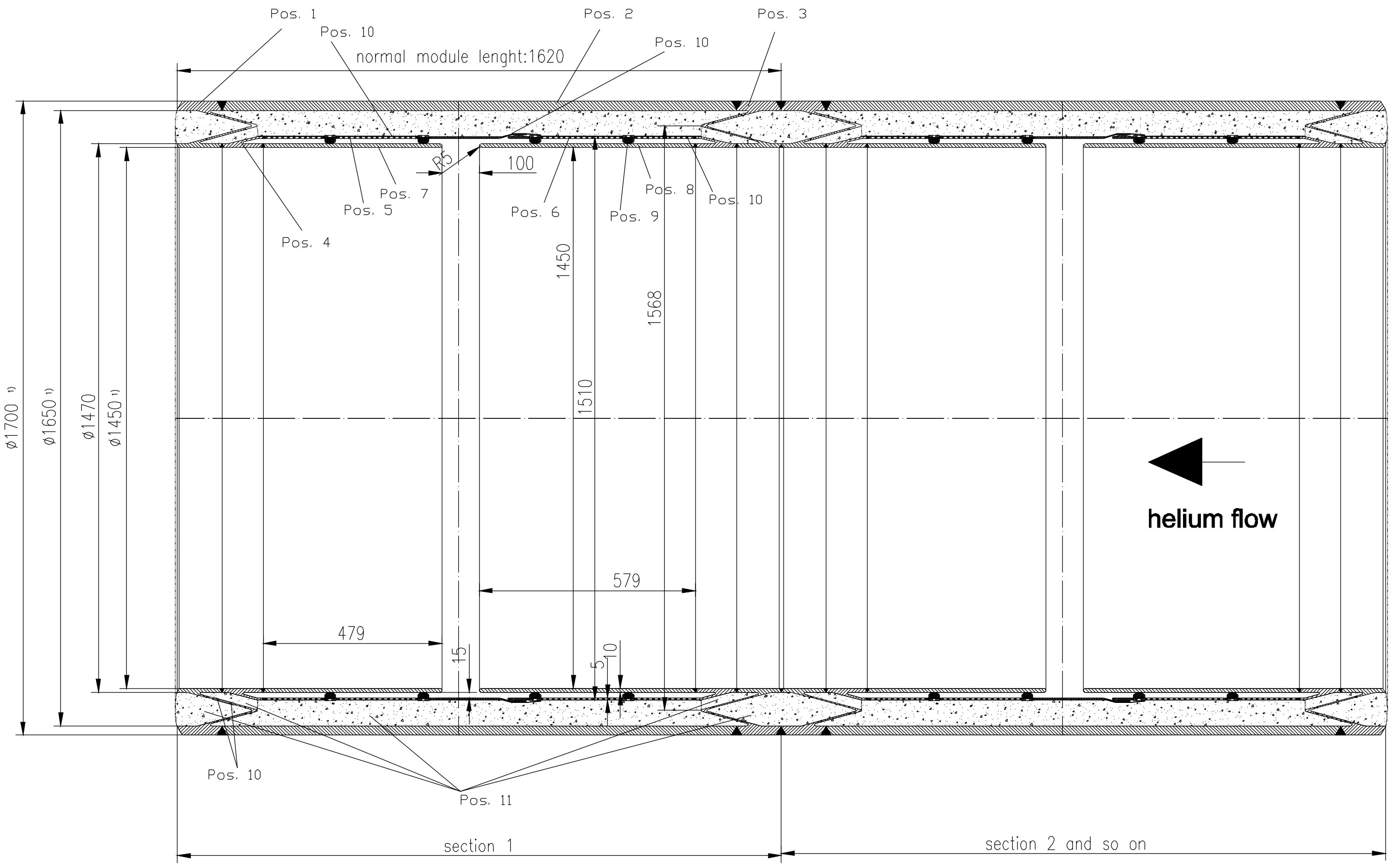

1) Basis Data:
Basis Date from E-Mail from 10. february 2003,
Alain Gerber, NFEVES
"GT-MHR: normal working conditions"

Pos. 9, scale 1:1

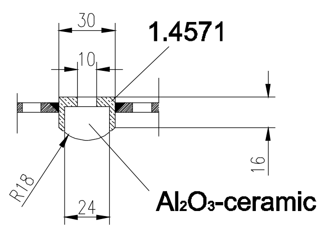

Detail: sliding system, scale 1:1

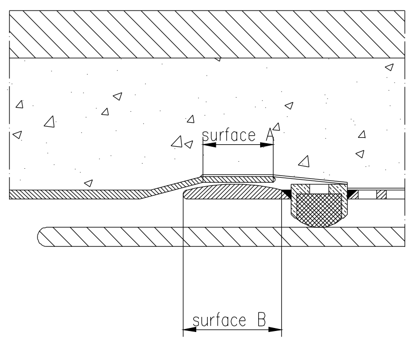

Coating for surface A and B:

dublex coating as NiCrAlY and $ZrO_2 + Y_2O_3$

ground surface with R_t= 50 µm,
NiCrAlY with 78,4/16,4/5,1 and 0,15 %
coating thickness 140 µm

cover coating as $ZrO_2 + Y_2O_3$, with >13 % Y_2O_3
ground surface with R_t= 25 - 50 µm
coating thickness 80 µm

--	fibre insulation	--	Al2O3	P 11	--
--	mesh cover	--	1.4876	P 10	--
64	ceramic spacer	ø30	--	P 9	see detail
1	liner	ø1450; th:10	1.4876	P 8	--
1	liner	ø1450; th:10	1.4876	P 7	--
1	perforated pipe	ø1510; th:5	1.4876	P 6	--
1	perforated pipe	ø1510; th:5	1.4876	P 5	--
2	depressurization spacer	ø1510; th:5	1.4876	P 4	see detail
1	Vee-shaped spacers	ø1700/ø1450; L:120	1.4876	P 3	see detail
1	support pipe	ø1700; Th: 25	1.4571	P 2	--
1	Vee-shaped spacers	ø1700/ø1450; L:120	1.4876	P 1	see detail
St. Qt.	Benenng. Title / Fertig-Abmessgn. Finished dim.	Norm-Nr./Stand.-No. Zeichng.-Nr./Drwg.-No.	Werkstoff Material	Lfd.Nr. Pos.	Bemerkungen Remarks

Ursprung/Original | Ursprung-Nr./Original-No. | Urspr.-PKZ-Nr. Orig.-PC

Projekt/Project: HTR-E | PKZ/PC: ZFY116

	Datum Date	Name
gezeichn. Drawn	24.02.03	Vanvor
bearb. Coord.	24.02.03	Vanvor
geprüft Checked		
Abtlg. Dept.	NGPS3	

Maßstab Scale: 1 : 5 (1:1)

UA / DCC Type of Doc.: XK09

Benennung/ Title:
Continuous Horizontal Hot Gas Duct
For GT-MHR Reactor Design
Deliverable 7b of WP1
Outline And Detail Drawing

Inhaltskennzeichen Contents Code: DS1600

Zähl.-Nr. Reg.No.: --

FRAMATOME ANP

Dienstst./Dept.: NGPS3 | UNID: 0600191634 | Index/Rev.: -- | Version: --

ZFY116-NGPS3-00-003327

Ang.-Var./Offer-Var.: -- | Var./Opt.: -- | Blatt-Nr./Page-No.: --

Erstellt mit / designed with: AutoCAD | Ersatz für Supersedes: in EDDA as PDF

Maße nicht abgreifbar/Not to Scale

Pos. 1
scale 1:2

Pos. 3:
manufatured in a reflected image

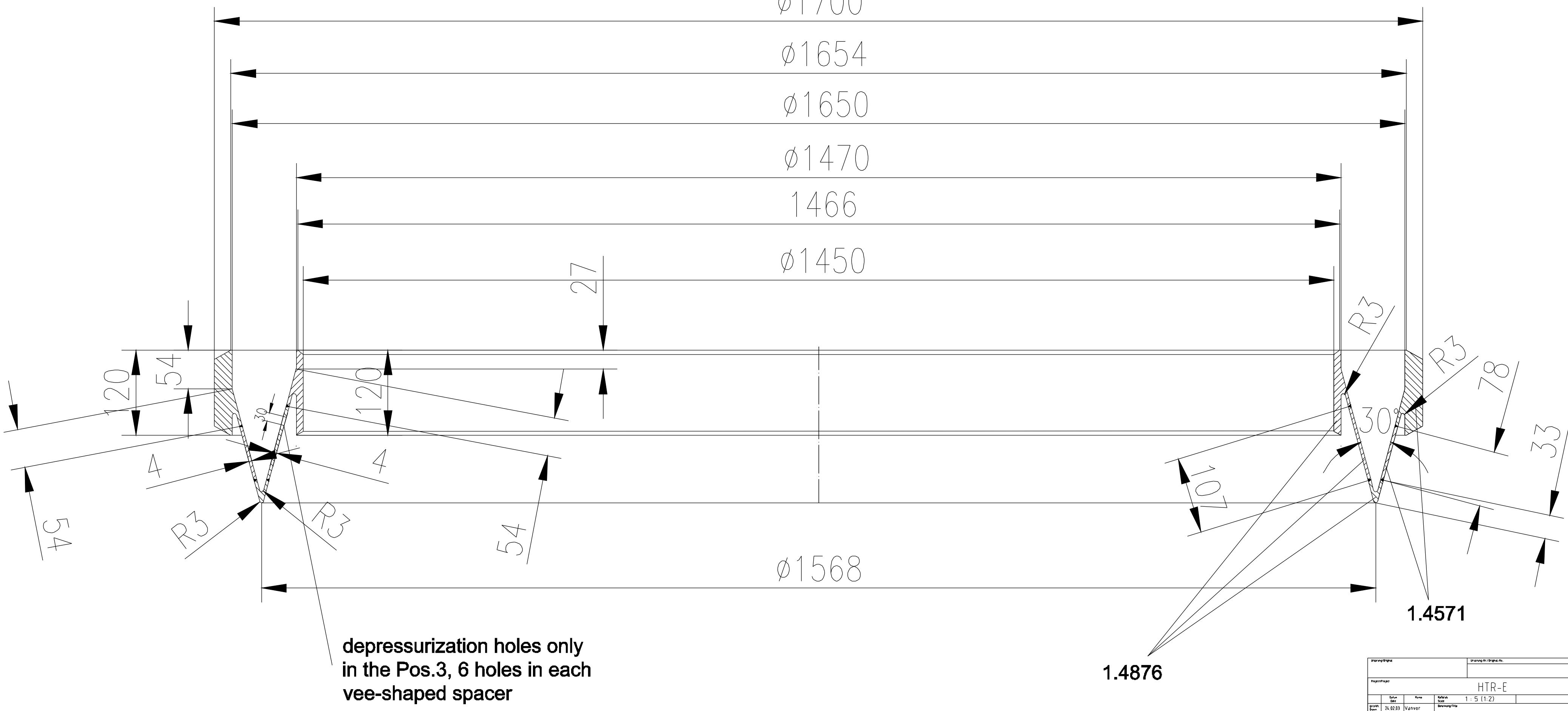

Ursprung/Original		Ursprung-Nr./Original-No.		Urspr.-PKZ-Nr. Orig.-PC
Projekt/Project		HTR-E		PKZ/PC ZFY116
	Datum Date	Name	Maßstab Scale 1 : 5 (1:2)	UA / DCC XK09 Type of Doc.
gezeichn. Drawn	24.02.03	Vanvor	Benennung/Title: Continuous Horizontal Hot Gas Duct For GT-MHR Reactor Design Deliverable 7b of WP1 Detail Drawing	Inhaltskennzeichen Contents Code 0S1600
bearb. Coord.	24.02.03	Vanvor		
geprüft Checked				
Abtlg. Dept.	NGPS3			Zähl.-Nr. Reg.No. --
FRAMATOME ANP		Dienstst./Dept. NGPS3	UNIQ 0600191641	Index/Rev. -- Version --
ZFY116-NGPS3-00-003328		Ang.-Var./Offer-Var. --	Var./Opt. --	Blatt-Nr./Page-No. --
Erstellt mit / designed with: AutoCAD		Ersatz für Supersedes	in EDDA as PDF	

Maße nicht abgreifbar/Not to Scale

Pos. 4, 5, 6
scale 1:2

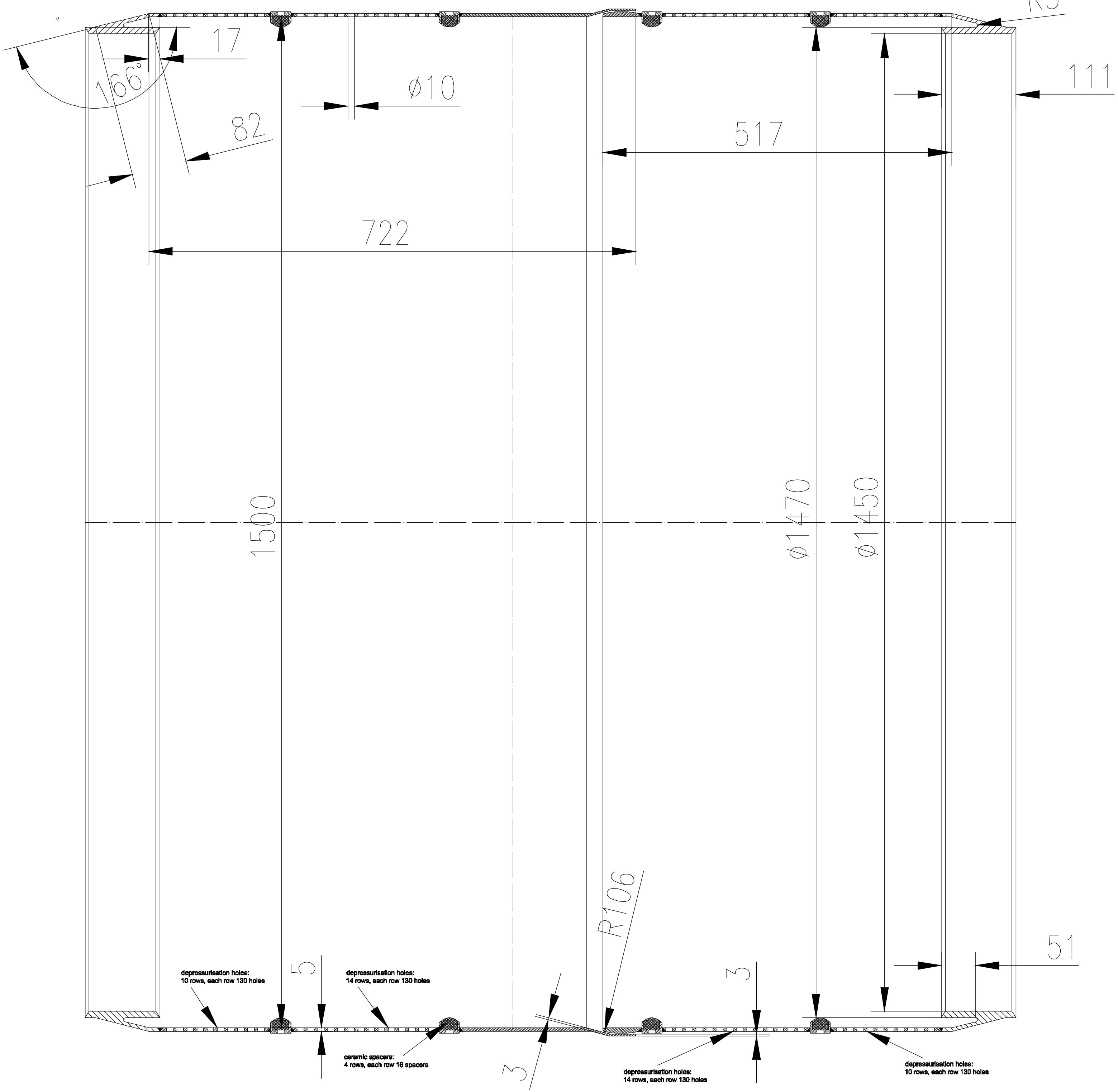

Ursprung/Original	Ursprung-Nr./Original-No.		Urspr.-PKZ-Nr. Orig.-PC
Projekt/Project	HTR-E		PKZ/PC ZFY116
Maßstab Scale	1 : 5 (1:2)		UA / DCC XK09 Type of Doc.
gezeich. Drawn	24.02.03	Vanvor	Inhaltskennzeichen Contents Code 0S1600
bearb. Coord.	24.02.03	Vanvor	
geprüft Checked			
Abtlg. Dept.	NGPS3		Zähl.-Nr. Reg.No. --
Benennung/Title	Continuous Horizontal Hot Gas Duct For GT-MHR Reactor Design Deliverable 7b of WP1 Detail Drawing		
FRAMATOME ANP	Dienststelle/Dept. NGPS3	UNQ 0600191658	Index/Rev. -- Version --
ZFY116-NGPS3-00-003329	Ang.-Var./Offer-Var. --	Var./Opt. --	Blatt-Nr./Page-No. --
Erstellt mit / designed with: AutoCAD	Ersatz für Supersedes	in EDDA as PDF	

Maße nicht abgreifbar/Not to Scale

Attachment 2

HTR Hot Gas Duct Configuration Trade-off Doc.N0 092-110-E-00002

EUROPEAN COMMISSION

Project:	**HIGH TEMPERATURE REACTOR COMPONENTS AND SYSTEMS (HTR-E)**

Title:	**HTR Hot Gas Duct Configuration Trade-off**

Document No:	**092-110-E-M-00002**	Issue: **0**
Purpose of issue: Information and Comments		Date: 22/09/03

Prepared: MAB, ABP

Reviewed: AOM

Approved: MDB

EMPRESARIOS AGRUPADOS

EMPRESARIOS AGRUPADOS INTERNACIONAL, S.A.

Magallanes, 3 28015 Madrid - España

CLASSIFICATION

Contains information for the design of structures, systems or components: Yes ☐ No ☒

Design verification : Not applicable ☒ Head of OU/Supervisor ☐ Verifier Level 1 ☐ Level 2 ☐

CONTROL OF MODIFICATIONS

Issue	Modifications
0	Preliminary issue

PRELIMINARY OR PENDING INFORMATION

Issue	Paragraphs	Subject	Status

DISTRIBUTION

External	Internal	No. copies/Format
	MDB, AOM, ABP, MAB, AGD	1/ Hardcopy

CONTENTS

Page No.

LIST OF ABBREVIATIONS

GT-MHR	Gas Turbine – Modular Helium Reactor
He	Helium
HP	High Pressure
HTR	High Temperature Reactor
LP	Low Pressure
PBMR	Pebble Bed Modular Reactor
PCU	Power Conversion Unit

1. PURPOSE

The purpose of this document is to present the trade off of the HTR hot gas duct.

The studies performed cover the different configurations for spacers between the support tube and the liner. In these studies, some alternatives for the components that serve as a filter during He pressure drop have been considered.

This report is Empresarios Agrupados' contribution to Deliverable 7b, "Thermal insulation of the turbine inlet" of HTR-E, WP1, "Turbine".

2. INTRODUCTION

The hot gas duct is part of the reactor Power Conversion Unit (PCU). It is the component that connects the HTR Module Reactor and the helium turbine.

The purpose of the hot gas duct is to conduct the high temperature helium coming out of the reactor core to the helium turbine and to feed the reactor with helium coming from the PCU Recuperator. It should be isolated in order to minimise thermal losses (improving cycle efficiency) and to limit the maximum material operating temperature.

The hot gas duct reference design · proposed by Framatome ANP Refs 1 and 2- consists of two coaxial ducts. High temperature helium flows through the inner part of the duct of minimum diameter, from the reactor to the turbine. The feed helium flows through the region limited by both the inner and outer ducts, from the recuperator to the reactor. The helium operating pressure is approximately the same in the "hot-gas side" and the "cold-gas side". Therefore, only the outer duct is part of the pressure boundary.

The advantage of this design is that the duct conducting the high temperature helium is not part of the pressure boundary. As a result, the material of this duct, working at temperatures over 800ºC, will not be subjected to the design pressure and will only be subjected to relatively small pressure differences during transient conditions. The analyses performed and reported in this document only refer to this inner duct of the hot gas duct. The outer duct is outside the scope of this study.

3. CALCULATION HYPOTHESES

3.1 REFERENCE HOT GAS DUCT

The different analyses have been carried out using a reference hot gas duct with the following geometrical characteristics (Ref. 2):

- Outside diameter of the support tube (cold duct side) De = 1700 mm
- Inside diameter of the liner (hot duct side) Di = 1450 mm
- Thickness of the support tube Te = 25 mm
- Thickness of the liner Ti = 10 mm
- Duct material $\Rightarrow$ Alloy 1.4876 or 1.4571

3.2 MATERIAL PROPERTIES

3.2.1 Metal Parts

The different metal parts of the hot duct are made of alloy 1.4876 or 1.4571, the properties of which are similar. Table 2-1 below shows their properties at different temperatures (Ref 4):

Table 2-1

Temp (ºC)	K (W/m K)	α (1/K)	Cp (J/kg K)	φ (kg/m^3)	E (MPa)	$Rp_{0.2}$ (MPa)
200	17	17 E-6	0.49	7850	186 E+9	150
400	20	18 E-6	0.52	7850	172 E+9	125
600	22.5	19 E-6	0.59	7850	155 E+9	115
850	26	19.5 E-6	0.63	7850	120 E+9	84

3.2.2 Insulating Material

A Saffil type material has been considered as insulation between the hot and cold duct sides. It is formed of ceramic fibres containing 95% Al_2O_3.

Ref 1 gives the equivalent thermal conductivity values measured for this material with a packing density of 160 kg/m^3 in an He fluid at 40 bar. These values are shown in Table 2-2 below:

Table 2-2

Temp (ºC)	400	600	800	1000
K (W/mK)	0.296	0.465	0.571	0.682

In accordance with Ref 2, a single equivalent conductivity value of 0.55 W/mK is used in the calculations.

The equivalent thermal conductivity value mainly affects the total heat transmitted in the hot duct and includes the material thermal conductivity, the convection and the radiation present during the test.

3.3 LOAD CASES CONSIDERED

In accordance with Ref 3, the maximum loads to be considered in the design of the hot duct will be based on the following events:

- Normal operating conditions ⇒ Conditions in accordance with section 3.3.1
- Thermal and pressure transient loads ⇒ Conditions in accordance with section 3.3.2

3.3.1 Normal Operating Conditions

The following are the He conditions considered on the "hot-gas" and "cold-gas" sides of the hot gas duct during normal operating conditions (Ref 2):

Hot gas side

- Helium temperature ⇒ 850ºC
- Helium pressure ⇒ 70.8 bar
- Helium mass flow ⇒ 316.19 kg/s

Cold gas side

- Helium temperature ⇒ 488ºC
- Helium pressure ⇒ 71.6 bar
- Helium mass flow ⇒ 318.2 kg/s

3.3.2 Thermal and Pressure Transient Loads

According to Ref. 3, the maximum transient loads to be considered are:

- Maximum temperature gradient of cold gas side He ⇒ ΔT = -23ºC/s for 8.83 s, starting from the operating conditions
- Maximum pressure gradient of cold gas side He ⇒ ΔP = 1.0 MPa/s for 7 s, starting from the operating conditions.

3.4 PRESSURE DROP IN THERMAL INSULATION

The hot duct pressure drop events will start a process to remove the He stored in the space occupied by the thermal insulation. It must be borne in mind that the thermal insulation occupies less than 10% of the total volume, so the remaining volume will therefore be occupied by He.

To evaluate the pressure differences between the hot gas side (thermal insulation chamber) and the cold gas side He, the pressure drop which will take place in the thermal insulation during a pressure drop event must be estimated.

This pressure drop is estimated on the basis of Ref 5 which gives the following values for pressure drop in air at 1 bar for each metre length of insulation:

- Compacted fibres → ΔP (N/m^2) ≈ 680 $V^{1.097}$ (V → Velocity of the air m/s)
- Tissues or wrapped fibres → ΔP (N/m^2) ≈ 600 $V^{1.155}$ (V → m/s)

These pressure drop values have been compared to the pressure drop values provided by the manufacturers of glass fibre materials used in filters and the results were similar to those obtained with the formulae.

These are only approximate values as there will be different factors to take into account, such as the extent to which the insulating material is compacted. In any event, we shall consider these pressure drop values to be multiplied by an increase coefficient of four (4) in order to perform conservative pressure drop calculations.

To extrapolate the values of pressure drop in air to values of pressure drop in He at pressures other than 1 bar and different temperature values, we shall consider a pressure drop value multiplied by the ratio of densities between the He and the air (≈1 kg/m^3).

3.5 He VELOCITY DURING PRESSURE DROP

The hot duct pressure drop events will start a process to remove the He stored in the space occupied by the thermal insulation. The following formula has been used to evaluate the velocity of He discharge during these events:

$$\frac{P_1}{P_2} = \left(\frac{d_1}{d_2}\right)^k \qquad \frac{T_1}{T_2} = \left(\frac{d_1}{d_2}\right)^{k-1} \qquad \frac{P_2}{d_2^{\,k}} = C$$

where:

- Point (1) is the initial state and point (2) is a state during the pressure drop event
- $P_{1,2}$ → pressure
- $T_{1,2}$ → temperature
- $d_{1,2}$ → density
- K = 1.666 (Cp/Cv of the He)

If during the pressure drop event we consider the following calculation data:

- Variation in pressure over time ⇒ $\partial P = \frac{\Delta P}{\Delta t}$ (Pa/s)
- Flow area in He discharge ⇒ As (m^2)
- Volume of He enclosed in the isolation chamber ⇒ Vo (m^3)
- He discharge flow ⇒ q_2 (kg/s)

With these data, the He discharge velocity (V_2) as it passes through the flow area As is calculated as follows:

$$\frac{\partial d_2}{\partial t} = \frac{\partial P}{C \times K \times d_2^{K-1}} \qquad q_2 = \frac{\partial d_2}{\partial t} Vo \qquad As \times V_2 = \frac{q_2}{d_2}$$

$$V_2 = \frac{Vo}{As} \frac{\partial P}{K \times P_2}$$

00 YYX 10302 -37 Issue 1

4. CONNECTING SPACERS BETWEEN SUPPORT TUBE AND LINER

4.1 GEOMETRICAL CONFIGURATIONS STUDIED

To connect the support tube structure and the liner, a metal spacer is installed which ensures that:

- The thermal dilations between the external support tube and the liner are compatible, so that the stresses on the connection are as low as possible
- A solid stiff connection is established between the external support tube and the liner

Three types of connecting spacers have been studied, as defined in Figures A, B and C of Appendix A. The geometrical and manufacturing characteristics of each of the connecting spacers are described below.

4.1.1 Type A — V-shaped Spacer (Reference Design)

- 4 mm-thick metal plate, forming a single V-shape part
- Each of these spacers is machine form forged. The machined part includes part of the support tube and the liner
- The dimensions considered are shown in Figure A of Appendix A

4.1.2 Type B — 2L-shaped Spacers

- Formed by a 5 mm thick cylindrical plate. This plate is connected to the liner by means of a 10 mm thick perpendicular plate and to the support tube by means of an 8 mm thick perpendicular plate
- The three plates which comprise the spacer are manufactured from cut plates which are welded together
- The spacer is connected to the liner and the support tube by means of welds
- The dimensions considered are shown in Figure B of Appendix A

4.1.3 Type C — LCL-shaped Spacer

- Formed by two 5 mm and 8 mm thick cylindrical plates. These plates are connected to the liner by means of a 10 mm thick perpendicular plate and to the support tube by means of an 5 mm thick perpendicular plate
- The plates which comprise the spacer are manufactured from cut plates which are welded together
- The spacer is connected to the liner and the support tube by means of welds
- The dimensions considered are shown in Figure C of Appendix A

4.2 THERMAL STRESSES ON THE SPACERS

4.2.1 Stress States in Normal Operating Conditions

Three types of spacers for a hot duct configuration have been analysed defined by the following:

- Geometry of the support tube and liner in accordance with the data given in section 3.1
- Thermal conductivity of the insulation between the support tube and liner in accordance with section 3.2.2
- Temperature of 488ºC considered on the external face of the support tube in accordance with section 3.3.1
- Temperature of 850ºC considered on the internal face of the liner in accordance with section 3.3.1

A finite element model has been built of each of the three types of spacers and thermo-mechanical analyses have been performed to obtain the maximum stress states on the spacers. The finite element models are illustrated in Figures 1, 4 and 7 of Appendix B.

The maximum stress and temperature values obtained on the three types of spacers are given in Table 3-1 below.

Table 3-1

Point		Type A	Type B	Type C
1	S (MPa)	353	370	382
	T (ºC)	550	550	550
2	S (MPa)	290	240	250
	T (ºC)	620	750	750
3	S (MPa)	200	100	170
	T (ºC)	820	820	820

Figures 2, 5 and 8 of Appendix B show the temperature distribution in each one of the three spacer configurations. Figures 3, 6 and 9 show the stress distribution in each one of the three spacer configurations.

Analyses of other geometrical configurations have been carried out and the following results obtained:

- Double-A configuration (Figure 10, Appendix B) ⇛ The resulting stress state is similar to that obtained with the Type A configuration
- Double-C configuration (Figure 11, Appendix B) ⇛ The resulting stress state is similar to that obtained with the Type C configuration
- Configuration Type B, with curved ends (Figure 12, Appendix B) ⇛ The stress state obtained in this configuration is more critical than that in configuration Type B

The following conclusions can be derived from the stress analyses carried out for normal operating conditions:

- Considering a maximum allowable secondary stress limit of 2 x Rp_{02}, the stress states obtained at different temperatures are higher than these maximum value
- This means that the material will suffer slight permanent/plastic deformations which will accumulate with the hot duct thermal cycles
- The maximum allowable number of thermal cycles subject to fatigue for this stress level can be estimated as $n > 10^5$ cycles, in accordance with ASME III Division 1-NH (Figure T-1420-1B)

- Since the allowable number of thermal cycles subjected to fatigue $n>10^5$ is far greater than the foreseen startup and shutdown number of cycles during the plant lifetime, it is considered that no cracks will appear in the different metal parts of the hot duct due to material fatigue

4.2.2 Stress States during Thermal Transients

Stress analyses have been carried out for the most unfavourable thermal transient load case, indicated in section 3.3.2. The following have been considered in these transient analyses:

- Variation in the external He temperature of ΔT = -23ºC/s (hot side) for ≈9 s. At the end of the transient, the He temperatures considered are ≈650ºC on the hot side and ≈375ºC on the cold side
- It has been considered that the He flow is maintained during the thermal transient, imposing He-wall heat exchange coefficients of ≈1500 W/m^2K in the hot duct and ≈1300 W/m^2K in the cold duct
- A thermal transient of 310 s was analysed so that after the first 9 s the external He temperature is kept constant, both on the hot side and the cold side

The analyses of the thermal transients for the different hot duct configurations A, B and C produced similar results:

- During the ≈9 s thermal transient, the following wall temperature variation values were produced: liner 850ºC → ≈845ºC; support tube 488ºC → ≈460ºC
- A period of time in excess of 300 s is required to raise the temperature of the pipe walls to a temperature close to that of the external He
- The maximum stress states on the metal connecting part are obtained approximately 200 s after the transient begins. The maximum stress states reached in the cold part of the connecting spacers increase by approximately 75-80% with respect to the stresses in normal operating conditions. The maximum stresses on the hot part of the connecting spacers are maintained approximately the same as the values obtained for normal operating conditions

The maximum stress states reached during thermal transients for the three types of spacers is S ≈650 MPa at a maximum temperature of about 550ºC.

This thermal stress state is more critical than that obtained during normal operating conditions. Therefore the accumulated deformation in the metal spacer would increase with these types of events.

Taking into account that the connecting spacer is axisymmetrical, the deformation and the thermal loads are also axisymmetrical. The deformation will practically have no effect on either the liner or the support tube because the stress states on these components are lower than the maximum values obtained.

The maximum allowable number of thermal cycles subject to fatigue for these levels of maximum stresses and temperatures obtained in the thermal transients can be estimated as $n > 500$ 1000 cycles, in accordance with ASME III Division 1-NH (Figure T-1420-1B).

If the number of cycles (n) is exceeded, small fissures may appear in the metal connecting part. This will not cause any significant problems, as long as the cracks are not big enough to considerably diminish the stiffness provided by the metal connecting spacer.

4.3 STRUCTURAL STIFFNESS OF THE SPACERS

The stiffness of each of the different types of connecting spacers have been analysed.

The stiffness is calculated under the following conditions:

- The radial displacement of the external face of the support tube is restricted
- To obtain the radial stiffness, a unit radial displacement is introduced into the liner and the axial displacement is restricted. The radial reaction between the liner and the metal spacer is obtained
- To obtain the axial stiffness, a unit axial displacement is introduced into the liner and the radial displacement is restricted. The axial reaction between the liner and the metal spacer is obtained

The following are the stiffness results obtained for the three types of connecting spacer analysed:

Stiffness	Type A	Type B	Type C
Radial (N/m)	2.8 E+9	7.3 E+9	8.1 E+9
Axial (N/m)	3.0 E+9	5.0 E+9	2.5 E+9

If we take the axial stiffness of the duct as the most representative stiffness, we can see that a Type B connection is practically equivalent to the double-A or double-C type connections.

4.4 HEAT TRANSFERRED THROUGH THE INSULATION

An analysis has been carried out of the heat transmitted through the insulating wall (thermal losses) between the liner and the external support tube, based on the following calculation conditions:

- Temperature of the external face of the support tube ⇒ 488ºC
- Temperature of the internal face of the liner ⇒ 850ºC
- Thermal conductivity of the insulation K = 0.55 W/mK
- Conductivity of the metal parts ⇒ see section 3.2

The analysis of the heat transferred has been carried out for a meter length hot gas duct, with the metal spacer centred in that portion of the duct. The results of the heat transferred for each of the different types of spacers are provided in the following table:

Type A	Type B	Type C	Type Double A	Type Double C
10.3 kW/m	12.0 kW/m	11.8 kW/m	11.0 kW/m	—

It can be seen that Type B spacers transmit 16% more heat than Type A spacers and 10% more than double-A type spacers.

4.5 CONCLUSIONS FOR THE DESIGN OF THE SPACERS

The following conclusions can be derived from the analyses of the different types of metal connection spacers between the support tube and the liner:

- From the manufacturing point of view, the Type A connection requires machining of the metal connecting parts. On the other hand, connection Types B and C would be formed by cut plates welded together and in turn welded to the support tube and the liner
- From the point of view of maximum thermal stresses, the three types of connections give similar stress results
- For spacer Types B and C, the stress states on the connections with the support tube and the liner are low, which means it would be acceptable to weld them together
- From the point of view of stiffness, the Type B connection is the stiffest, being equivalent to a double-A or double-C type connection
- From the point of view of heat transferred through the insulating wall (thermal losses), the Type A connection gives better thermal insulation compared to the other types of connections

5. FIBRE FILTERING DURING PRESSURE DROP

5.1 GEOMETRICAL CONFIGURATIONS OF FILTERS STUDIED

Sudden external He pressure drop events can give rise to the entrainment of insulation fibres from the thermal insulation chamber into the hot duct. To prevent this, a filter system shall be installed which guarantees that:

- The thermal dilations between the external support tube and the liner are compatible, so that the stresses on the connecting part are as low as possible
- Insulation fibres are prevented from getting inside the hot duct

Two types of filters have been studied and are defined in Figures D and E of Appendix A. The geometrical manufacturing characteristics of each of the filters are described below.

5.1.1 Type A Filter — (Reference Design, Ref 2), Figure D, Appendix A

- The thermal insulation is separated from the liner by a 5 mm thick, perforated internal pipe which is welded to a machined part installed in the liner
- Axial thermal deformation is made compatible by allowing the axial dilation of the 5 mm pipe in a contact area between the two pipe sections (see Figure D, Appendix A). Given the high temperatures (850ºC) of this contact area, it requires very precise machining and surface treatment
- To prevent the entry of fibres in the helium flow, a closed chamber is created between the liner and the 5 mm perforated pipe. This chamber is sealed by machined ceramic rings which are connected to the 5 mm pipe and are in contact with the liner pipe
- The chamber is approximately 20 mm thick and reduces the space occupied by the thermal insulation. A comparison of filter Type A with filter Type B shows that filter Type A will transfer approximately 20% more heat through the hot duct than filter Type B

5.1.2 Type B Filter — Ring-type Filter, Figure E, Appendix A

- The filter is manufactured in the form of a ring, as a part independent of the hot duct. This filter comprises the following parts:

- 5 mm perforated internal and external pipes
- 2 lateral, cut plates on which the perforated pipes are mounted and welded. The filter is installed between the two 5 mm perforated pipes
- Filter formed by wrapped fibre insulation arranged circumferentially and compacted. The filter fibre is separated from the 5 mm perforated pipes by means of metal wire mesh

- The ring-type filter is installed in the hot duct by means of two lateral L-shaped profiles welded to the liner. The joint is made using a flexible temperature-resistant material and screws with axially elongated holes for thermal dilation. Once the screws have been inserted they can be spot welded

5.2 PRESSURE DROP IN THE INSULATING CHAMBER

5.2.1 Type A Filter (Reference Design, Ref. 2)

During He pressure drop events with this type of filter, the maximum pressure drop between the He of the internal thermal insulation chamber and the external He is produced in the gap section located in the contact between the ceramic rings and the liner. The pressure drop in the thermal insulation is considered negligible (see pressure drop with Type B filter).

A finite model was built of a hot duct section with a Type A filter (see Figure 13, Appendix B). Analyses were carried out with this model and the following results obtained:

- If it is assumed that the ceramic rings make contact with the liner before the hot duct is heated to operating temperatures, when these temperatures are reached the liner is displaced in radial direction to a value 5 mm more than that of the ceramic rings due to the different thermal expansion coefficients. Both parts will continue to be in contact and there will be a radial compression force of Fr = 8E+5 N/m between each of the ceramic rings and the liner

- A higher pressure inside the thermal insulation chamber with respect to the cold gas side He (between 1 and 7 MPa) will not cause any significant relative opening between the rings and the liner, especially the outer ceramic ring, which is the ring that retains the pressure

Therefore, assuming contact between the rings and the liner, the cold gas side He pressure drop events will not cause any opening between the ceramic rings and the liner. The thermal insulation chamber could therefore become overpressurised and give rise to unallowable stress states.

Therefore, in order to control the pressure drop process in the insulating chamber, it must be ensured that there is a discharge opening between the ceramic rings and the liner during hot duct operating conditions and during the different thermal transients.

This required discharge opening will have to be calculated to obtain the desired differential pressure in the insulating chamber with respect to outside pressure, so as to produce acceptable stress states.

5.2.2 Type B Filter

To calculate the pressure drop inside the thermal insulation during He pressure drop events in accordance with section 3.4, the following values were used:

- Variation in maximum pressure ⇒ ΔP = 1.0 MPa/s
- Volume of He enclosed between the two spacers ⇒ $Vo \approx 0.7\ m^3$, considering a distance of ≈ 1.6 m between spacers
- Minimum He flow area ⇒ $As \approx 0.2\ m^2$, section between the filter and the wall of the support tube. A length of $Lp \approx 0.2$ m is conservatively considered as maximum length with a minimum flow area section (As)

If we assume that the pressure drop ΔP occurs from normal operating conditions ⇒ P_1 = 7.2 MPa; T_1 = 850ºC; d_1 = 3 kg/m^3, in accordance with section 3.5 the maximum velocity reached by the He in the section As will be V_2 = 0.3 m/s. In accordance with section 3.4 the pressure drop value in the section As for an insulation material length Lp can be estimated as:

$$\Delta P \approx 4 \times Lp \times d_1 \times 680 \times V_2^{1.097} = 0.435\ E\text{-}3\ MPa$$

If we assume that the pressure drop ΔP occurs in low pressure operating conditions ⇒ P_1 = 2.0 MPa; T_1 = 500ºC; d_1 = 1.2 kg/m^3, in accordance with section 3.5 the maximum velocity reached by the He in the section As is V_2 = 1.0 m/s. In accordance with section 3.4 the pressure drop value in the section As for an insulation material length Lp can be estimated as:

$$\Delta P \approx 4 \times L_p \times d_1 \times 680 \times V_2^{1.097} = 0.787\ E\text{-}3\ MPa$$

A similar pressure drop value would be obtained in the fabric insulation (see section 3.4).

As may be seen, the pressure drop value in the insulation can be considered insignificant compared to the value ΔP. It can therefore be ensured that the pressure inside the insulating chamber will be practically the same as the pressure of the cold side gas He during pressure drop events.

5.3 STRESSES ON THE FILTER STRUCTURE

5.3.1 Type A Filter (Ref. 2)

If the joint between the ceramic rings and the 5 mm perforated pipe which supports them is rigid, very high stress states will occur in the ceramic rings due to the different thermal expansion coefficients between the steel and the ceramic material.

The ceramic rings should therefore be connected to the 5 mm pipe in such a way that the joint is not rigid, allowing a different radial displacement between the two components. It would be recommendable that the rings were not continuous, but rather that they were assembled in segments so that dilation of the ceramic material would not produce circumferential stresses.

5.3.2 Type B Filter

The filter is manufactured in the form of a ring, as a part independent of the hot duct.

The fibre fabric which serves as a filter is enclosed within the structure of two metal perforated pipes, which ensures that the filter wrapped fibre will not suffer relative axial displacements due to axial dilation of the hot duct.

The external metal perforated pipe of the filter will reach a temperature different to that of the internal perforated pipe which will generate a stress state between the two pipes. These thermal stress values can be very conservatively estimated as follows:

$$\sigma = \frac{850 - 488}{2} \cdot E \cdot \alpha \cdot \frac{1}{2} \cong 275\ MPa$$

This secondary stress state could cause the material to suffer slight deformations which will accumulate during the startup and shutdown cycles, but they are far from the stress states that can cause cracks due to material fatigue.

The ring-type filter is installed in the hot duct by means of two lateral L-shaped profiles welded to the liner. The joint is made using a flexible temperature-resistant material and screws with axially elongated holes for thermal dilation.

The use of flexible joints between the filter and the connecting part to the liner allows different radial displacements of the liner and the filter structure so that stress states are not generated due to these relative displacements. In addition, these joints must prevent the entrainment of insulation fibres through the joints during He pressure drop events.

6. CONCLUSIONS

Based on the hot gas duct reference design (Ref. 2), thermomechanical calculations have been carried out for the both the normal operating conditions and transients. In particular, the design of the connecting spacers and the behaviour of the thermal insulation was analysed.

Connecting spacers:

Three types of connecting spacers have been analysed (A, B and C), which are defined in Figures A, B and C of Appendix A. Type A being the reference design (Ref. 2).

From the point of view of manufacturing and assembly, spacer Types B and C do not require any kind of special machining and can be welded directly to the support tube and the liner.

From the point of view of mechanical stiffness, spacer Type B is the most rigid with a stiffness comparable to a double-A type spacer or a double-C type spacer.

The maximum stress state on the spacers is reached during the thermal transient event analysed, which gave stress states of the order of 75-80% greater than those in normal operating conditions. This maximum stress state is reached approximately 200 s after initiation of the event.

The maximum stress states can reach values which give rise to cracks in the spacer due to metal fatigue, based on a number of thermal transient cycles of the order of $n \cong 500$ 1000 cycles.

Regarding the heat transferred through the insulation, Type A has better thermal insulation with 10.3 Kw/m of thermal losses.

Fibre filtering:

Two types of filters (A and B) have been studied, as defined in Figures D and E of Appendix A, filter type A being the reference design.

From the point of view of manufacturing and assembly, filter Type B is made as an independent part which is mounted on the liner structure and joined to it by sealed, flexible joints and screwed to parts with elongated holes so that the joint is not subjected to thermally induced forces.

During external He pressure drop events, with the Type B filter there will be no significant differential pressure between the insulating chamber and the external He. With the Type A filter, the differential pressure in the insulating chamber could be significant and it would be necessary to control this pressure drop by ensuring some depressurisation openings.

7. REFERENCES

1. ZFY16-400636724, *Final Report*, Framatome ANP
2. ZFY16-0600191597, *Intermediate Report*, Framatome ANP
3. 092-110-CE-SV-EA-03/0007, *Hot Duct Transient Operating Conditions*
4. ASME III, Parts A, B and C, 1998 Edition
5. *Handbook of Hydraulic Resistance*. 3rd Edition

APPENDIX A

FIGURES

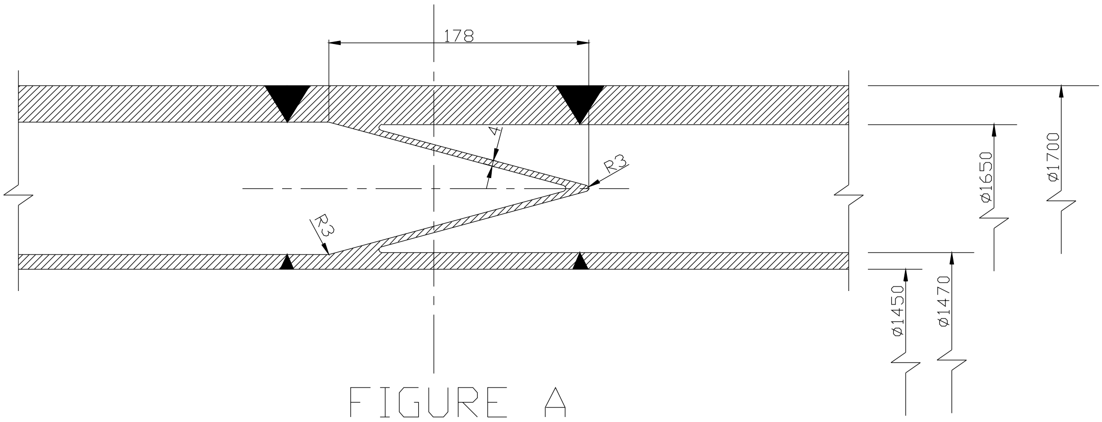

FIGURE A
(TYPE A SPACER)

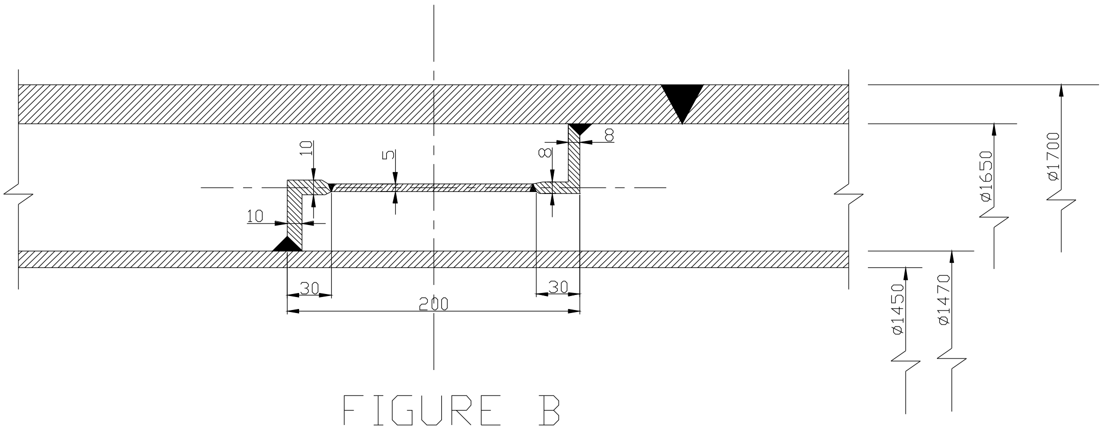

FIGURE B
(TYPE B SPACER)

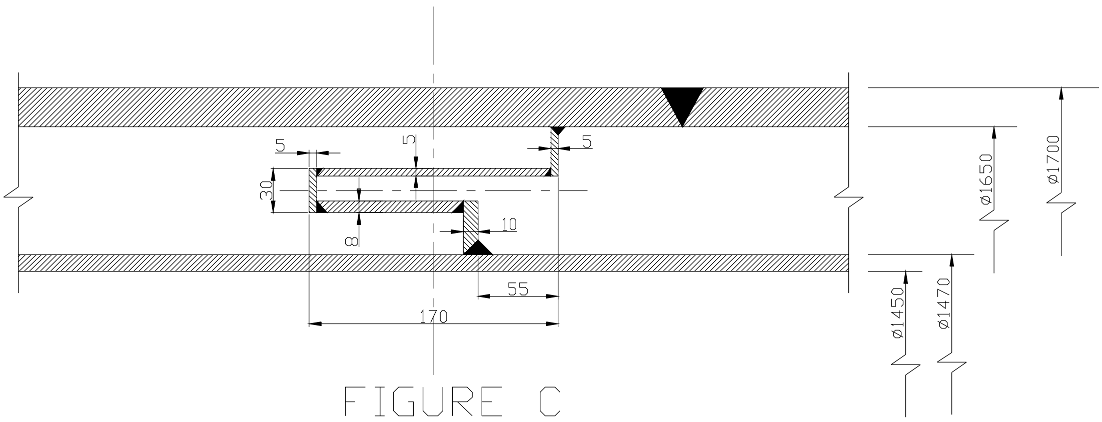

FIGURE C
(TYPE C SPACER)

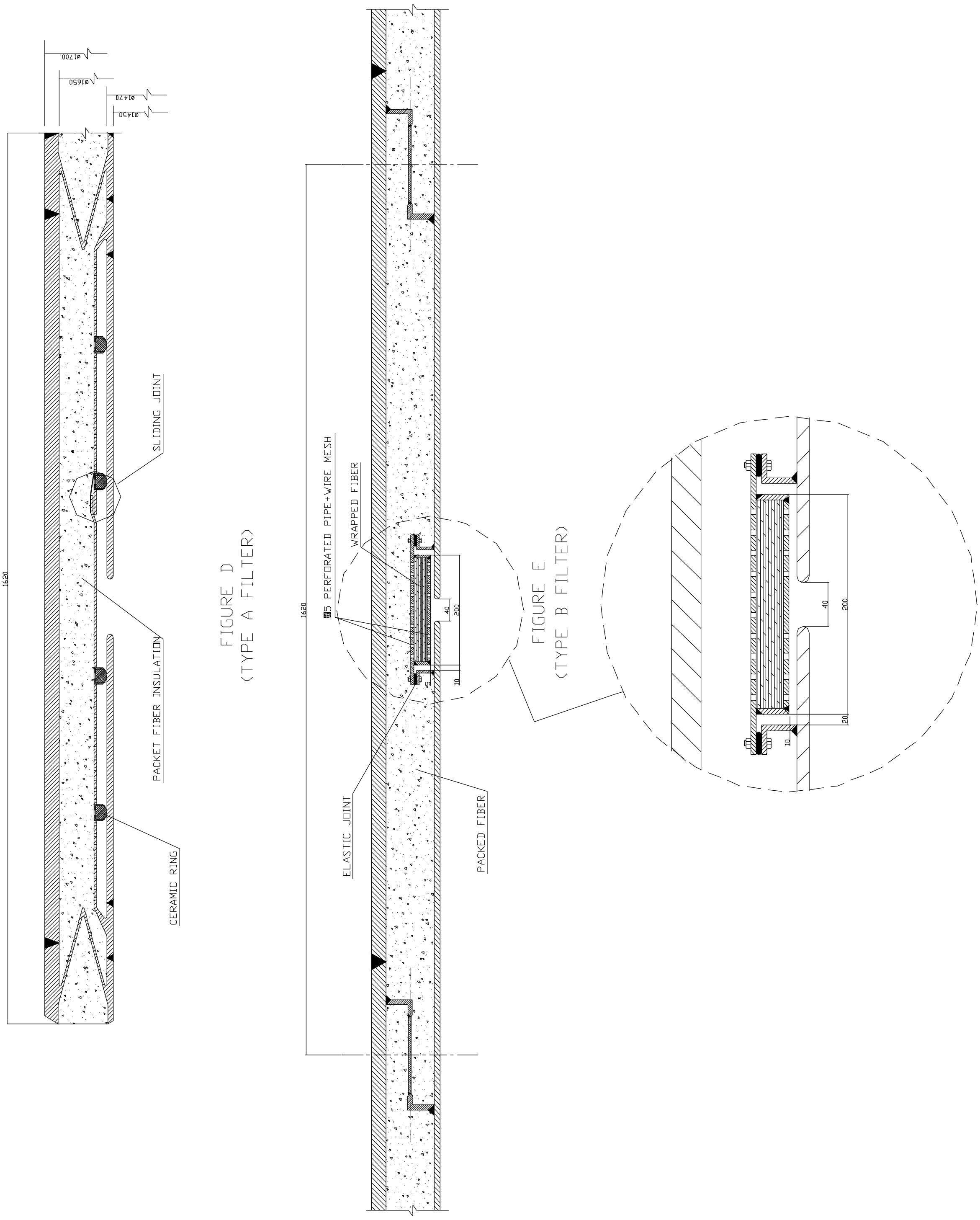
ø1700
ø1650
ø1470
ø1450
1620
SLIDING JOINT
PACKET FIBER INSULATION
CERAMIC RING
FIGURE D
(TYPE A FILTER)
ø5 PERFORATED PIPE+WIRE MESH
WRAPPED FIBER
ELASTIC JOINT
PACKED FIBER
40
200
10
FIGURE E
(TYPE B FILTER)
20

APPENDIX B

F.E.M FIGURES

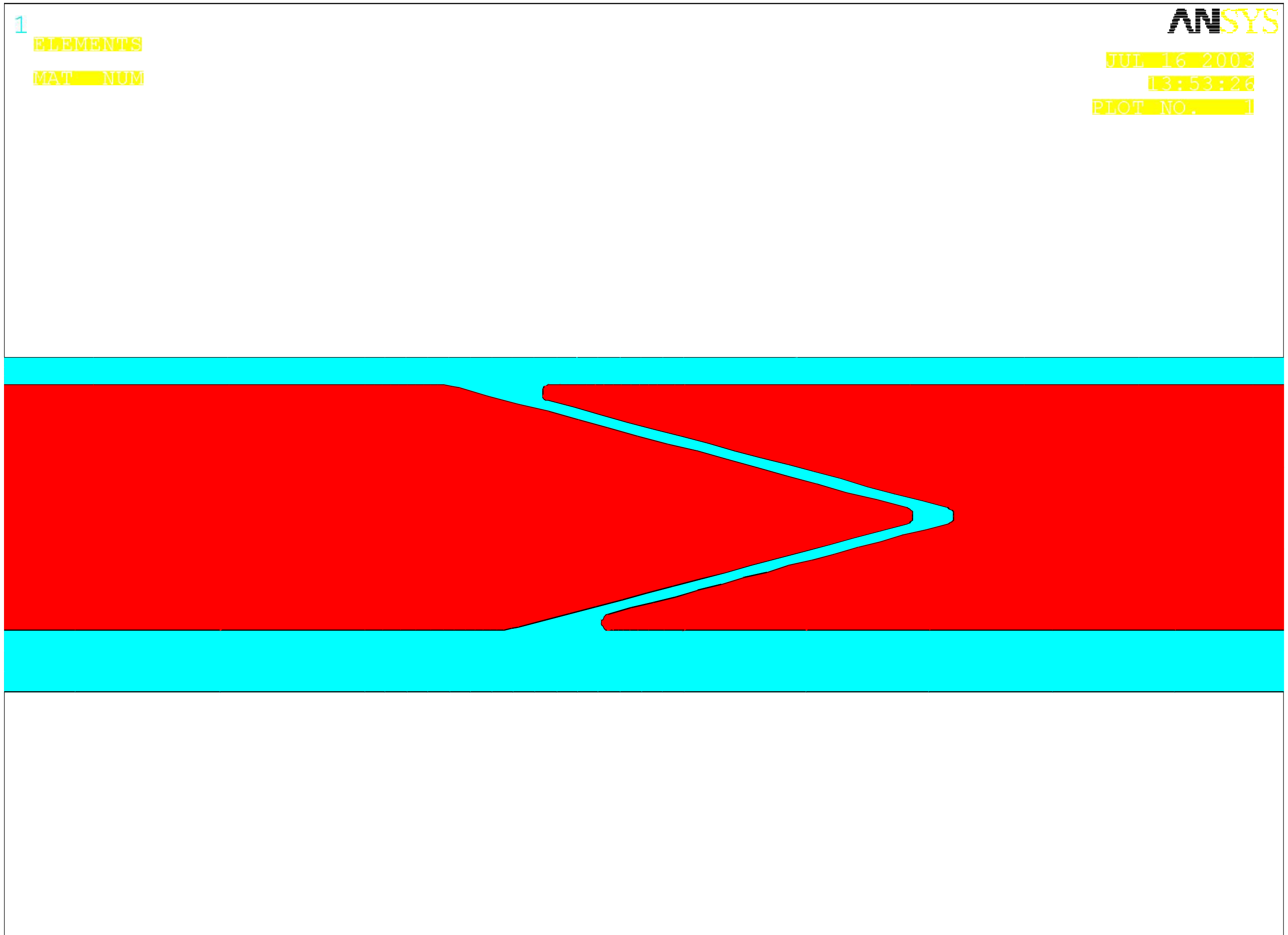

FIGURE 1. TYPE A. F.E.M

00048539

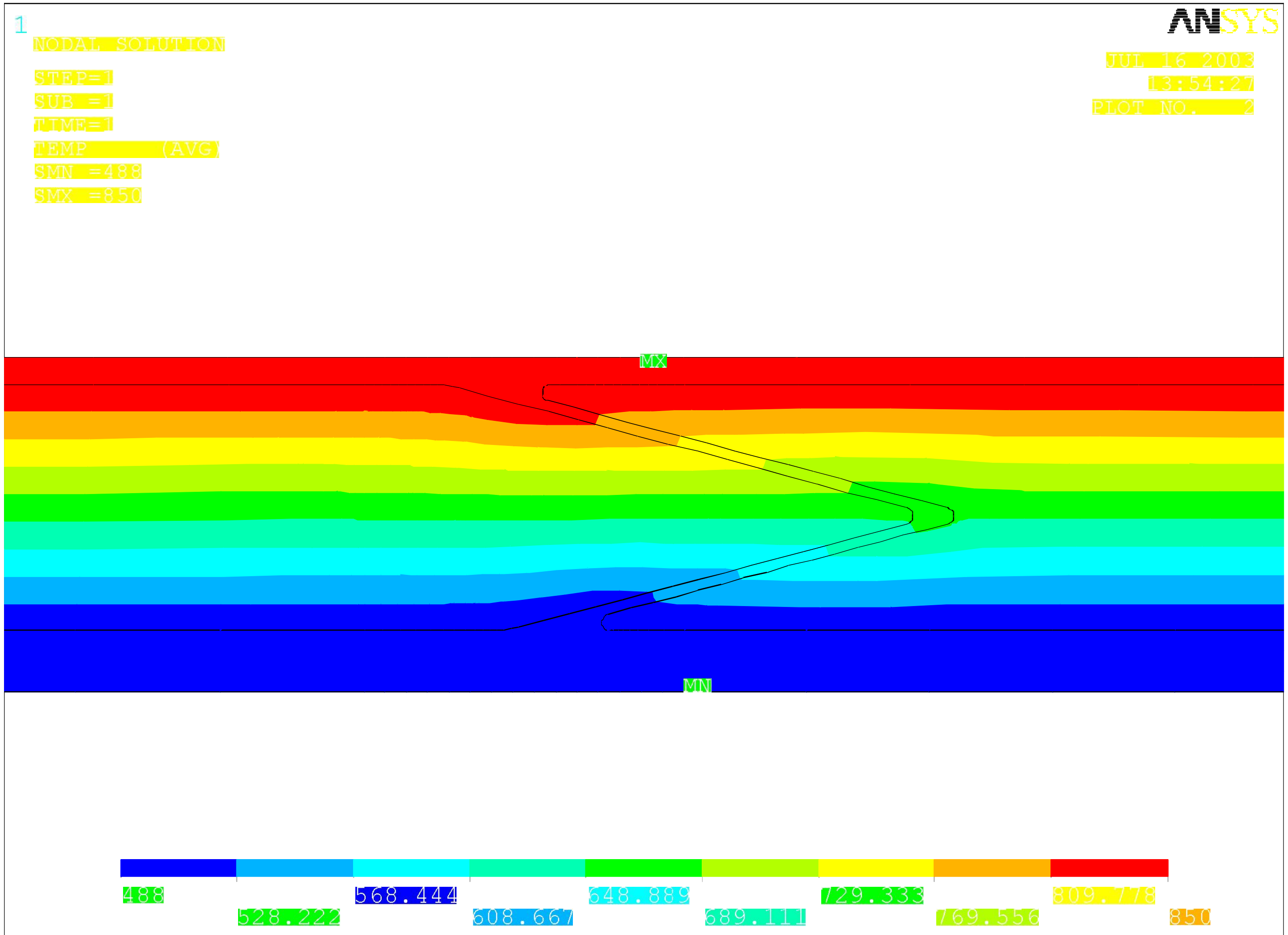

FIGURE 2. TYPE A. TEMPERATURE DISTRIBUTION

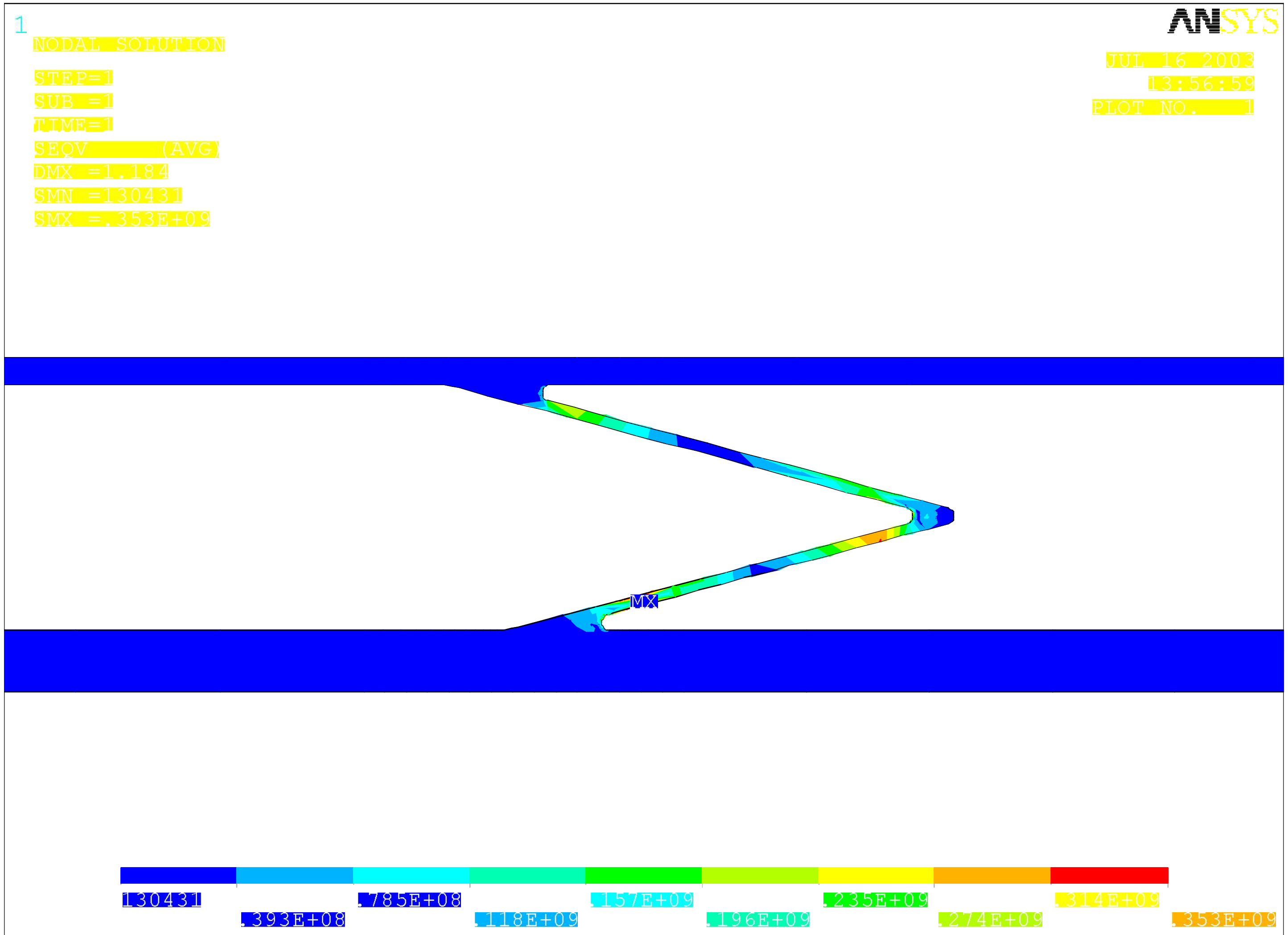

FIGURE 3. TYPE A. STRESS DISTRIBUTION (N/M2)

00048539

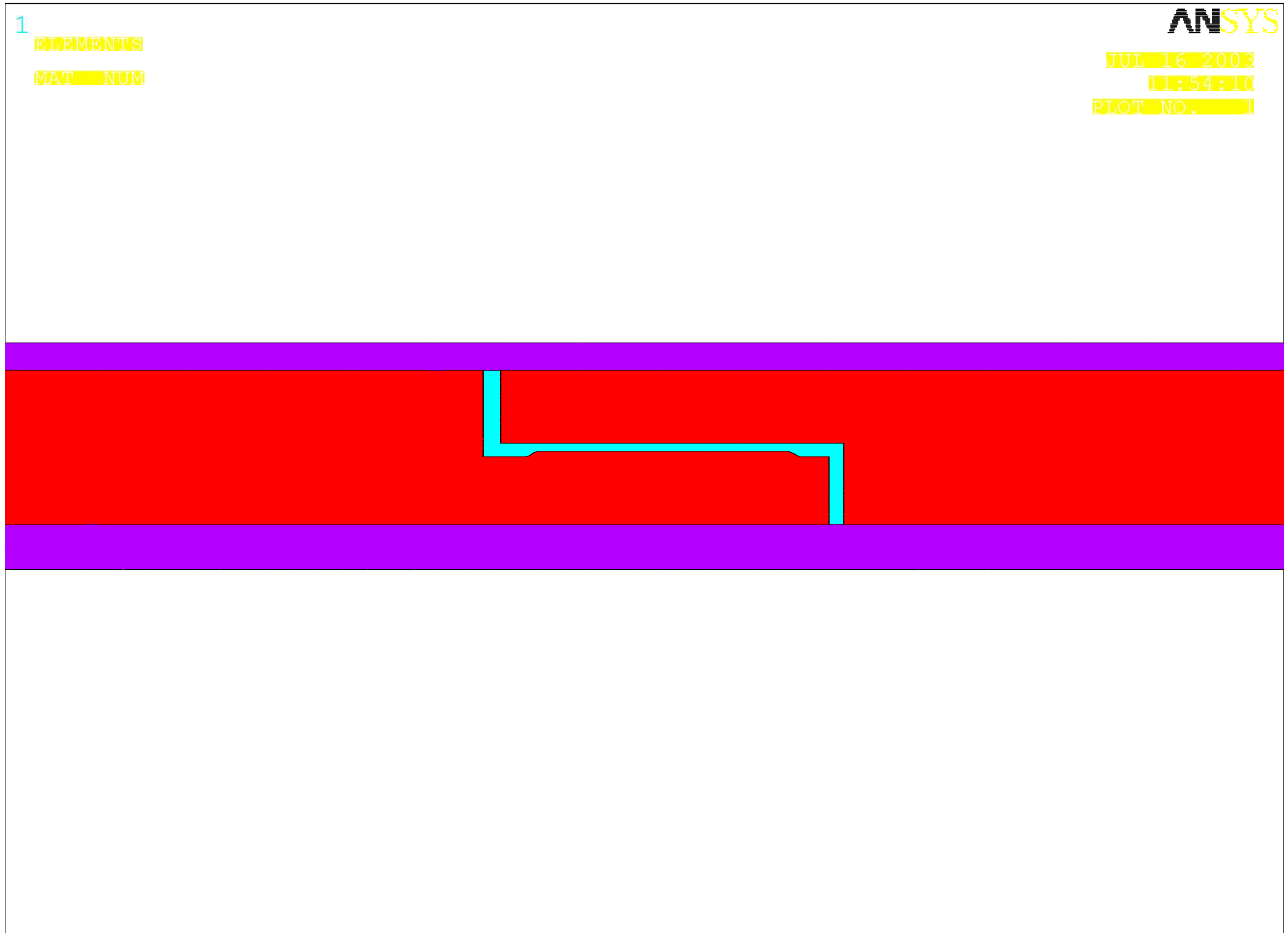

FIGURE 4. TYPE B. F.E.M

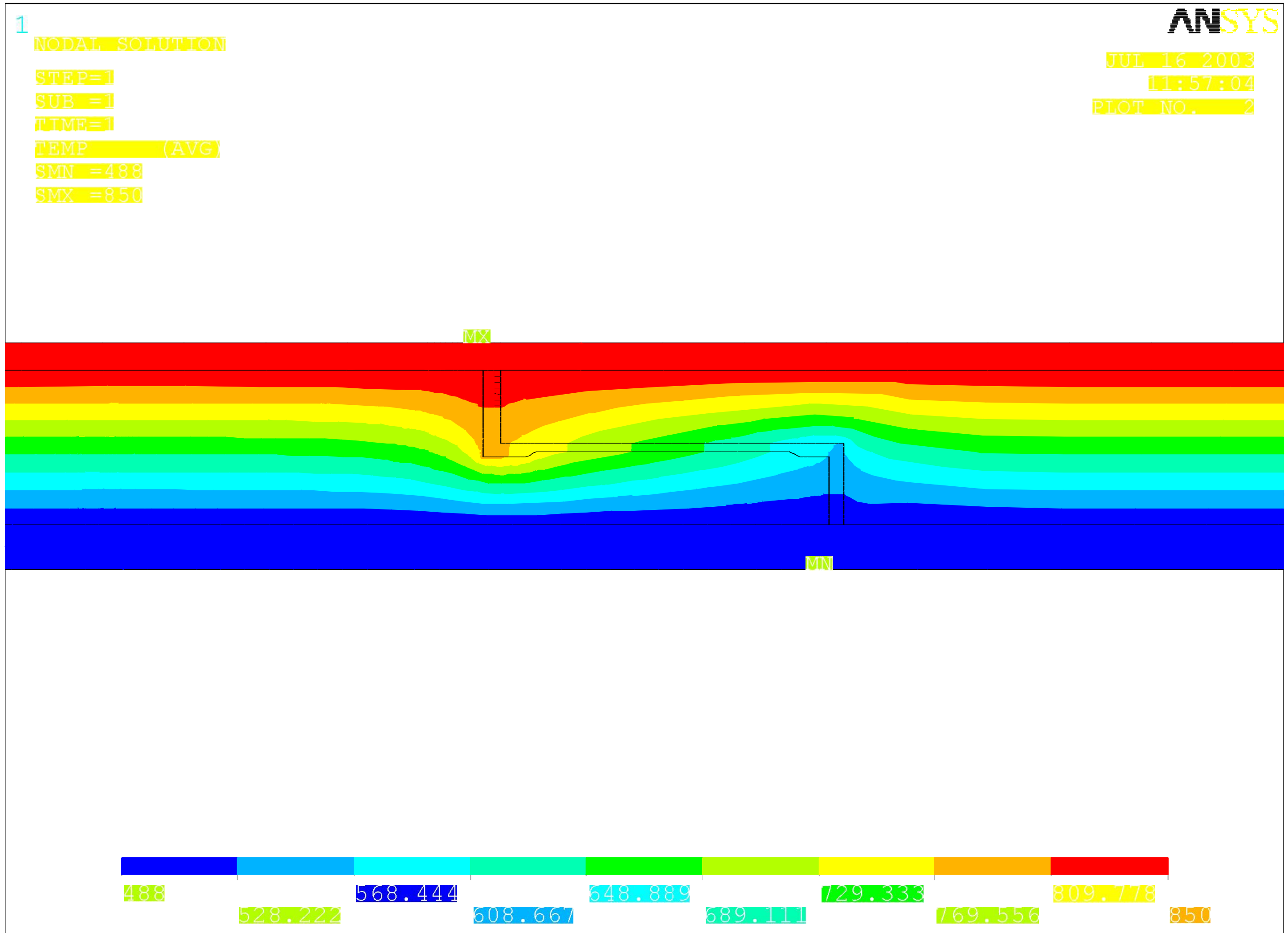

FIGURE 5. TYPE B. TEMPERATURE DISTRIBUTION

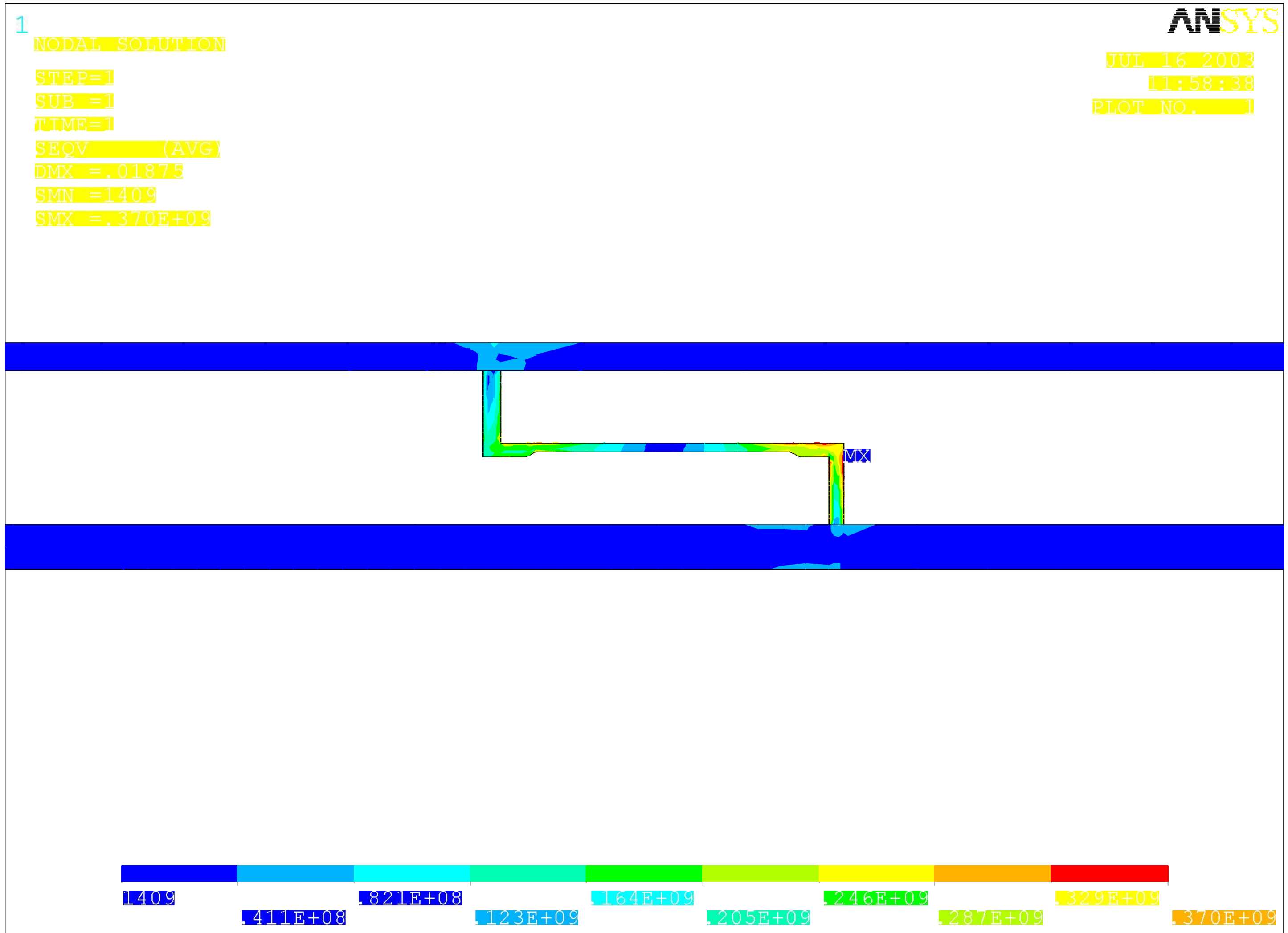

FIGURE 6. TYPE B. STRESS DISTRIBUTION (N/M2)

00048539

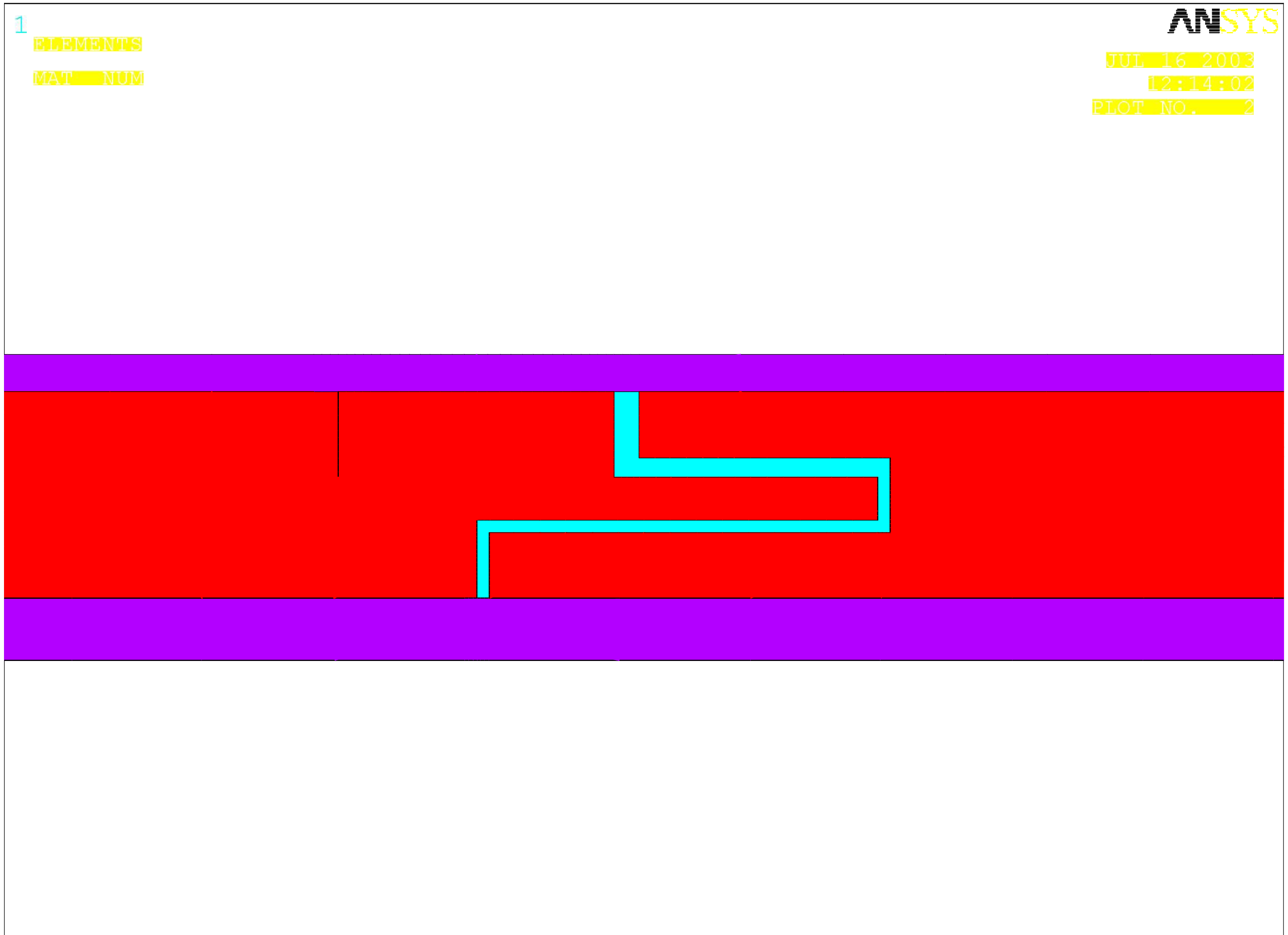

FIGURE 7. TYPE C. F.E.M

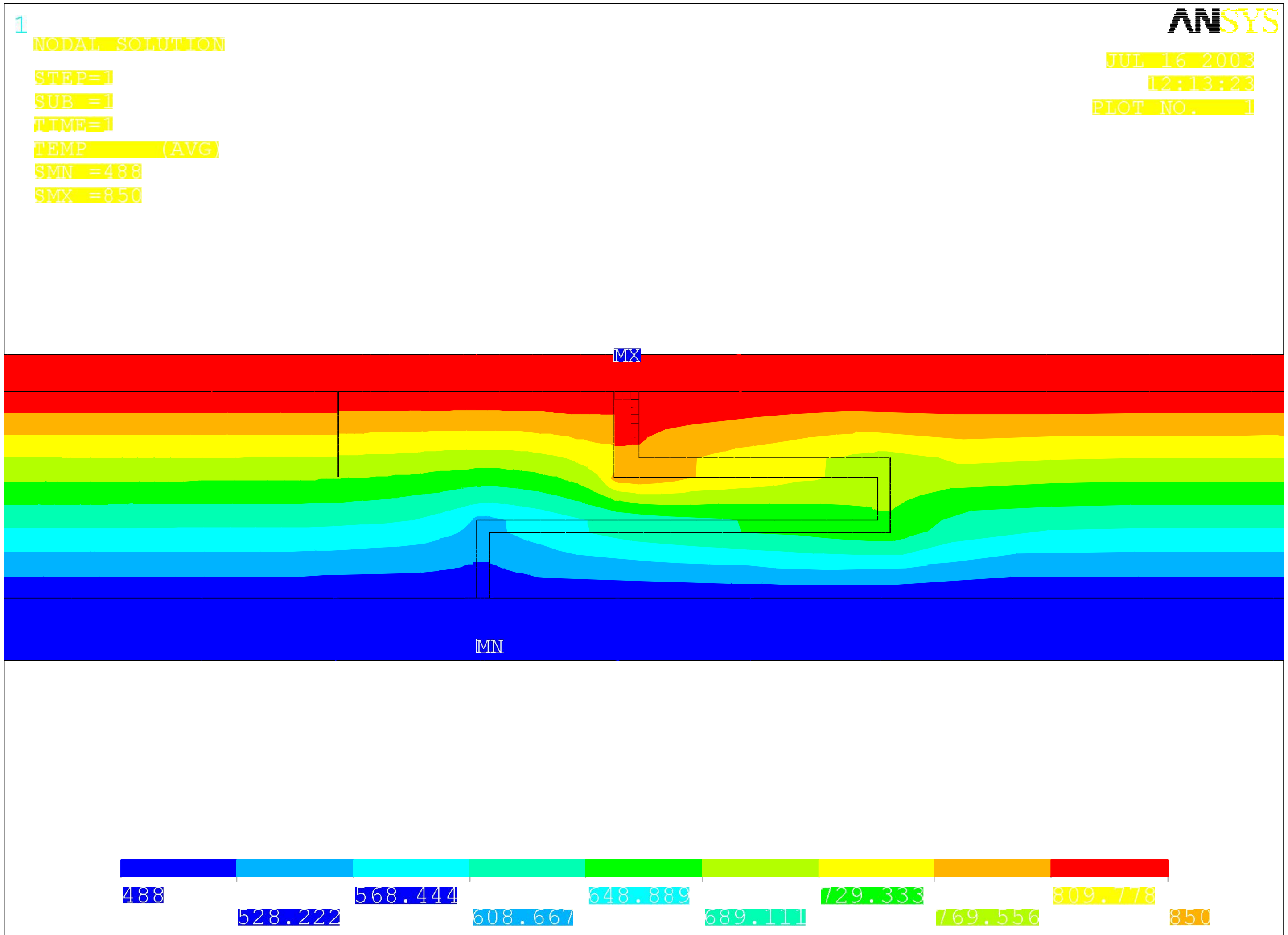

FIGURE 8. TYPE C. TEMPERATURE DISTRIBUTION

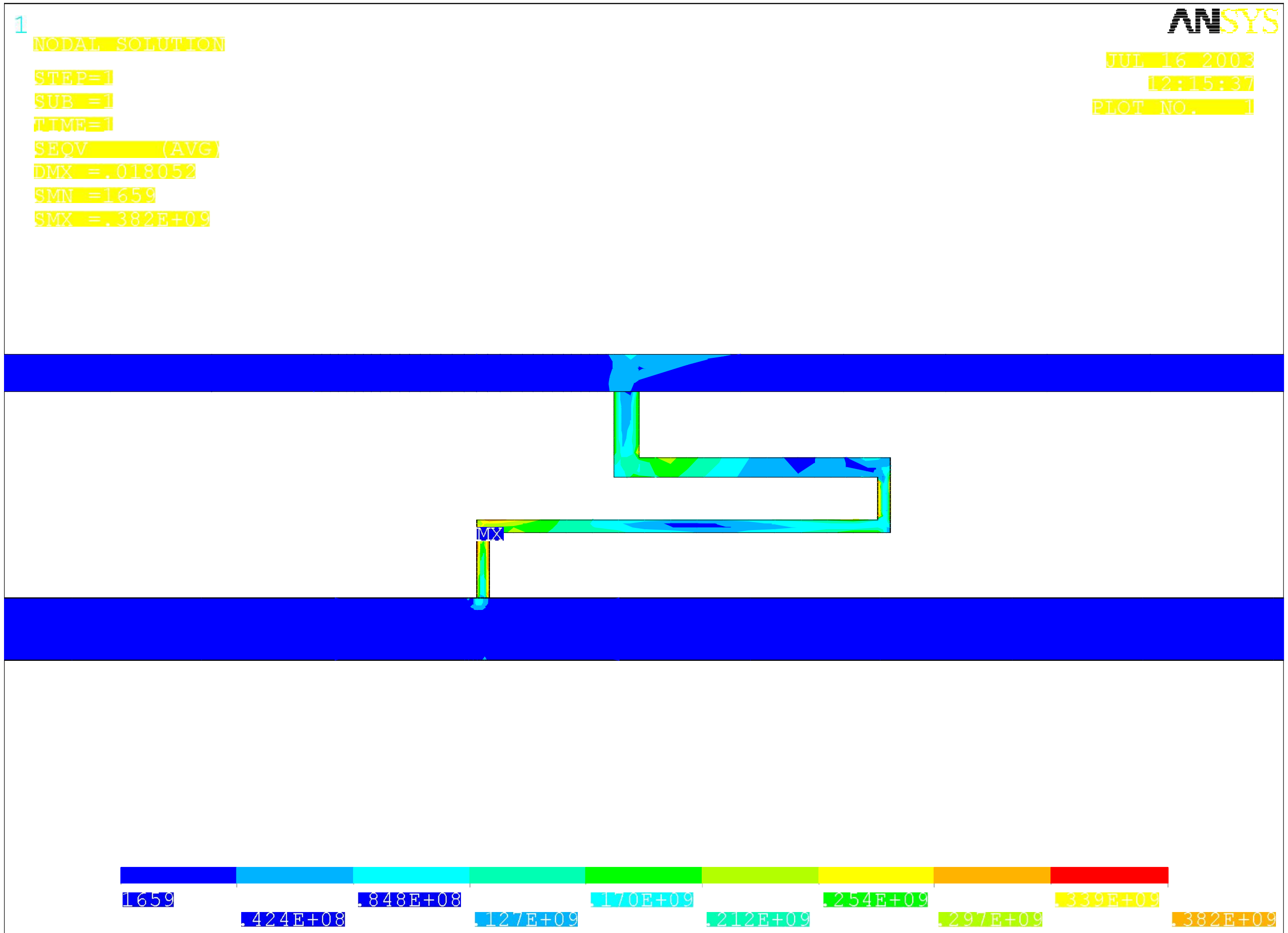

FIGURE 9. TYPE C.STRESS DISTRIBUTION (N/M2)

00048539

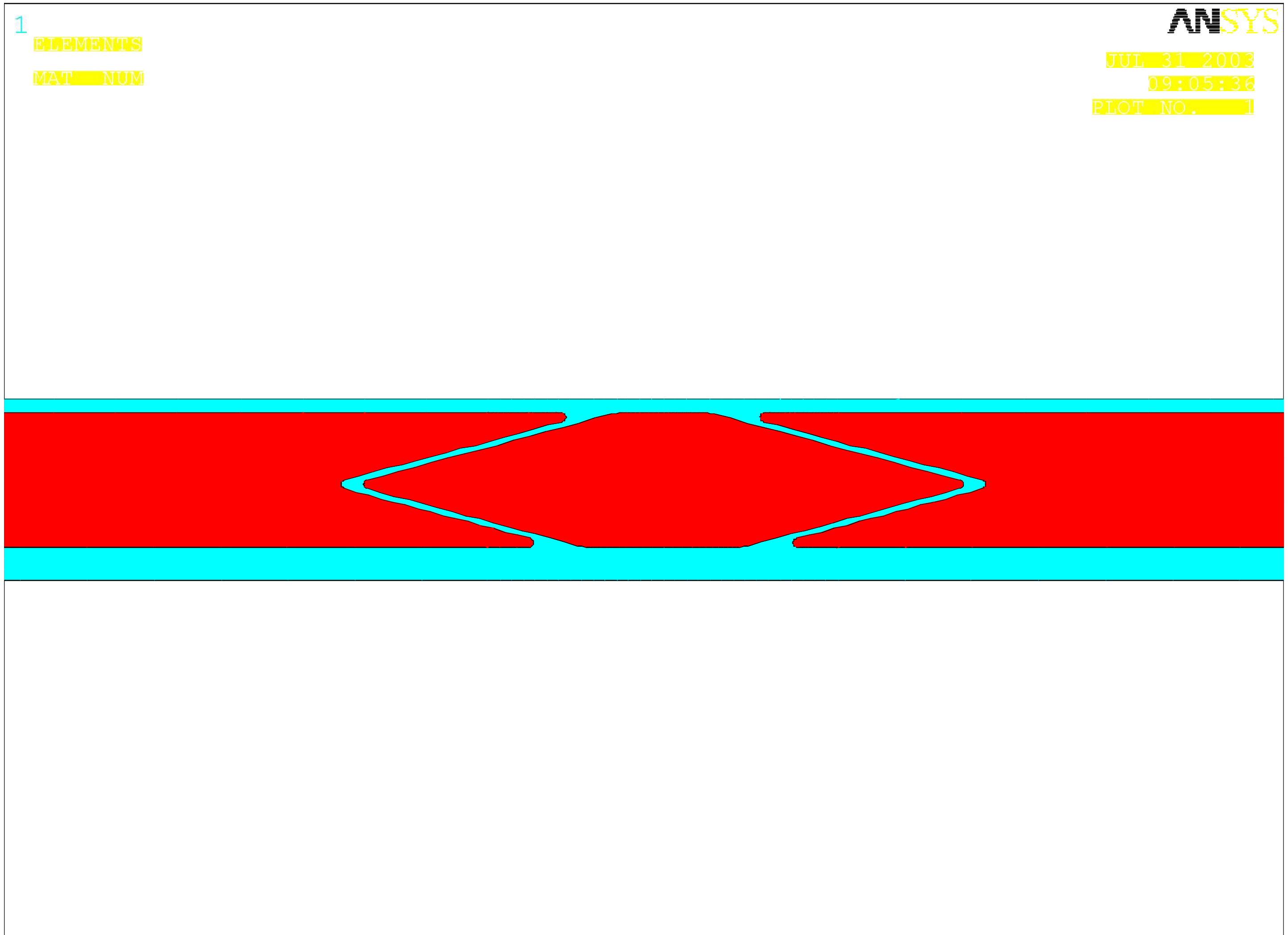

FIGURE 10. TYPE A-DOUBLE

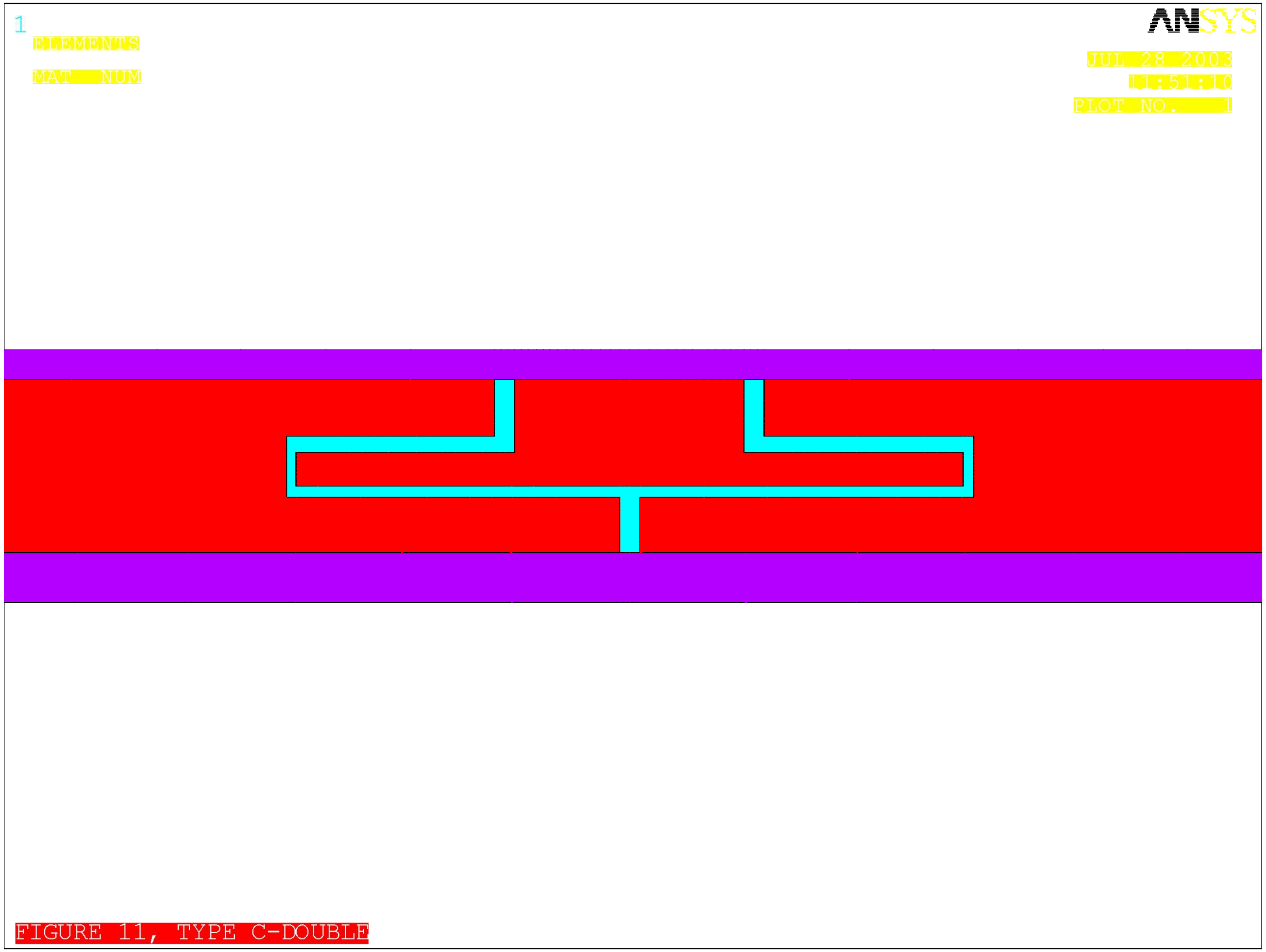

FIGURE 11, TYPE C-DOUBLE

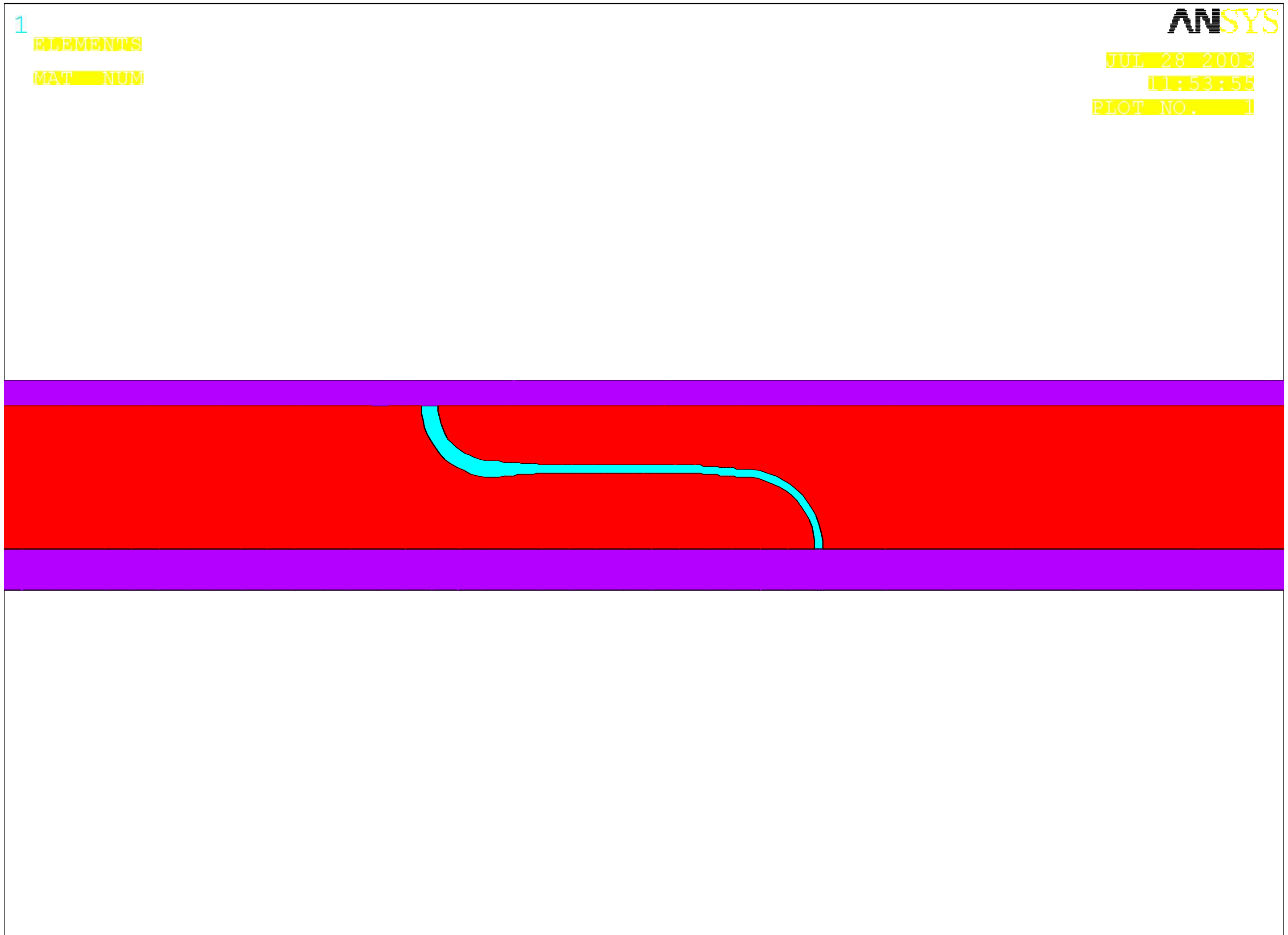

FIGURE 12

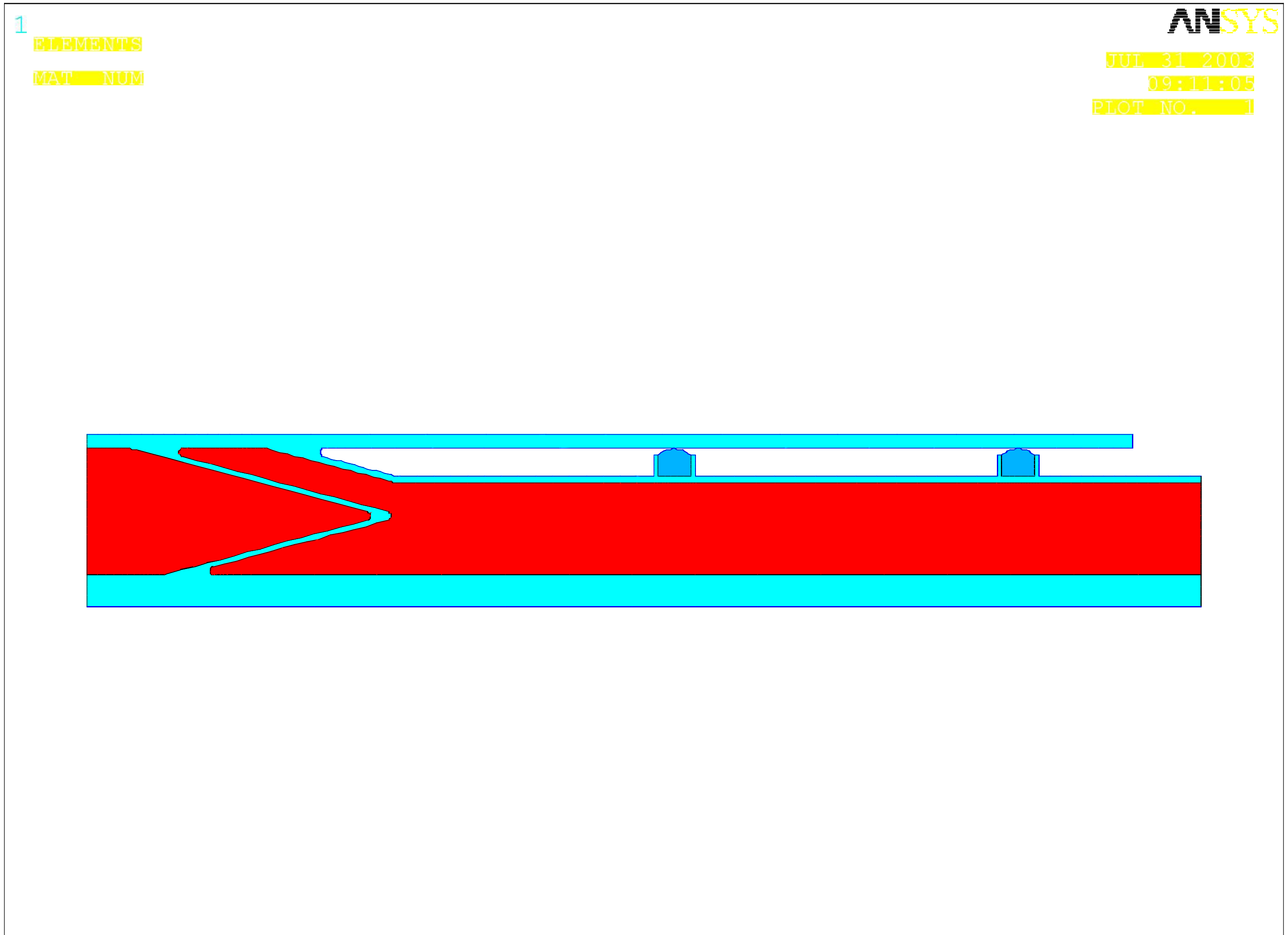

FIGURE 13, FILTER TYPE A

Attachment 3

Work-Report NGPM5/2003/en/0285 from 30.12.2003, FANP GmbH

FRAMATOME ANP

Work-Report

Ref. (Department/Year/Language/Serial No.)	Rev.
NGPM5/2003/en/0285	A

Subject/Title
Design study for the fatigue evaluation for the Hot Gas Duct of the High Temperature Reactor.

Place	Date
Offenbach	2004-01-27

Prepared by	Department	Tel.	Signature
M.Schippers	NGPM5	94451	
G. Müller	NGPM5	94228	

Project
HTR-Modul F+E

Reviewed by

W.Kratschmann	NGPM5	92947	

Handling Instructions
restriktiv

Export Classification (Reports with techn. content)
AL: N ECCN: N

M.Schippers — Released by concerned department (content, handling, distribution)

D. Vanvor — released for external distribution

Proj.-Code	UA	DCC	Contents Code	Doc. Ident. No.
ZFY114		M BB		0600265007

Pages of Text: 19 Appendices 12 Pages total: 31

Summary

The present design for the Hot Gas Duct, especially the distance pieces between the inner liner and the support tube, is evaluated for the operational conditions and one Accident Load Case. For the incident and accident conditions conclusions are made.

The evaluation based on the preliminary KTA 3221.1 and KTA 3221.2. The Hot-Gas-Duct with operating conditions of 488°C at the support tube und 850°C at the inner liner is classified for Temperature category III. With respect to the classification include the structural analysis evaluation of primary and secondary strains and stresses and the consideration of elastic-plastic material behaviour together with the assessment of creep behaviour. The threshold values are time-temperature depending values.

The evaluation is done by the FE-Method with the computer code ANSYS 7.1.

With respect to the available information and made estimations we can conclude that the design resist the load for the normal operation (usage factor 0,11). Critical items are stress concentration with respect to material and geometrical discontinuities. Welds has to be minimized in principle and not considered here.

Distribution

Mr. Vanvor	NGPS4
Dr. Brinkmann	NGPS4
Mr. Wirtz	NGPM5 f.i.o.
Mr. Ballot	NZ f.i.o.
Members of WP 1	of HTR-E

List of revisions

Rev.	Date	Scope of revision	Section/Page
A	2004-01-27	First Edition	

Table of Content

1 Introduction

The report describe the investigation of the present design for the Hot-Gas-Duct for the High-Temperature-Reactor. The duct is part of the reactor power conversion unit and connect the reactor with the helium turbine. The duct has the purpose to conduct the high temperature helium from the reactor to the helium turbine (inside) and to feed the reactor with helium coming from the recuperator (outside).

To ensure the functionality a coaxial duct is designed. The support tube is protected with a thermal sleeve (liner) at the inner side. The liner is connected to the support tube via Vee-shape pieces. The Vee-shape has to be designed for thermal and mechanical loads coming from the different helium temperatures at both sides of the duct. Investigated are normal operating conditions and accident conditions. The normal operating conditions investigated with two different models. The first model is designed with two different materials. The chosen material for the support tube is the standard austenitic material 1.4571. The Vee-shape and the liner are designed with the Alloy 800H. The second model is using for all parts Alloy 800 H.

2 Design Data

2.1 Geometry

The geometrical dimension is taken from Ref. [1] to [3] (Appendices 1 to 3) and Ref. [10].

2.2 Material Data Base

Considered materials are taken from Ref. [1] to [3]. Material properties are taken from Ref. [4] and Ref. [5]. The temperature depending material properties are shown in the following graphs.

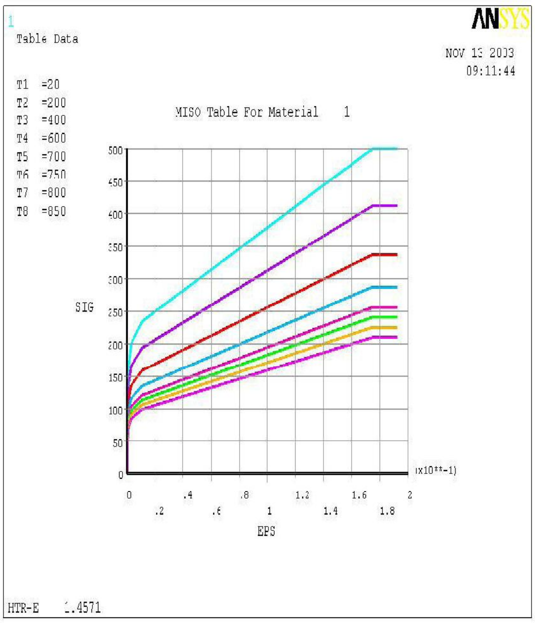

Figure 2-1: Multi linear Isotropic Hardening for 1.4571

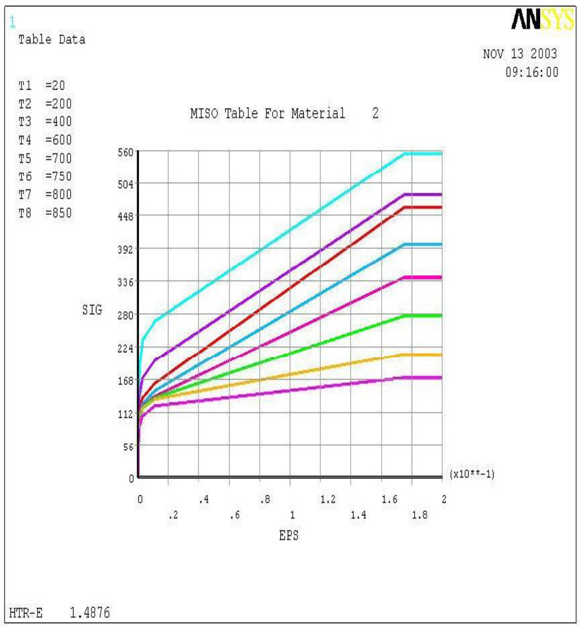

Figure 2-2: Multi linear Isotropic Hardening for Alloy 800H

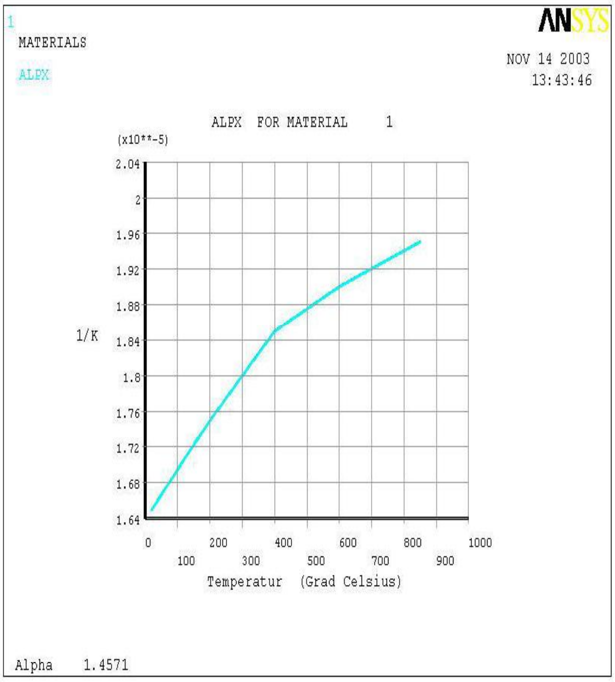

Figure 2-3: Thermal Expansion Coefficient 1.4571

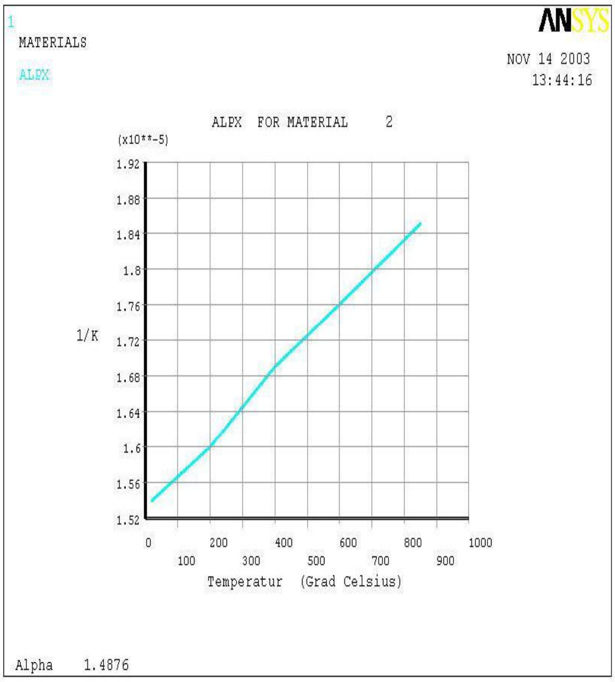

Figure 2-4: Thermal Expansion Coefficient Alloy 800H

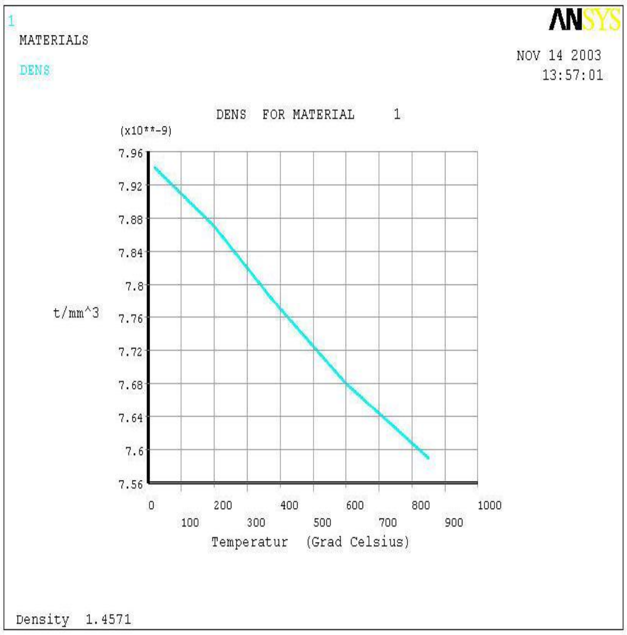

Figure 2-5: Density 1.4571

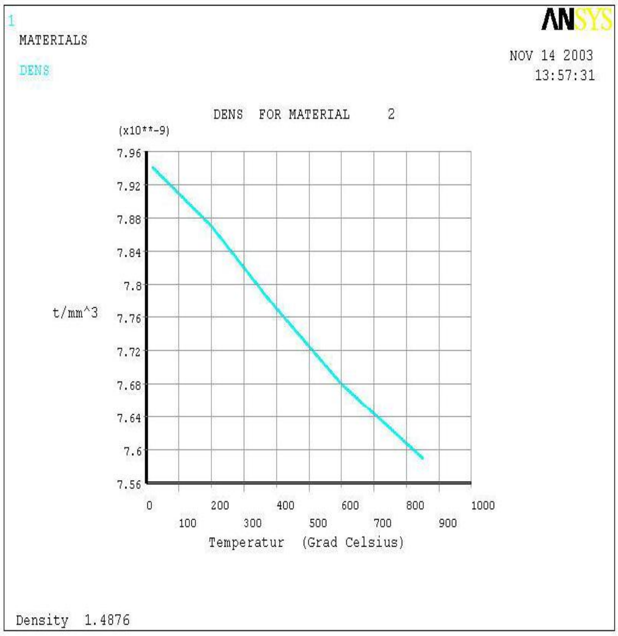

Figure 2-6: Density Alloy 800H

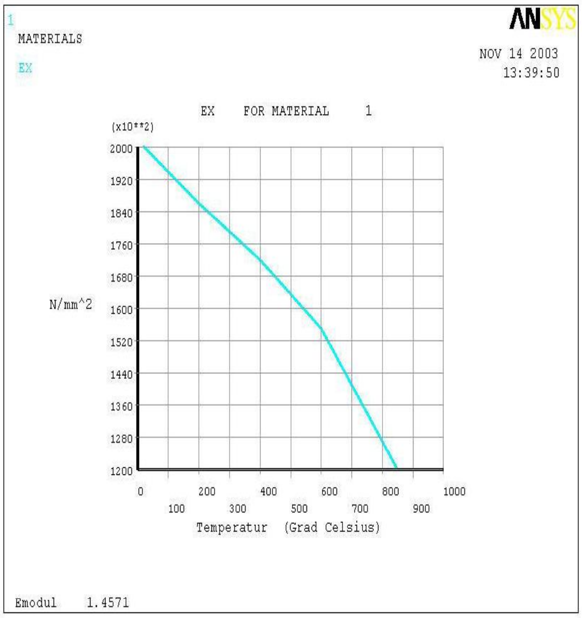

Figure 2-7: E-Module 1.4571

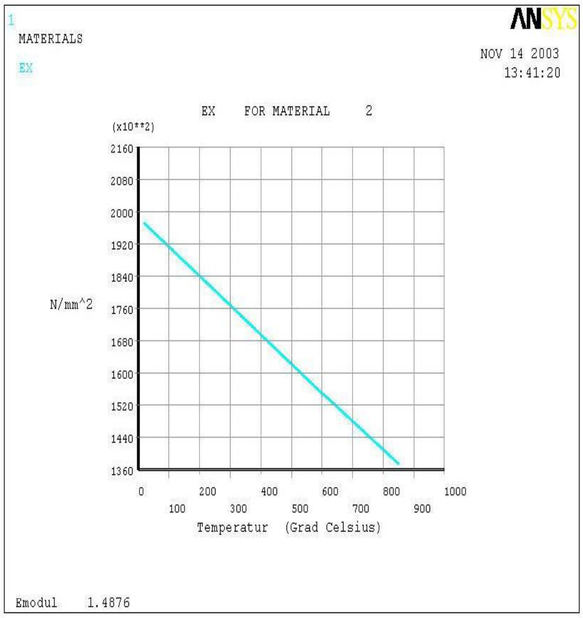

Figure 2-8: E-Module Alloy 800H

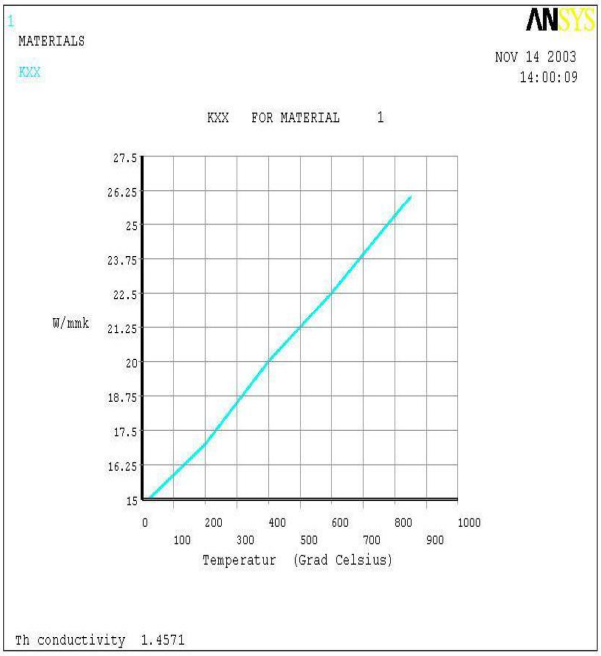

Figure 2-9: Thermal Transfer Coefficient 1.4571

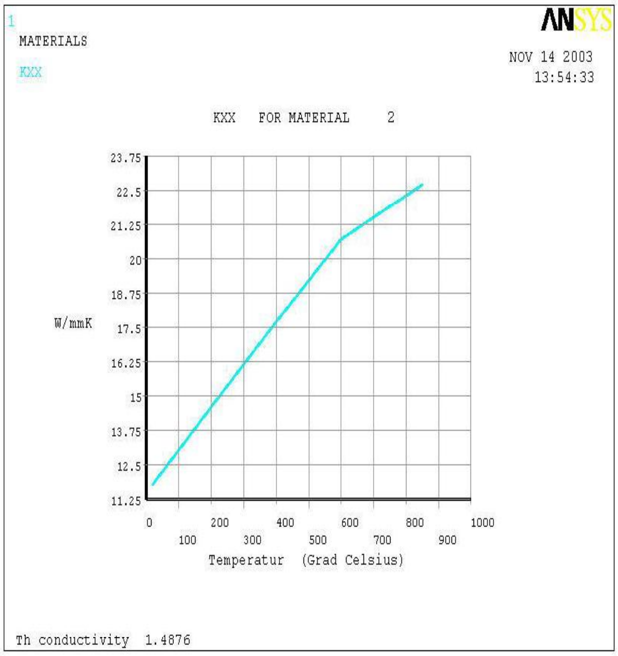

Figure 2-10: Thermal Transfer Coefficient Alloy 800H

With respect to the high temperature and the classification is the creep behaviour to consider. This effect is implemented for the secondary creep behaviour by using the implicit creep equation in accordance to Norton described as follow:

acc. to Norton: $\dot{\varepsilon}_{st}=k\sigma^{n}$

ANSYS creep model: $\dot{\varepsilon}_{cr}=C_{1}\sigma^{C2}e^{-C3/T}$

The coefficients are taken from Ref. [4] where the temperature depending values are published.

2.3 Loadings

The specified loads for pressure and temperature are described in Ref. [6] and Ref. [11]. Other external loads e.g. from seismic or pipe loads from supports or components are not considered.

2.3.1 Normal Operation Conditions

The investigated loads for normal operation consider for the primary stresses pressure differences of 0,8 MPa and 0,2 MPa for the liner and the vee-shape and1,5 MPa for the support tube. Load cycles are considered from Ref. [11] "Tabel 1: Functional specifications" with 1100 cycles in 6 years and a temperature variation of +/- 240°C/h.

2.3.2 Accident Condition

Considered are the loads from Ref. [6] "Table 1: functional specification" and herein the Accident conditions for the Primary Coolant Leak (DN<250). The specified transient is the maximal load with respect to the maximal range of pressure and temperature and the strong gradients.

3 Structural Analysis

3.1 Principles of used Methodology

The evaluation will be based on the methodology described in Ref. [4]. If the component have to be designed for transient load conditions together with time dependant material properties, is during the dimensioning not only the dimensioning level with the analysis of the primary stresses to evaluate, then the secondary stresses under consideration of the different operational levels and the fatigue aspect have to be analysed (see Ref.[4] Chapter 4.3.2).

Depending on the mechanical behaviour and with respect to Temperature-Time-Limitcurves different classifications are defined. The Hot-Gas-Duct is in the class of high temperature with significant creep behaviour.

Primary stresses related to the outer loads and can be separated in ordinary membrane stress Pm, local membrane stress Pl or local bending stress Q. Within the evaluation of the Hot-Gas-Duct is the relevant load for the primary stresses the inner pressure and will be analysed in Chapter 3.4.1.

Secondary stresses e.g. related to unsteady geometry and or because of different temperature distributions be separated in membrane stress Q and bending stress Q for the component geometry we have to consider herein. The secondary stresses analysed in Chapter 3.4.2 (time history of temperature distribution) and 3.4.3. The assessment of secondary stresses have to be seen in the scope of the fatigue evaluation.

The evaluation of fatigue with relevant creep behaviour based on the assessment of strains and will be analysed in Chapter 3.4.4.

3.2 Structural FE-Model

The structural model is considering the geometry, material properties and loads are described in Chapter 2. The chosen model is a two dimensional axial symmetric model. At both ends of the model the boundary conditions defined in a way, that the radial displacements are taken the ongoing duct in to account. It is also valid for the axial displacements. The "hole-plate" is modelled for free axial strain. Furthermore is the mesh generated to guarantee adequate results for high thermal transient load and for the geometric nonlinearities. The elements are plane and axisymmetric defined by 4 nodes by having 2 degrees of freedom per node. The model and the boundary conditions are shown in the following picture.

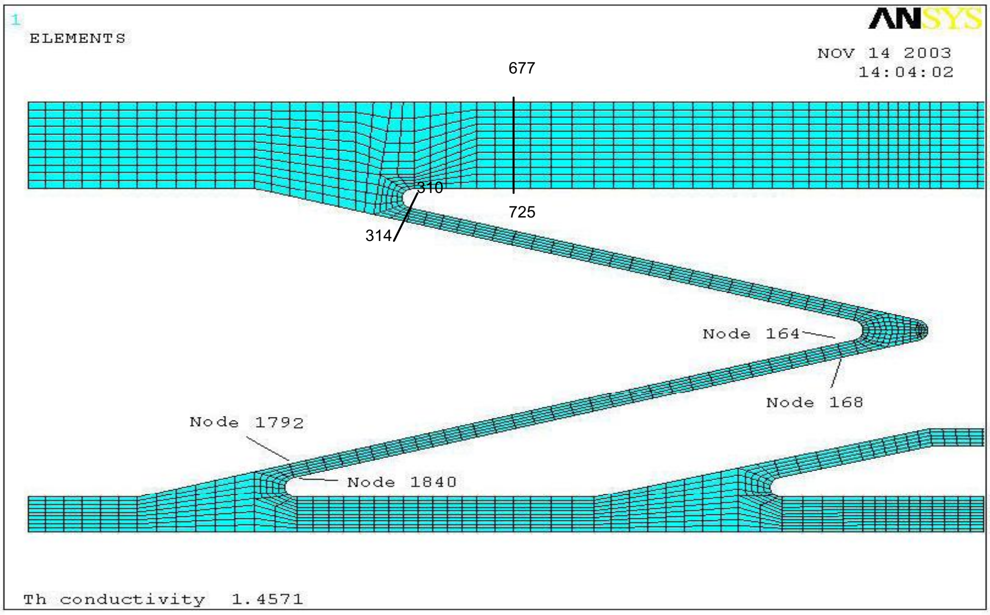

Figure 3-1: Element Mesh

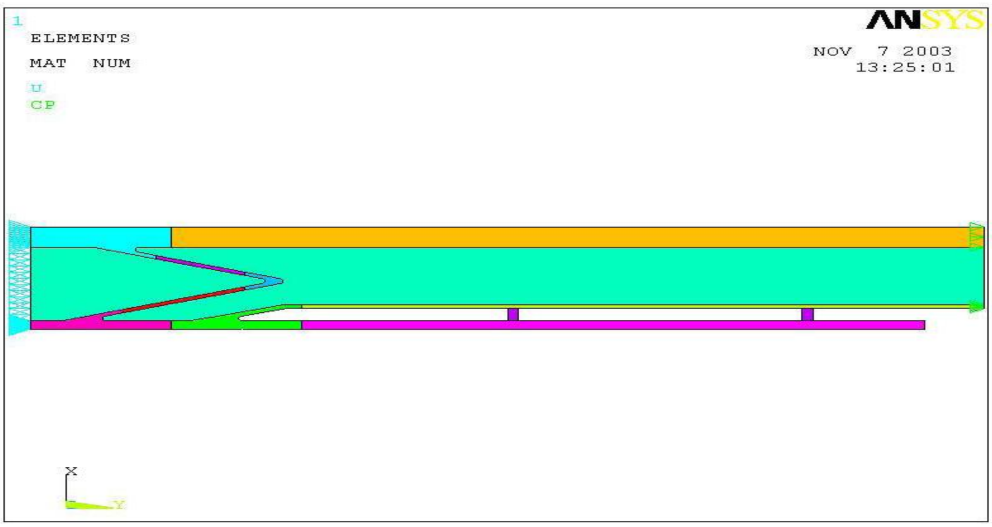

Figure 3-2: Boundary Conditions

3.3 FE-Solution Method

The implicit Finite-Element-Method is used to get adequate results with respect to the transient analysis under consideration of geometry and material nonlinearities e.g. plastic strain and creep.

For the analysis of normal operating conditions is the temperature distribution calculated by a transient analysis with 124 time steps and 305 cumulative iterations. The following quasi static structural analysis takes into account 48 time steps with 288 cumulative iterations. The adequate chosen time steps considering the time period where changes in temperature or pressure happened. In particular temperature differences over the wall thickness are considered to evaluate effects for membrane and bending strain and stress. The same procedure is used for the analysis of the accident conditions.

3.4 Results

3.4.1 Primary Stress (Membrane stress related to inner pressure)

The primary stress for the pressure load is calculated for cylindrical parts with shell characteristic:

$$\sigma_u = pi \cdot \frac{di}{2 \cdot s}$$ Circumferential stress

$$\sigma_r = \frac{-pi}{2}$$ Radial stress

$$\sigma_l = \frac{\sigma_u}{2}$$ Logitudenal stress

$$\sigma_v = \sigma_u - \sigma_r$$ Equivalent stress acc. to Tresca (max-min)

The results for the primary stress at the liner, the vee-shape und the support tube are shown in Table 3-1.

Part / σ_v [MPa]	liner	vee-shape	support tube
p= 0,2 MPa*1	1,46	3,635	0,67
p= 0,8 MPa*1	5,84	14,54	2,68
p= 1,5 MPa*1	-	-	5,025
p= 4,5 MPa*2	-	-	15,075

Table 3-1: Primary stresses
*1 normal operating conditions
*2 accident conditions

Dimensions [mm]	liner	vee-shape	support tube
Inner diameter	1450	1450	1650
Wall thickness [s]	10	4	25

Table 3-2: Geometrical Parameter

3.4.2 Time History of Temperature Distribution

Adiabatic conditions are considered. The insulating material is implemented with a thermal conductivity of 0,426 W/mK in acc. to Ref. [7]. The heat transfer coefficient at the outside of the support tube is chosen 1300 W/m^2K and 1500 W/m^2K for the inner side. The solution for temperature distribution at several time steps is shown in the following figures . The distribution is showing the expected linear distribution from the outside of the support tube to the inner side of the liner. The figures will show the temperature distribution for three several time steps.

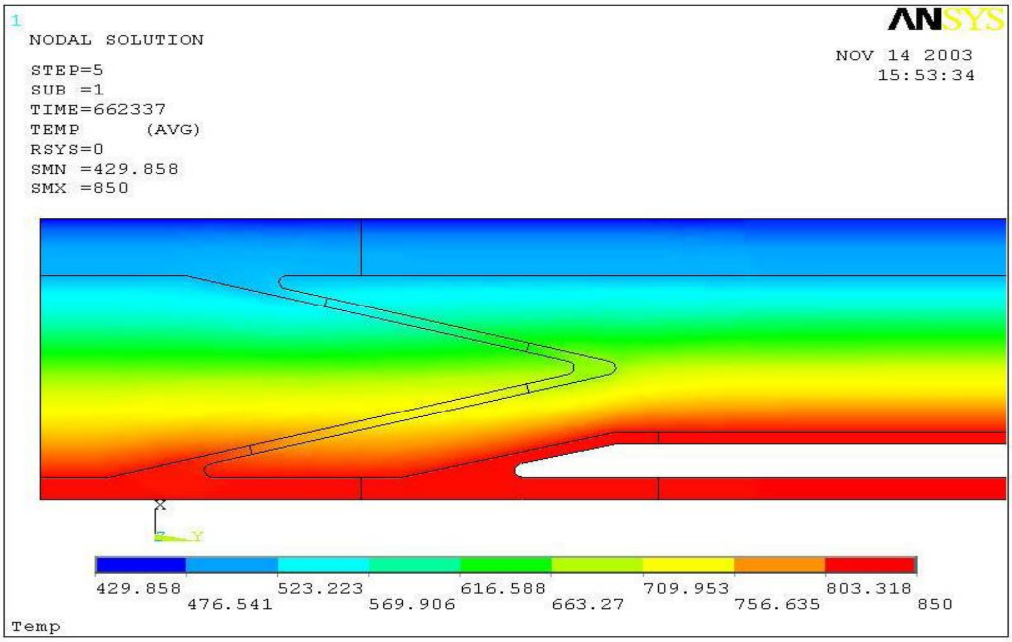

Figure 3-3: Temperature Distribution at 662337 sec (Normal Operation)
Cold shock at the outside of the support tube with 60K/sec.

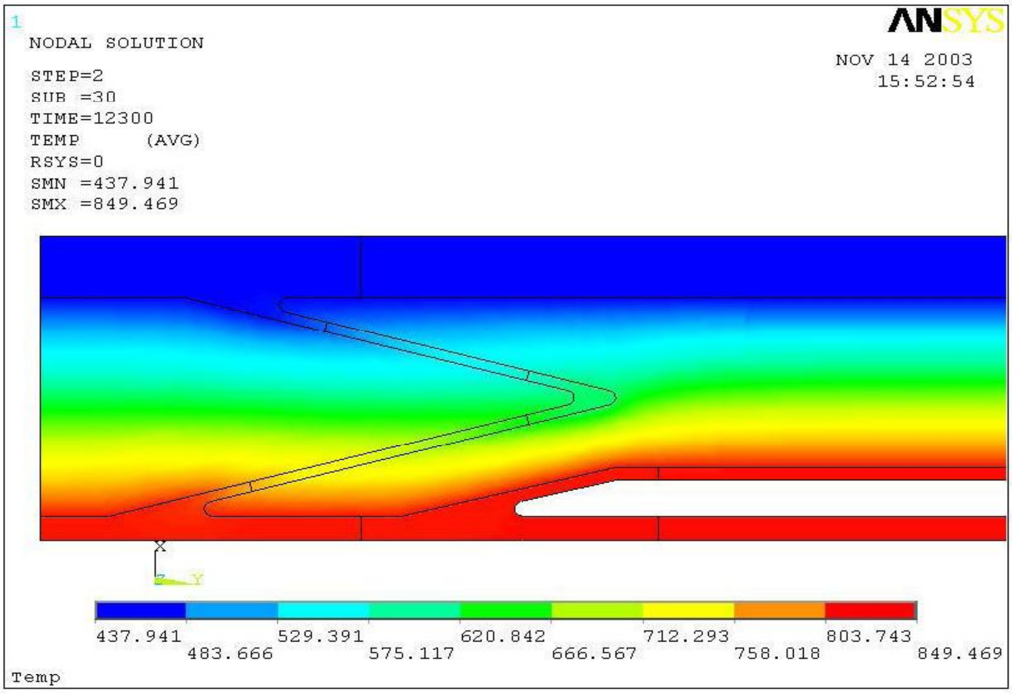

Figure 3-4: Temperature Distribution at 12300 sec. - 3,4 h after start up (Normal Operation)

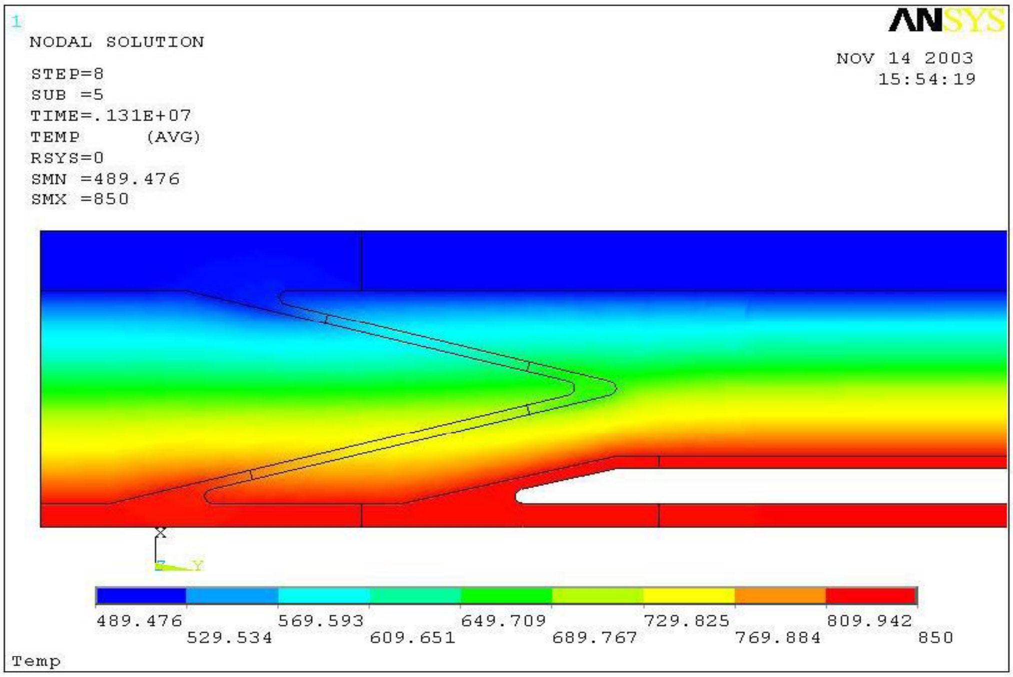

Figure 3-5: Temperature Distribution at 131E+7 sec.

Before cooling down

(Normal Operation)

The following figures are showing the temperature – time-history for selected nodes 164 and 168 for the load case Normal Operating and Accident Conditions. The selected time steps for the stress evaluation are marked in the listed output in Appendix 4 and 5.

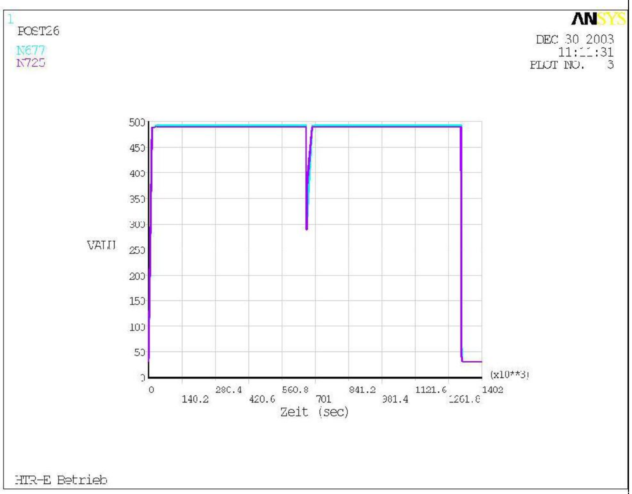

Figure 3-7: Temperature-Time node 164, 168 (Normal Operation)

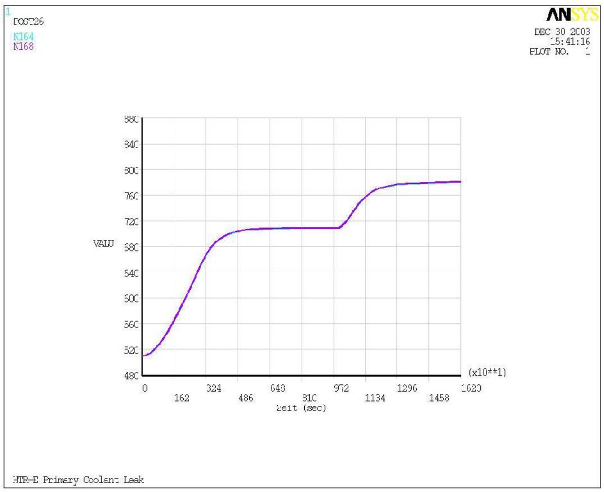

Figure 3-6: Temperature-Time at nodes 164, 168 (Accident Conditions)

3.4.3 Secondary Stresses (Membrane and Membrane+Bending Stresses related to the Temperature Load)

The evaluated nodes (path for the linearization) are shown in Figure 3-1. The following table shows the secondary stresses membrane and membrane + bending for selected time steps.

Model (Load Case)	Path of Lineariza-tion	Time [sec]	Temp. [°C]	$Q_{membrane}$ [MPa]	$Q_{memb.+bend.}$ [MPa]
Different materials as described in Chapter 1 (Normal Operation)	**1792 / 1840**	**3280**	**823**	**25,3**	**193,8**
		56979	**650**	**1,6**	**12.9**
		1,4E+7	**30**	**63,3**	**394**
	164 / 168	**3280**	**800**	**106,8**	**216,6**
		56979	**628,4**	**32.8**	**46.0**
		1,4E+7	**30**	**221,5**	**292,8**
All Parts Alloy 800H (Normal Operation)	**1792 / 1840**	**12300**	**823**	**11,7**	**37,3**
		665956	**829,6**	**10,5**	**32,32**
		1,4E+7	**30**	**63,2**	**393,7**
	164 / 168	**12300**	**628,4**	**20,2**	**136,1**
		665956	**622,9**	**30,1**	**123,6**
		1,4E+7	**30**	**220,1**	**292,9**
All Parts Alloy 800H (Accident Conditions)	**310 / 314**	**3000**	**522,9**	**136,6**	**284,0**
		10003	**530,4**	**158,2**	**318,3**
		16011	**717**	**4,6**	**31,5**
	164 / 168	**3000**	**654,1**	**89,3**	**157,4**
		10003	**709,5**	**101,2**	**164,3**
		16011	**780,9**	**12,0**	**37,1**

Table 3-3: Linearized Secondary Stress (membrane and bending)

The values are taken from the listed output in Appendices 6 to 8.

The following figure is showing the equivalent stress in acc. to v.Mises at the model with different materials during normal operation time at 56579 sec. The maximum value is near the location where the material changed and in the area of heat affection zone of the weld.

This model will not be further investigated for the evaluation of strains and the fatigue. More remarks made under Conclusions in Chapter 4.2.

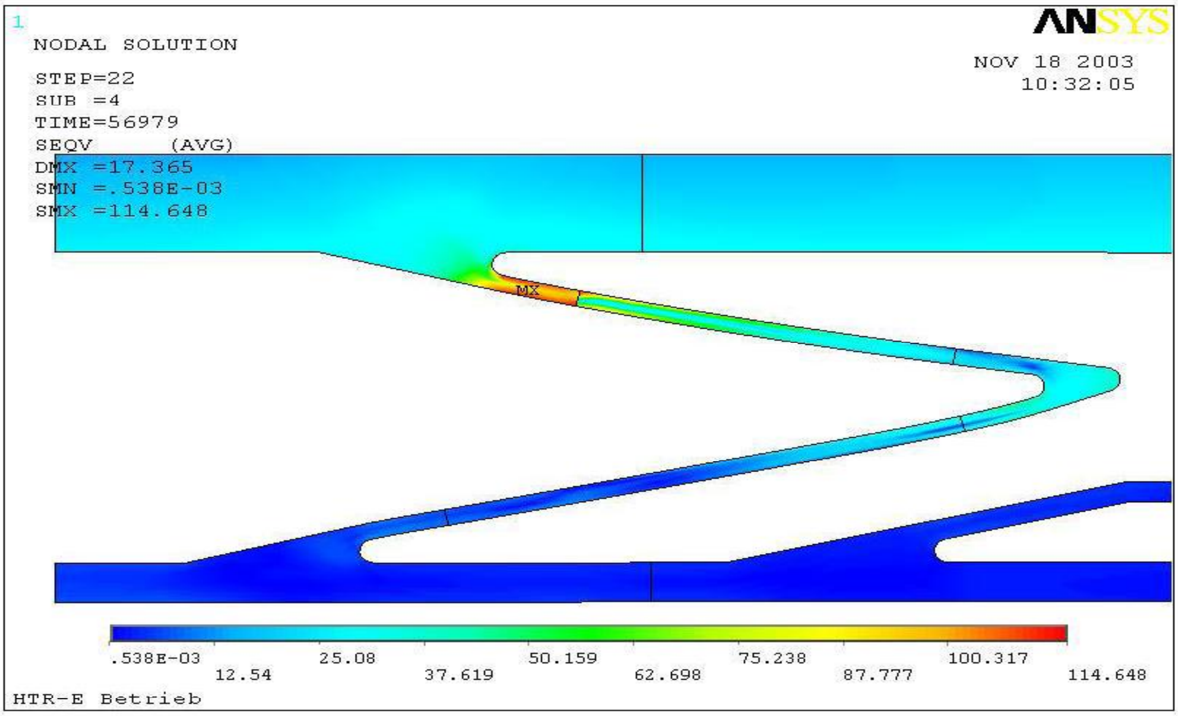

Figure 3-8: Equivalent Stress during Normal Operation for the Model with Different Material

3.4.4 Fatigue Evaluation (elastic, plastic, thermal and creep strains)

The results for strains are shown as time histories for the elastic, plastic, thermal and creep strains for the nodes equivalent to the stress evaluation. The figures are related to the model with single material Alloy 800 H and the load case Normal Operation. The equivalent strains are not linearized and the smaller share of membrane and membrane+bending strains is not shown. The maximum equivalent strain including peak share of 0,8% in Figure 3-10 is shown.

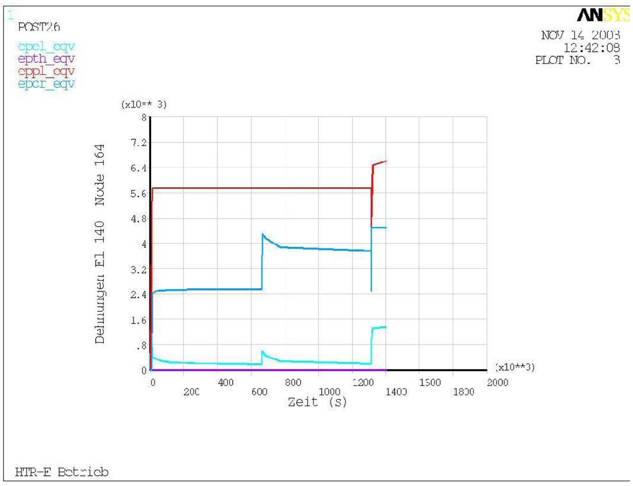

Figure 3-9: Equivalent Strains at Node 164

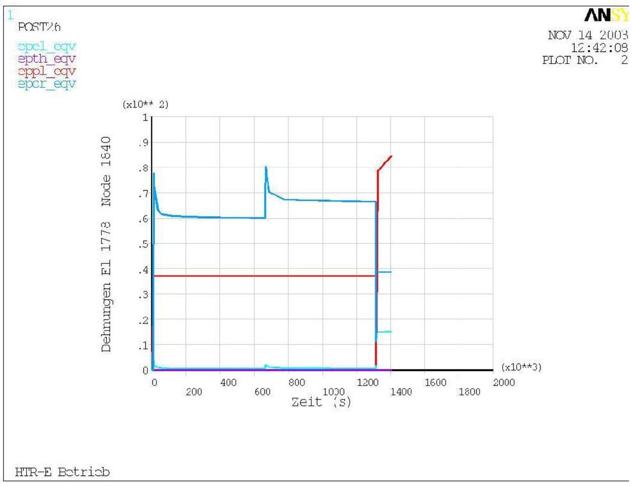

Figure 3-10: Equivalent Strains at Node 1840

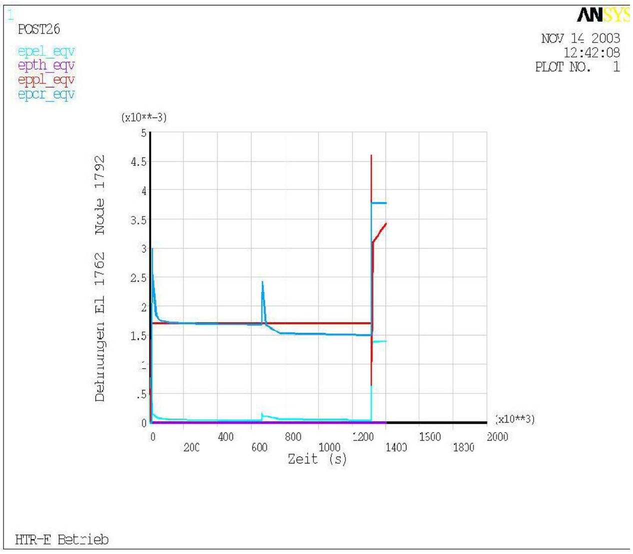

Figure 3-12: Equivalent Strains at Node 1792

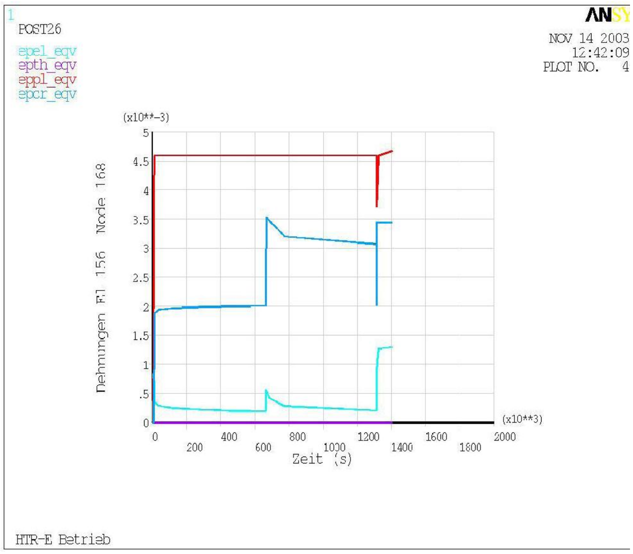

Figure 3-11: Equivalent Strains at Node 168

4 Assessment

The analysis for the hot gas duct has with the temperature of ~850°C significant creep behaviour. To consider the creep effect are different aspects to investigate. The analysis required elastic-plastic material behaviour for the adequate determination of strains and stresses. The threshold values are time, temperature and depending on the number of load cycles. The separate analysis should show the influence of creep for the strain accumulation.

4.1 Comparison of Evaluation Criteria and Analytical Results

For the pressure related membrane stress are threshold values (St) depending of the material, operating time and temperature given as follow from Ref. [4] for Alloy 800H:

Oper. Temperature	Operating time [h]	St [MPa]
850	10^5	8
775	10^5	17
700	10^5	30

Table 4-1: Evaluation Criteria Membrane Stress

The maximum membrane stress is ~15 MPa (Table 3-1) for Normal Operation. To consider linear interpolation for the location of the vee-shape, with temperature of not more then 775°C, is the criteria for the membrane stress fulfilled. For 850°C and 100 h operating time is the St-value given with 35 MPa. For the accident conditions was the primary membrane stress 15,075 MPa.

Q		
Temperature [°C]	S_m [MPa]	$3S_m$ [MPa]
20-250	115	345
500	101	303
650	95	285
700	91	273
750	88	264
800	83	252
850	72	216

Stresses in MPa, the given values valid for Alloay 800H. The criteria is for the dimensioning the same for membrane or membrane +bending.

Table 4-2: Evaluation Criteria in acc. to Ref. [4]

The $3S_m$ criteria is not for all stresses given in Table 3-3 fulfilled. The following strain evaluation has to be done if the 3Sm criteria is exceeded. With respect to the temperature classification is the strain evaluation with limited plastic and creep strains necessary anyway.

Following limitations for equivalent strains in principal are required for all Load Classes without Accident Cases:

- membrane strain to $\leq$ 1%
- membrane+bending strain to $\leq$ 2%
- local membrane+bending strain to $\leq$ 5%

For the load case Normal Operation is a maximal membrane strain of 0,45 % at the path node 1840-1792 (Appendix 9, page 28) evaluated. The membrane + bending strain is 1,66 % at the same path (Appendix 9, page 28). The limits above are fulfilled.
For the Accident conditions is a maximal total equivalent strain of 13,8 % evaluated (Appendix 10, page 29). It has to be considered that the linearized strains total strain and contain elastic, plastic and creep strains. It is not to understand as strain range.

For the thermal fatigue evaluation is the separated evaluation for the influence of creep strain (D_{cr}) and plastic strain (D_{pl}) required. The relevant criteria in acc. to Ref. [4] for the plastic strain:

$$\sum_i \frac{n_i}{n_{iallowable}} = D_{pl} \leq$$

n_i – amount of cycles per load case

$n_{iallowable}$ – allowable number of cycles for $\Delta\varepsilon_i$ at load cycle$_i$ at temperature t_i

$n_{iallowable\ (Normal\ Operation)} \sim 10^4$ (at 850°C and $\Delta\varepsilon/2$=0,427%/2~0,2% taken from Appendix 11); n_i=1100
$n_{iallowable\ (Accident\ Conditionsn)}$ ~ 5 (at 700°C and $\Delta\varepsilon/2$=9,7%/2~4,9% taken from Appendix 12); n_i=2

$D_{pl\ Normal\ Operation} + D_{pl\ Accident\ Conditions} \leq 1$

The usage factor for the normal operation is D=0,11. For the accident conditions are app. 5 load cycles allowable.

To consider the creep strain in acc. to Ref. [2]:

$$\sum_i n_i \int_0^{\Delta t_i} \frac{dt}{t_{o.all}} + \sum_i \frac{n_i}{n_{iallowable}} = D_{cr} + D_{pl} \leq 1$$

Δti - time per cycle
$t_{o.all}$ - allowable load time based on 1,1St see Table 4-1

For normal operation are 1100 cycles in 6 years specified. It would be 46 hour per cycle, which is not realistic. More realistic are 12 cycles in 6 years with a time per cycle of 4000 h.
The used Input values are:

Load case	Δti	$t_{o.all}$	n_i	$n_{iallowable}$
Normal operation:	4000	100.000	12	10.000
Accident Condition:	2	100	2	5

Plastic Strain: $D_{pl} = D_{pl\ Normal\ Operation} + D_{pl\ Accident\ Condition} = 0{,}0012 + 0{,}4 = 0{,}4012$
Creep Strain: $D_{Cr} = D_{Cr\ Normal\ Operation} + D_{cr\ Accident\ Condition} = 0{,}48 + 0{,}04 = 0{,}52$
$D_{total} = 0{,}92$

4.2 Conclusions

The investigated design for the hot gas duct seems to resist the defined loadings. To take care of the estimations and that not all load case considered, material discontinuities should be neglected. Furthermore it should be considered that welds have to be minimized and the geometrical design should preclude any stress concentration. A final statement and design optimization should include further load cases and the check if any further loads from boundary conditions has to be considered (e.g. pipe- or seismic loads).

5 References

[1] FANP Drawing ZFY116-NGPS3-00-003327 Date: 2003-02-24
Continuous Horizontal Hot Das Duct
For GT-MHR Reactor design
Deliverable 7b of WP1
Outline And Detail Drawing

[2] FANP Drawing ZFY116-NGPS3-00-003328 Date: 2003-02-24
Continuous Horizontal Hot Das Duct
For GT-MHR Reactor design
Deliverable 7b of WP1
Detail Drawing

[3] FANP Drawing ZFY116-NGPS3-00-003329 Date: 2003-02-24
Continuous Horizontal Hot Das Duct
For GT-MHR Reactor design
Deliverable 7b of WP1
Detail Drawing

[4] KTA 3221.1 Metallische HTR-Komponenten, Ausgabe Dez. 1992

[5] Stahlschlüssel 18. Ausgabe 1998

[6] FANP Report ZFY116-400636724

[7] FANP Report NGES3/2002/en/0044 Rev.0; Data Summery for materials for the hot gas duct
Date: 2002-11-20

[8] Fuchs/Stephens; Metal fatigue in engineering, A Wiley-Interscience Publication 1980

[9] ANSYS Release 7.1 UP20030501

[10] FANP Report NGPS3/2003/en/0005 Rev.0, date 2003-02-25

[11] FANP Report HTR-E 02/12 D1-1-1-2, Rev.A,

6 List of Figures

7 List of Tabel

8 List of Appendices

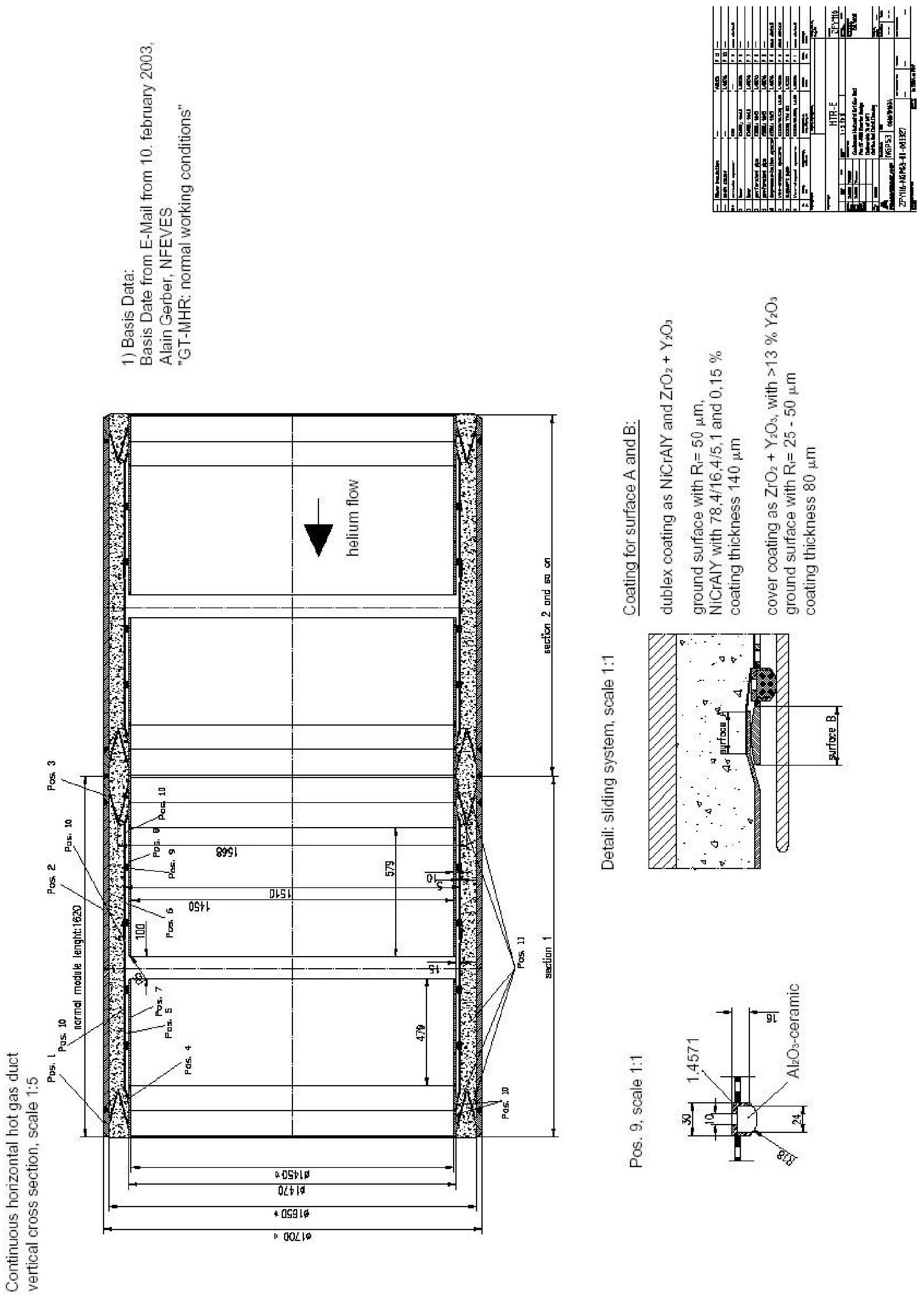

Appendix 1: Drawing-1 of HOT-Gas-Duct (acc. to [1])

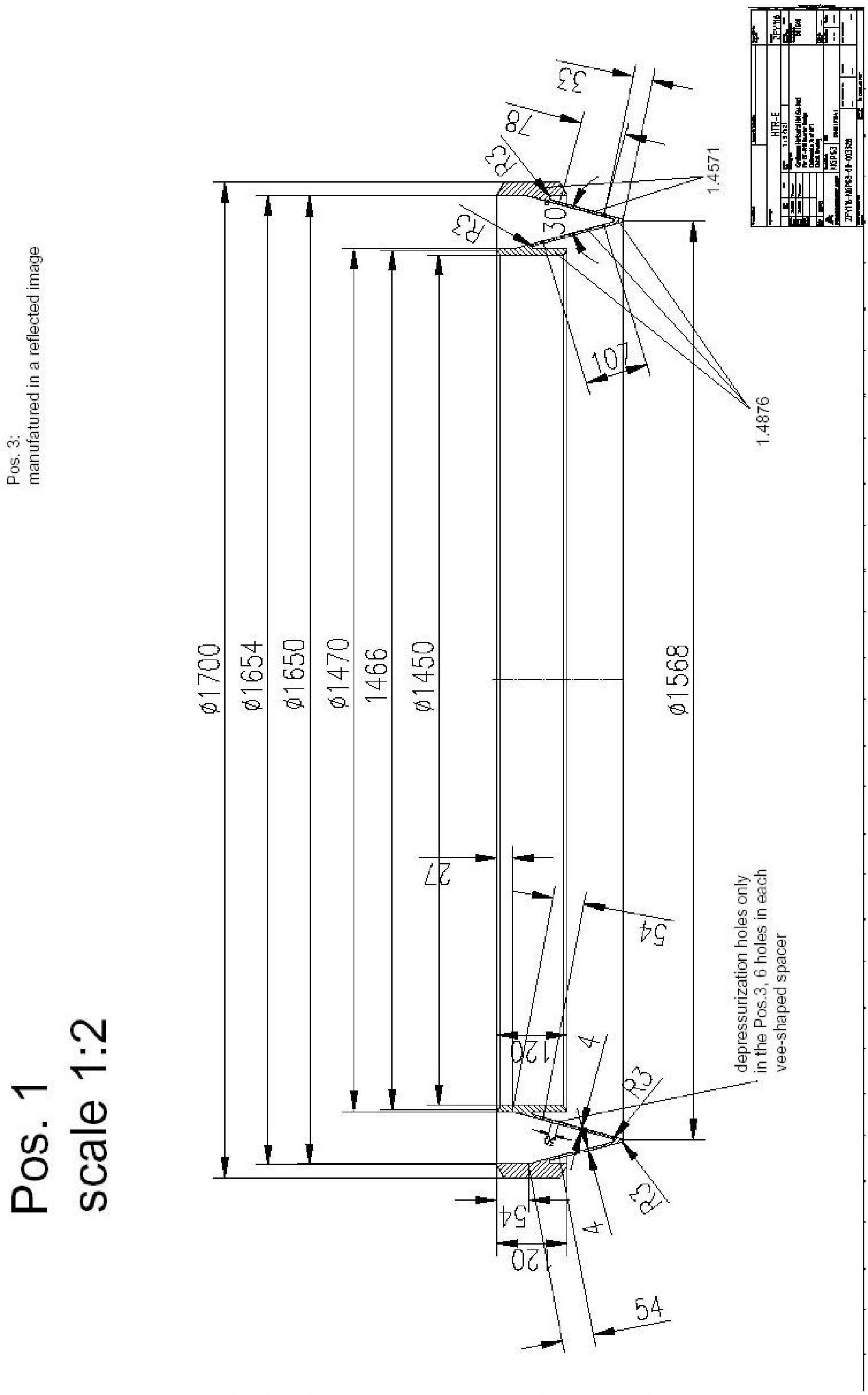

Appendix 2: Drawing of HOT-Gas-Duct -Detail 1 (acc. to [2])

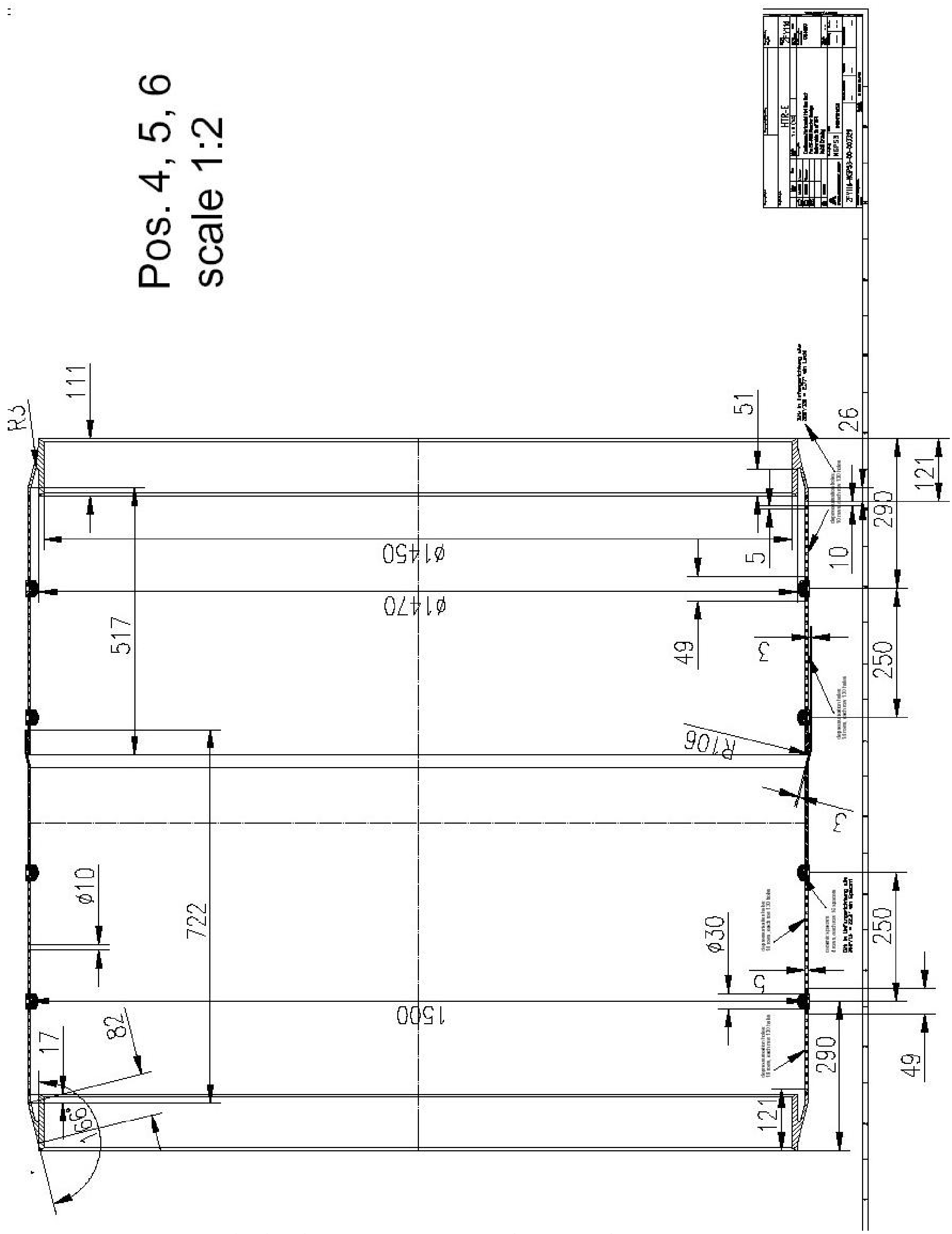

Appendix 3: Drawing of HOT-Gas-Duct -Detail 2 (acc. to [3])

Appendix 4: Listed Output Temperature-Time History - Normal Operation

***** ANSYS POST26 VARIABLE LISTING *****

LS	TIME	164 TEMP N164	168 TEMP N168	1792 TEMP N1792	1840 TEMP N1840	677 TEMP N677	725 TEMP N725
1	0.10000000E-05	30.0000	30.0000	30.0000	30.0000	30.0000	30.0000
	410.00000	33.1734	33.2006	48.8367	48.9825	39.2289	41.7884
	820.00000	40.0867	40.1440	72.7248	72.9610	51.5074	54.9099
.							
.							
.							
	11890.000	605.460	605.952	795.694	796.463	424.739	425.037
2	12300.000	627.925	628.436	822.537	823.325	438.678	438.809
	12710.000	645.450	645.939	829.318	830.003	452.560	452.560
.							
.							
.							
	121838.00	694.486	694.882	835.174	835.697	493.032	490.034
	316414.40	694.486	694.882	835.174	835.697	493.032	490.034
3	489371.20	694.486	694.882	835.174	835.697	493.032	490.034
	662328.00	694.486	694.882	835.174	835.697	493.032	490.034
	662336.83	694.486	694.882	835.174	835.697	490.679	428.204
.							
.							
.							
	665937.50	622.368	622.943	828.819	829.566	293.143	287.961
4	665956.00	622.312	622.888	828.815	829.562	302.218	370.038
	687575.60	691.103	691.506	834.875	835.408	491.608	489.314
	709195.20	694.374	694.770	835.164	835.687	493.019	490.028
	774054.00	694.486	694.883	835.175	835.698	493.032	490.034
	968630.40	694.487	694.883	835.174	835.697	493.032	490.034
5	1314544.0	694.486	694.882	835.174	835.697	493.032	490.034
	1314727.0	673.470	673.601	705.025	704.219	380.150	320.666
	1314788.0	663.922	663.959	651.973	650.742	332.852	256.495
.							
.							
.							
	1315177.5	554.426	553.995	254.130	250.821	82.5462	49.1221
	1315187.2	550.804	550.365	243.964	240.609	80.5613	48.3239
	1315193.6	548.388	547.943	237.214	233.829	79.2910	47.8145
6	1315200.0	545.960	545.511	230.466	227.050	78.0666	47.3248
7	1318080.0	186.767	186.590	54.0684	53.4463	36.4472	32.1009
	1320960.0	76.2578	76.2023	34.9890	34.8546	31.3586	30.4217
	1323840.0	43.4246	43.4082	31.2665	31.2327	30.3515	30.1073
	1332480.0	31.5926	31.5907	30.1413	30.1375	30.0399	30.0121
	1358400.0	30.0680	30.0679	30.0059	30.0057	30.0017	30.0005
8	1401600.0	30.0018	30.0018	30.0002	30.0001	30.0000	30.0000

Appendix 5: Listed Output Temperature-Time History - Accident Conditions

***** ANSYS POST26 VARIABLE LISTING *****

LS	TIME	164 TEMP N164	168 TEMP N168	314 TEMP N314	310 TEMP N310	677 TEMP N677	725 TEMP N725
1	0.10000E-05	510.000	510.000	510.000	510.000	510.000	510.000
	100.00	510.328	510.337	510.004	510.004	510.000	510.000
	200.00	511.126	511.151	510.021	510.020	510.003	510.001
	2600.0	626.509	626.904	520.141	519.798	512.264	510.913
	2700.0	633.211	633.620	520.820	520.456	512.423	510.978
	2800.0	639.969	640.393	521.510	521.124	512.586	511.045
	2900.0	646.781	647.219	522.210	521.802	512.751	511.112
2	3000.0	653.640	654.093	522.919	522.488	512.918	511.180
	3233.3	666.940	667.388	524.489	524.011	513.298	511.335
	3466.7	677.372	677.807	525.854	525.336	513.640	511.476
	3700.0	685.375	685.799	526.966	526.419	513.929	511.596
	3933.3	691.439	691.854	527.836	527.266	514.160	511.692
	4166.7	695.996	696.404	528.499	527.912	514.340	511.767
	4400.0	699.401	699.804	528.997	528.397	514.477	511.824
	4633.3	701.936	702.334	529.368	528.759	514.580	511.867
	4866.7	703.817	704.212	529.643	529.028	514.657	511.899
	5100.0	705.211	705.604	529.846	529.226	514.714	511.923
	5333.3	706.243	706.634	529.996	529.373	514.756	511.941
	5566.7	707.006	707.395	530.107	529.481	514.787	511.954
	5800.0	707.569	707.958	530.189	529.561	514.810	511.964
	6033.3	707.985	708.374	530.249	529.620	514.827	511.971
	6266.7	708.293	708.680	530.294	529.663	514.840	511.976
	6500.0	708.519	708.907	530.327	529.695	514.849	511.980
	6733.3	708.687	709.074	530.350	529.718	514.856	511.983
	6966.7	708.811	709.198	530.368	529.736	514.861	511.985
	7200.0	708.902	709.289	530.381	529.749	514.864	511.986
	7900.0	709.034	709.421	530.400	529.767	514.870	511.988
3	10000.	709.129	709.515	530.414	529.781	514.874	511.990
4	10003.	709.129	709.516	530.418	529.785	514.945	544.029
5	10006.	709.129	709.516	530.439	529.811	515.288	589.387
6	10008.	709.129	709.516	530.478	529.856	515.821	605.492
	10010.	709.129	709.515	530.555	529.945	516.723	614.975
	10012.	709.129	709.515	530.690	530.099	518.052	620.955
	10014.	709.128	709.514	530.903	530.339	519.819	624.632
	10016.	709.127	709.513	531.213	530.682	521.993	626.643
	10019.	709.126	709.511	531.633	531.141	524.514	627.382
	10021.	709.124	709.509	532.172	531.724	527.311	627.103
	10023.	709.121	709.505	532.835	532.435	530.306	625.987
	10024.	709.119	709.503	533.292	532.923	532.218	625.009
	10026.	709.117	709.500	533.796	533.458	534.169	623.775
	10358.	718.581	718.887	645.058	645.301	659.689	683.292
	10691.	733.152	733.406	688.662	688.758	695.017	702.029
7	11023.	746.902	747.120	704.974	704.936	705.843	707.756
	11356.	757.704	757.898	711.376	711.258	709.415	709.608
	11688.	765.489	765.667	714.115	713.954	710.710	710.262
	12021.	770.854	771.023	715.418	715.232	711.240	710.520
	13018.	777.313	777.470	716.542	716.332	711.630	710.702
8	16010.	780.728	780.879	717.040	716.818	711.787	710.773
	20000.	781.349	781.500	717.124	716.900	711.813	710.785

Appendix 6: Listed Output of Linearized Stresses for Normal Operation Different Materials

		Equivalent stress (MPa)			
Step	Time	Membran/M+B(C)	Bending	M+B (I)	M+B(O)
1	0.0	4.9	3.7	7.1	4.9
2	5330.0	82.8	178.3	211.8	180.1
3	12300.0	21.0	123.6	136.5	113.2
4	56979.0	32.8	23.9	46.0	34.3
5	662340.0	27.9	14.0	35.7	26.0
6	1401600.0	221.5	175.5	292.8	271.9
Max		221.5	178.3	292.8	271.9

Cross Section: 12 = Path Node 168 - 164

		Equivalent stress (MPa)			
Step	Time	Membran/M+B(C)	Bending	M+B (I)	M+B(O)
1	0.0	0.9	0.3	0.7	1.2
2	5330.0	23.4	167.1	151.5	184.3
3	12300.0	12.3	25.8	15.9	37.1
4	56979.0	1.6	12.2	11.7	12.9
5	662340.0	2.1	6.8	4.9	8.8
6	1401600.0	63.3	363.8	342.8	394.0
Max		63.3	363.8	342.8	394.0

Cross Section: 14 = Path Node 1840 - 1792

Appendix 7: Listed Output of Linearized Stresses for Normal Operation

		Equivalent stress (MPa)			
Step	Time	Membran/M+B(C)	Bending	M+B (I)	M+B(O)
1	1.0000E-06	21.8	1.9	23.0	20.6
2	1.2300E+04	22.5	6.2	25.5	20.9
3	4.8937E+05	20.1	12.6	30.5	14.0
4	6.6596E+05	30.0	112.0	91.8	135.8
5	1.3145E+06	25.1	31.4	55.6	12.2
6	1.3152E+06	22.0	42.7	61.5	28.9
7	1.3181E+06	38.1	38.1	33.0	68.7
8	1.4016E+06	39.5	49.8	40.2	80.4
Max		39.5	112.0	91.8	135.8

Cross Section: 5 = Path Node 677 – 725

		Equivalent stress (MPa)			
Step	Time	Membran/M+B(C)	Bending	M+B (I)	M+B(O)
1	1.0000E-06	5.9	4.2	5.9	8.4
2	1.2300E+04	20.2	123.8	113.8	136.1
3	4.8937E+05	22.3	19.5	26.6	32.4
4	6.6596E+05	30.1	108.9	101.3	123.6
5	1.3145E+06	10.4	34.5	33.7	38.2
6	1.3152E+06	98.8	137.3	160.3	177.5
7	1.3181E+06	174.5	87.3	188.6	201.4
8	1.4016E+06	220.1	177.5	272.3	292.9
Max		220.1	177.5	272.3	292.9

Cross Section: 12 = Path Node 168 - 164

		Equivalent stress (MPa)			
Step	Time	Membran/M+B(C)	Bending	M+B (I)	M+B(O)
1	1.0000E-06	1.2	0.4	1.5	0.9
2	1.2300E+04	11.7	26.5	37.3	17.0
3	4.8937E+05	1.4	6.4	7.3	5.7
4	6.6596E+05	10.5	22.2	32.3	12.6
5	1.3145E+06	1.5	5.8	6.5	5.3
6	1.3152E+06	59.8	237.5	257.3	231.9
7	1.3181E+06	94.0	320.8	353.4	314.0
8	1.4016E+06	63.2	363.6	393.7	342.6
Max		94.0	363.6	393.7	342.6

Cross Section: 14 = Path Node 1840 - 1792

Appendix 8: Listed Output of Linearized Stresses for Accident Conditions

		Equivalent stress (MPa)			
Step	Time	Membran/M+B(C)	Bending	M+B (I)	M+B(O)
1	1.0000E-06	2.6	0.1	2.6	2.5
2	3.0000E+03	180.1	14.6	179.3	182.0
3	1.0000E+04	182.3	2.8	181.1	183.6
4	1.0003E+04	198.2	20.4	199.3	199.2
5	1.0006E+04	119.8	97.6	162.6	146.0
6	1.0008E+04	47.9	131.4	143.4	136.2
7	1.1023E+04	1.9	26.2	27.0	25.6
8	1.6011E+04	1.0	23.4	23.0	23.8
Max		198.2	131.4	199.3	199.2

Cross Section: 5 = Path Node 677 – 725

		Equivalent stress (MPa)			
Step	Time	Membran/M+B(C)	Bending	M+B (I)	M+B(O)
1	1.0000E-06	0.5	0.3	0.4	0.6
2	3.0000E+03	89.3	121.0	143.0	157.4
3	1.0000E+04	19.6	49.1	49.7	55.7
4	1.0003E+04	101.2	121.2	151.2	164.3
5	1.0006E+04	73.5	97.2	118.6	125.0
6	1.0008E+04	54.6	83.2	98.9	100.1
7	1.1023E+04	12.8	51.6	62.0	42.4
8	1.6011E+04	12.0	32.3	31.6	37.1
Max		101.2	121.2	151.2	164.3

Cross Section: 12 = Path Node 168 - 164

		Equivalent stress (MPa)			
Step	Time	Membran/M+B(C)	Bending	M+B (I)	M+B(O)
1	1.0000E-06	0.7	1.0	1.1	1.3
2	3.0000E+03	136.6	242.5	284.0	272.6
3	1.0000E+04	171.3	186.3	260.7	245.2
4	1.0003E+04	158.2	268.7	318.3	305.3
5	1.0006E+04	122.4	219.0	261.7	239.6
6	1.0008E+04	78.9	164.7	197.8	166.1
7	1.1023E+04	9.5	105.6	105.0	107.0
8	1.6011E+04	4.6	27.1	22.8	31.5
Max		171.3	268.7	318.3	305.3

Cross Section: 6 = Path Node 310 - 314

Appendix 9: Listed Output of Linearized total Equivalent Strain for Normal Operation

---- Load Case: Normal Operation ---Strain: EPTO ----- Cross Section: 5 ---------

Step	Time	Membran/M+B(C)	Bending	M+B(I)	M+B(O)
1.	0.10000000E-05	0.96088841E-04	0.82269668E-05	0.91133260E-04	0.10147032E-03
2.	0.12300000E+05	0.11712159E-03	0.32146924E-04	0.10898010E-03	0.13275963E-03
3.	0.48937000E+06	0.10751937E-03	0.67619791E-04	0.75374425E-04	0.16304723E-03
4.	0.66595600E+06	0.24217173E-03	0.76989917E-03	0.99422695E-03	0.56062157E-03
5.	0.13145000E+07	0.22756565E-03	0.47793938E-04	0.26860900E-03	0.18971024E-03
6.	0.13152000E+07	0.12873651E-03	0.59103705E-03	0.48823479E-03	0.70244042E-03
7.	0.13181000E+07	0.19639505E-03	0.22996134E-03	0.16122943E-03	0.39612062E-03
8.	0.14016000E+07	0.20265524E-03	0.17842334E-03	0.14287205E-03	0.35411248E-03
Max		0.24217173E-03	0.76989917E-03	0.99422695E-03	0.70244042E-03

Cross Section: 5 = Path Node 677 - 725

---- Load Case: Normal Operation ---Strain: EPTO ----- Cross Section: 12 ---------

Step	Time	Membran/M+B(C)	Bending	M+B(I)	M+B(O)
1.	0.10000000E-05	0.26461844E-04	0.24568336E-04	0.42165302E-04	0.28805415E-04
2.	0.12300000E+05	0.15996321E-02	0.10273586E-01	0.11608314E-01	0.90253994E-02
3.	0.48937000E+06	0.13408125E-02	0.99463967E-02	0.11204097E-01	0.87135177E-02
4.	0.66595600E+06	0.17199772E-02	0.12727440E-01	0.14280478E-01	0.11223192E-01
5.	0.13145000E+07	0.14773715E-02	0.11192728E-01	0.12586269E-01	0.98237166E-02
6.	0.13152000E+07	0.36651519E-02	0.24613278E-02	0.44667251E-02	0.43624893E-02
7.	0.13181000E+07	0.16904136E-02	0.44892772E-02	0.50336516E-02	0.45480290E-02
8.	0.14016000E+07	0.81141049E-03	0.60433054E-02	0.66458523E-02	0.54947704E-02
Max		0.36651519E-02	0.12727440E-01	0.14280478E-01	0.11223192E-01

Cross Section: 12 = Path Node 168 - 164

---- Load Case: Normal Operation ---Strain: EPTO ----- Cross Section: 14 ---------

Step	Time	Membran/M+B(C)	Bending	M+B(I)	M+B(O)
1.	0.10000000E-05	0.65850777E-05	0.29093848E-05	0.43799455E-05	0.91908440E-05
2.	0.12300000E+05	0.40447239E-02	0.12334707E-01	0.83099413E-02	0.16369315E-01
3.	0.48937000E+06	0.38132917E-02	0.10059221E-01	0.62610051E-02	0.13865716E-01
4.	0.66595600E+06	0.45157231E-02	0.12131613E-01	0.76342245E-02	0.16638937E-01
5.	0.13145000E+07	0.42939395E-02	0.10429020E-01	0.61516690E-02	0.14716037E-01
6.	0.13152000E+07	0.19238972E-02	0.12212380E-01	0.12512197E-01	0.12211966E-01
7.	0.13181000E+07	0.18902828E-02	0.18119027E-02	0.36962412E-02	0.22388006E-03
8.	0.14016000E+07	0.34348396E-02	0.71966190E-02	0.38503817E-02	0.10599691E-01
Max		0.45157231E-02	0.12334707E-01	0.12512197E-01	0.16638937E-01

Cross Section: 14 = Path Node 1840 - 1792

Appendix 10: Listed Output of Linearized total Equivalent Strain for Accident Conditions

---- Load Case: Primary Coolant Leak ---Strain: EPTO ----- Cross Section: 5 -----

Step	Time	Membran/M+B(C)	Bending	M+B(I)	M+B(O)
1.	0.10000000E-05	0.11265149E-04	0.26323593E-06	0.11013813E-04	0.11517016E-04
2.	0.30000000E+04	0.26854301E-01	0.33348165E-02	0.27808730E-01	0.26291130E-01
3.	0.10000000E+05	0.28182621E-01	0.32558361E-02	0.29055724E-01	0.27667419E-01
4.	0.10003000E+05	0.38284144E-01	0.44139305E-02	0.39302002E-01	0.37758040E-01
5.	0.10006000E+05	0.37864779E-01	0.48226666E-02	0.38874873E-01	0.37453217E-01
6.	0.10008000E+05	0.37476374E-01	0.50212950E-02	0.38488929E-01	0.37121238E-01
7.	0.11023000E+05	0.37208425E-01	0.42234095E-02	0.38257748E-01	0.36619022E-01
8.	0.16011000E+05	0.37225594E-01	0.41267012E-02	0.38258854E-01	0.36630713E-01
Max		0.38284144E-01	0.50212950E-02	0.39302002E-01	0.37758040E-01

Cross Section: 5 = Path Node 677 725

---- Load Case: Primary Coolant Leak ---Strain: EPTO ----- Cross Section: 6 -----

Step	Time	Membran/M+B(C)	Bending	M+B(I)	M+B(O)
1.	0.10000000E-05	0.28949373E-05	0.64810885E-05	0.69171348E-05	0.72748600E-05
2.	0.30000000E+04	0.26042734E-01	0.88037166E-01	0.99391438E-01	0.83539663E-01
3.	0.10000000E+05	0.27148965E-01	0.89352022E-01	0.10091352E+00	0.85194841E-01
4.	0.10003000E+05	0.36844008E-01	0.11819809E+00	0.13312134E+00	0.11373322E+00
5.	0.10006000E+05	0.36652620E-01	0.11780018E+00	0.13268500E+00	0.11329292E+00
6.	0.10008000E+05	0.36421912E-01	0.11735796E+00	0.13220231E+00	0.11278937E+00
7.	0.11023000E+05	0.36289069E-01	0.12408390E+00	0.13899411E+00	0.11877735E+00
8.	0.16011000E+05	0.36204409E-01	0.12338801E+00	0.13830845E+00	0.11807409E+00
Max		0.36844008E-01	0.12408390E+00	0.13899411E+00	0.11877735E+00

Cross Section: 12 = Path Node 168 164

---- Load Case: Primary Coolant Leak ---Strain: EPTO ----- Cross Section: 12 ----

Step	Time	Membran/M+B(C)	Bending	M+B(I)	M+B(O)
1.	0.10000000E-05	0.18576538E-05	0.16847603E-05	0.29059874E-05	0.20331816E-05
2.	0.30000000E+04	0.10070572E-01	0.21729004E-01	0.27104889E-01	0.20309039E-01
3.	0.10000000E+05	0.10151936E-01	0.22694908E-01	0.28099292E-01	0.21134594E-01
4.	0.10003000E+05	0.13619840E-01	0.28755236E-01	0.35978654E-01	0.27023394E-01
5.	0.10006000E+05	0.13530878E-01	0.28693737E-01	0.35866851E-01	0.26951796E-01
6.	0.10008000E+05	0.13426943E-01	0.28593465E-01	0.35709120E-01	0.26843935E-01
7.	0.11023000E+05	0.13197514E-01	0.27559957E-01	0.34518148E-01	0.25999013E-01
8.	0.16011000E+05	0.12790167E-01	0.26161578E-01	0.32845085E-01	0.24844183E-01
Max		0.13619840E-01	0.28755236E-01	0.35978654E-01	0.27023394E-01

Cross Section: 6 = Path Node 310 - 314

Appendix 11: Listed Output of Linearized Equivalent Plastic Strain - Normal Operation

---- Load Case: Normal Operation ---Strain: EPPL ----- Cross Section: 5 ---------

Step	Time	Membran/M+B(C)	Bending	M+B(I)	M+B(O)
1.	0.10000000E-05	0.00000000E+00	0.00000000E+00	0.00000000E+00	0.00000000E+00
2.	0.12300000E+05	0.00000000E+00	0.00000000E+00	0.00000000E+00	0.00000000E+00
3.	0.48937000E+06	0.00000000E+00	0.00000000E+00	0.00000000E+00	0.00000000E+00
4.	0.66595600E+06	0.10111226E-03	0.21313140E-03	0.31420680E-03	0.11212249E-03
5.	0.13145000E+07	0.10111226E-03	0.21313140E-03	0.31420680E-03	0.11212249E-03
6.	0.13152000E+07	0.29596486E-04	0.40039423E-03	0.37239106E-03	0.42861157E-03
7.	0.13181000E+07	0.29596486E-04	0.40039423E-03	0.37239106E-03	0.42861157E-03
8.	0.14016000E+07	0.29596486E-04	0.40039423E-03	0.37239106E-03	0.42861157E-03
Max		0.10111226E-03	0.40039423E-03	0.37239106E-03	0.42861157E-03

Cross Section: 5 = Path Node 677 - 725

---- Load Case: Normal Operation ---Strain: EPPL ----- Cross Section: 12 ---------

Step	Time	Membran/M+B(C)	Bending	M+B(I)	M+B(O)
1.	0.10000000E-05	0.00000000E+00	0.00000000E+00	0.00000000E+00	0.00000000E+00
2.	0.12300000E+05	0.10645853E-02	0.64134140E-02	0.72313872E-02	0.56778061E-02
3.	0.48937000E+06	0.10645853E-02	0.64134140E-02	0.72313872E-02	0.56778061E-02
4.	0.66595600E+06	0.10645853E-02	0.64134140E-02	0.72313872E-02	0.56778061E-02
5.	0.13145000E+07	0.10645853E-02	0.64134140E-02	0.72313872E-02	0.56778061E-02
6.	0.13152000E+07	0.55900757E-03	0.51767964E-02	0.57236993E-02	0.46327839E-02
7.	0.13181000E+07	0.10624031E-02	0.56941086E-02	0.65230052E-02	0.49551539E-02
8.	0.14016000E+07	0.19991709E-02	0.67579918E-02	0.80673785E-02	0.58524935E-02
Max		0.19991709E-02	0.67579918E-02	0.80673785E-02	0.58524935E-02

Cross Section: 12 = Path Node 168 - 164

---- Load Case: Normal Operation ---Strain: EPPL ----- Cross Section: 14 ---------

Step	Time	Membran/M+B(C)	Bending	M+B(I)	M+B(O)
1.	0.10000000E-05	0.00000000E+00	0.00000000E+00	0.00000000E+00	0.00000000E+00
2.	0.12300000E+05	0.75963714E-03	0.35148075E-02	0.27614659E-02	0.42703802E-02
3.	0.48937000E+06	0.75963714E-03	0.35148075E-02	0.27614659E-02	0.42703802E-02
4.	0.66595600E+06	0.75963714E-03	0.35148075E-02	0.27614659E-02	0.42703802E-02
5.	0.13145000E+07	0.75963714E-03	0.35148075E-02	0.27614659E-02	0.42703802E-02
6.	0.13152000E+07	0.12363265E-02	0.74574955E-02	0.65417781E-02	0.84552128E-02
7.	0.13181000E+07	0.41876146E-03	0.11858561E-02	0.15632530E-02	0.84821680E-03
8.	0.14016000E+07	0.19984310E-02	0.78739136E-02	0.58785801E-02	0.98705004E-02
Max		0.19984310E-02	0.78739136E-02	0.65417781E-02	0.98705004E-02

Cross Section: 14 = Path Node 1840 - 1792

max $\Delta\varepsilon$=0,427%

(max strain range within the load case)

Appendix 12: Listed Output of Linearized Equivalent Plastic Strain - Accident Condition

---- Load Case: Primary Coolant Leak ---Strain: EPPL ----- Cross Section: 5 -----

Step	Time	Membran/M+B(C)	Bending	M+B(I)	M+B(O)
1.	0.10000000E-05	0.00000000E+00	0.00000000E+00	0.00000000E+00	0.00000000E+00
2.	0.30000000E+04	0.25886702E-01	0.32592336E-02	0.26832050E-01	0.25328421E-01
3.	0.10000000E+05	0.27202634E-01	0.32676389E-02	0.28077523E-01	0.26701577E-01
4.	0.10003000E+05	0.37215925E-01	0.43038644E-02	0.38223390E-01	0.36688815E-01
5.	0.10006000E+05	0.37216514E-01	0.43072217E-02	0.38226117E-01	0.36687956E-01
6.	0.10008000E+05	0.37216514E-01	0.43072217E-02	0.38226117E-01	0.36687956E-01
7.	0.11023000E+05	0.37215448E-01	0.43225401E-02	0.38224939E-01	0.36690624E-01
8.	0.16011000E+05	0.37215448E-01	0.43225401E-02	0.38224939E-01	0.36690624E-01
Max		0.37216514E-01	0.43225401E-02	0.38226117E-01	0.36690624E-01

Cross Section: 5 = Path Node 677 - 725

---- Load Case: Primary Coolant Leak ---Strain: EPPL ----- Cross Section: 12 ----

Step	Time	Membran/M+B(C)	Bending	M+B(I)	M+B(O)
1.	0.10000000E-05	0.00000000E+00	0.00000000E+00	0.00000000E+00	0.00000000E+00
2.	0.30000000E+04	0.10261309E-02	0.24645721E-02	0.29886706E-02	0.23069393E-02
3.	0.10000000E+05	0.10261309E-02	0.24645721E-02	0.29886706E-02	0.23069393E-02
4.	0.10003000E+05	0.33362643E-02	0.67695389E-02	0.85919507E-02	0.63319047E-02
5.	0.10006000E+05	0.33362643E-02	0.67695389E-02	0.85919507E-02	0.63319047E-02
6.	0.10008000E+05	0.33362643E-02	0.67695389E-02	0.85919507E-02	0.63319047E-02
7.	0.11023000E+05	0.33362643E-02	0.67695389E-02	0.85919507E-02	0.63319047E-02
8.	0.16011000E+05	0.33362643E-02	0.67695389E-02	0.85919507E-02	0.63319047E-02
Max		0.33362643E-02	0.67695389E-02	0.85919507E-02	0.63319047E-02

Cross Section: 12 = Path Node 168 - 164

---- Load Case: Primary Coolant Leak ---Strain: EPPL ----- Cross Section: 6 -----

Step	Time	Membran/M+B(C)	Bending	M+B(I)	M+B(O)
1.	0.10000000E-05	0.00000000E+00	0.00000000E+00	0.00000000E+00	0.00000000E+00
2.	0.30000000E+04	0.25309754E-01	0.86100992E-01	0.97233487E-01	0.81569468E-01
3.	0.10000000E+05	0.26254227E-01	0.87866520E-01	0.99190198E-01	0.83551926E-01
4.	0.10003000E+05	0.35989584E-01	0.11604582E+00	0.13071317E+00	0.11152504E+00
5.	0.10006000E+05	0.35989584E-01	0.11604582E+00	0.13071317E+00	0.11152504E+00
6.	0.10008000E+05	0.35989584E-01	0.11604582E+00	0.13071317E+00	0.11152504E+00
7.	0.11023000E+05	0.35989584E-01	0.11604582E+00	0.13071317E+00	0.11152504E+00
8.	0.16011000E+05	0.35989584E-01	0.11604582E+00	0.13071317E+00	0.11152504E+00
Max		0.35989584E-01	0.11604582E+00	0.13071317E+00	0.11152504E+00

Cross Section: 6 = Path Node 310 - 314

max $\Delta\varepsilon$=9,723%

(max. strain range within the load case)